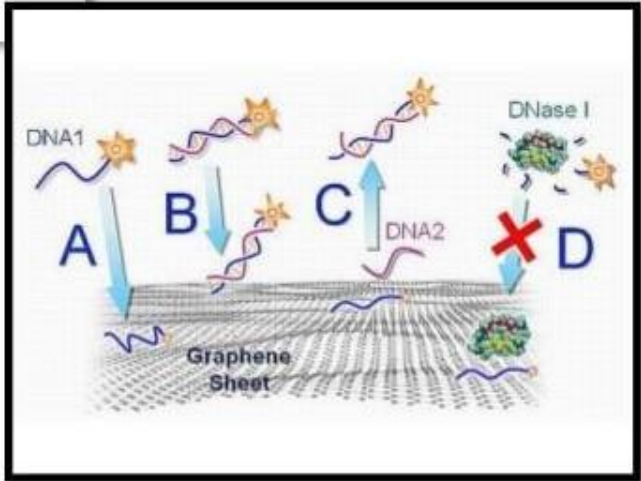
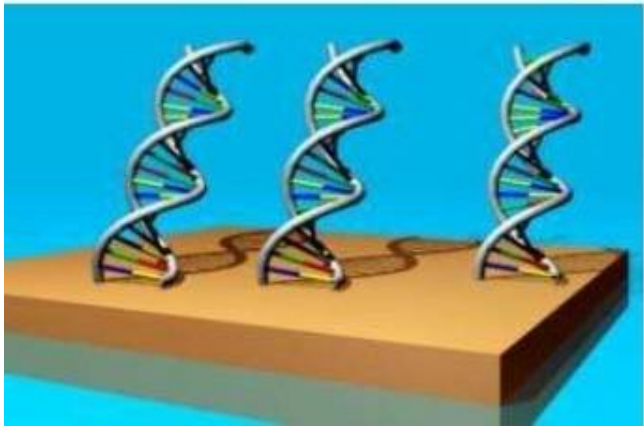
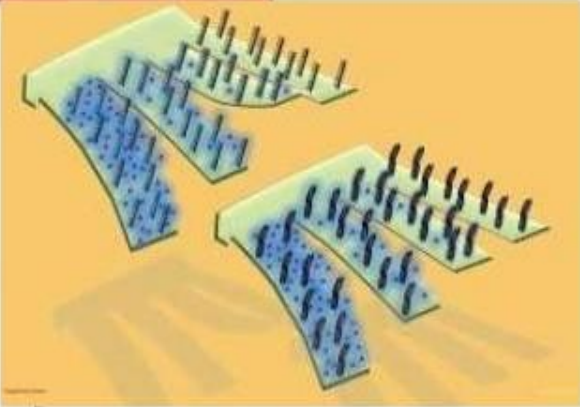
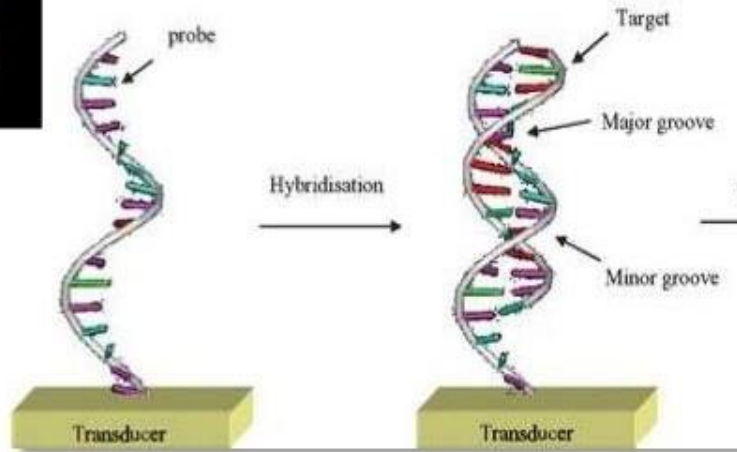
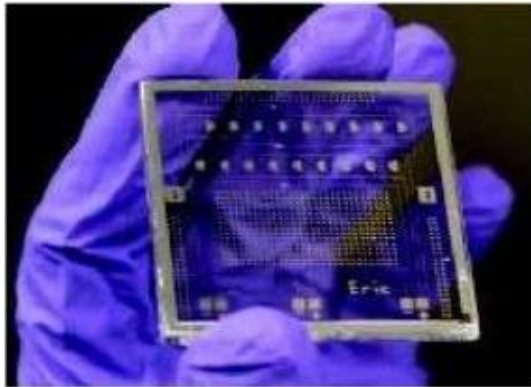


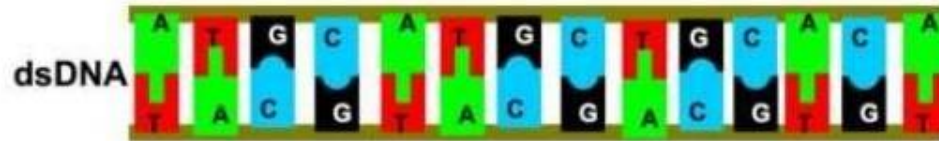
DNA biosensors



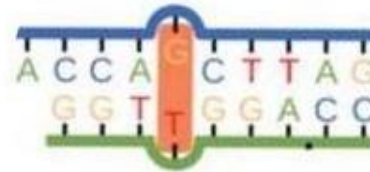
Principles of DNA biosensors

❖ Nucleic acid hybridization

- **Perfect match**
stable dsDNA, strong hybridization



- **One or more base mismatches**
weak hybridization



❖ **Forms of DNA Biosensors**

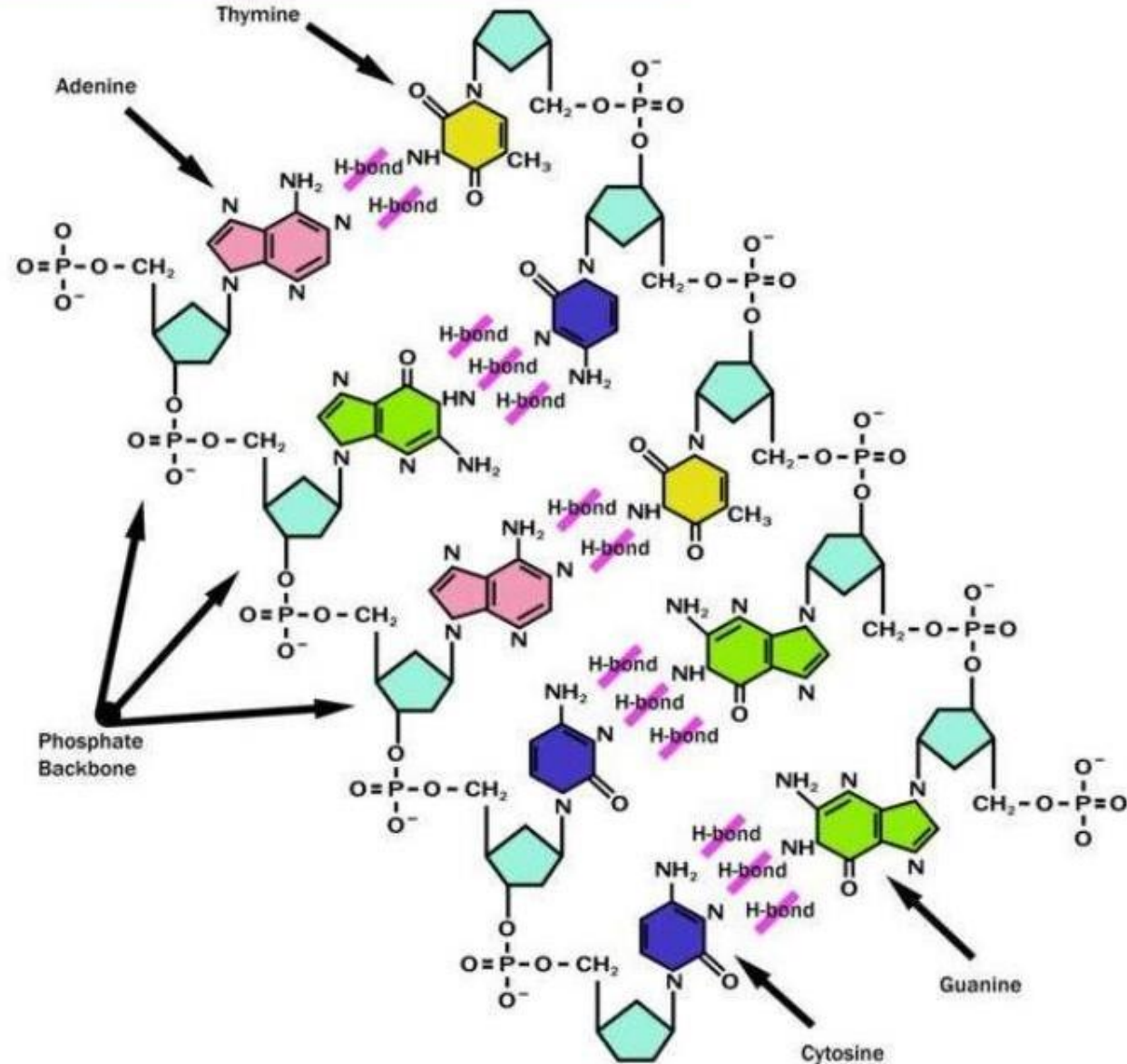
- Electrodes
- Chips
- Crystals

❖ **Types of DNA Based Biosensors**

- Optical
- Electrochemical
- Piezoelectric

Immobilization of DNA Probe onto Transducer Surface

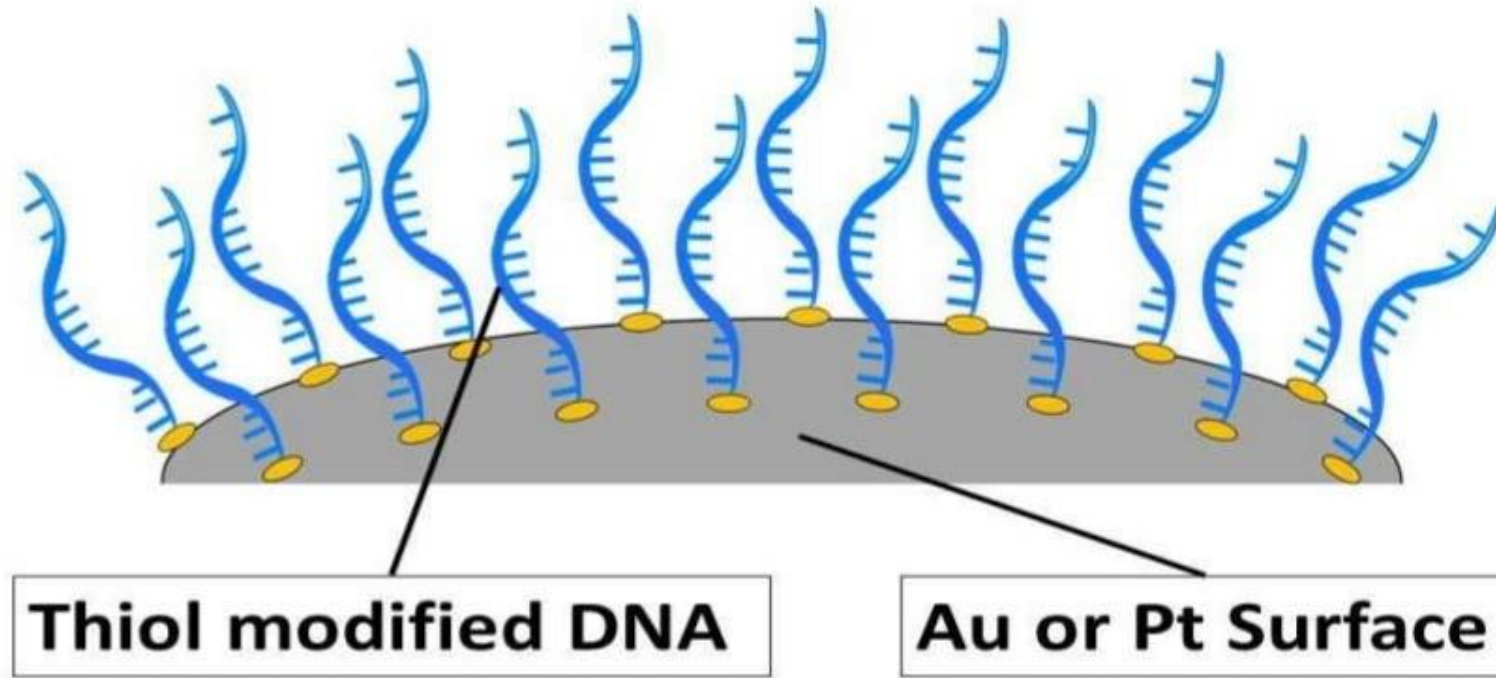
- simple adsorption onto carbon surfaces



Immobilization of DNA Probe onto Transducer Surface

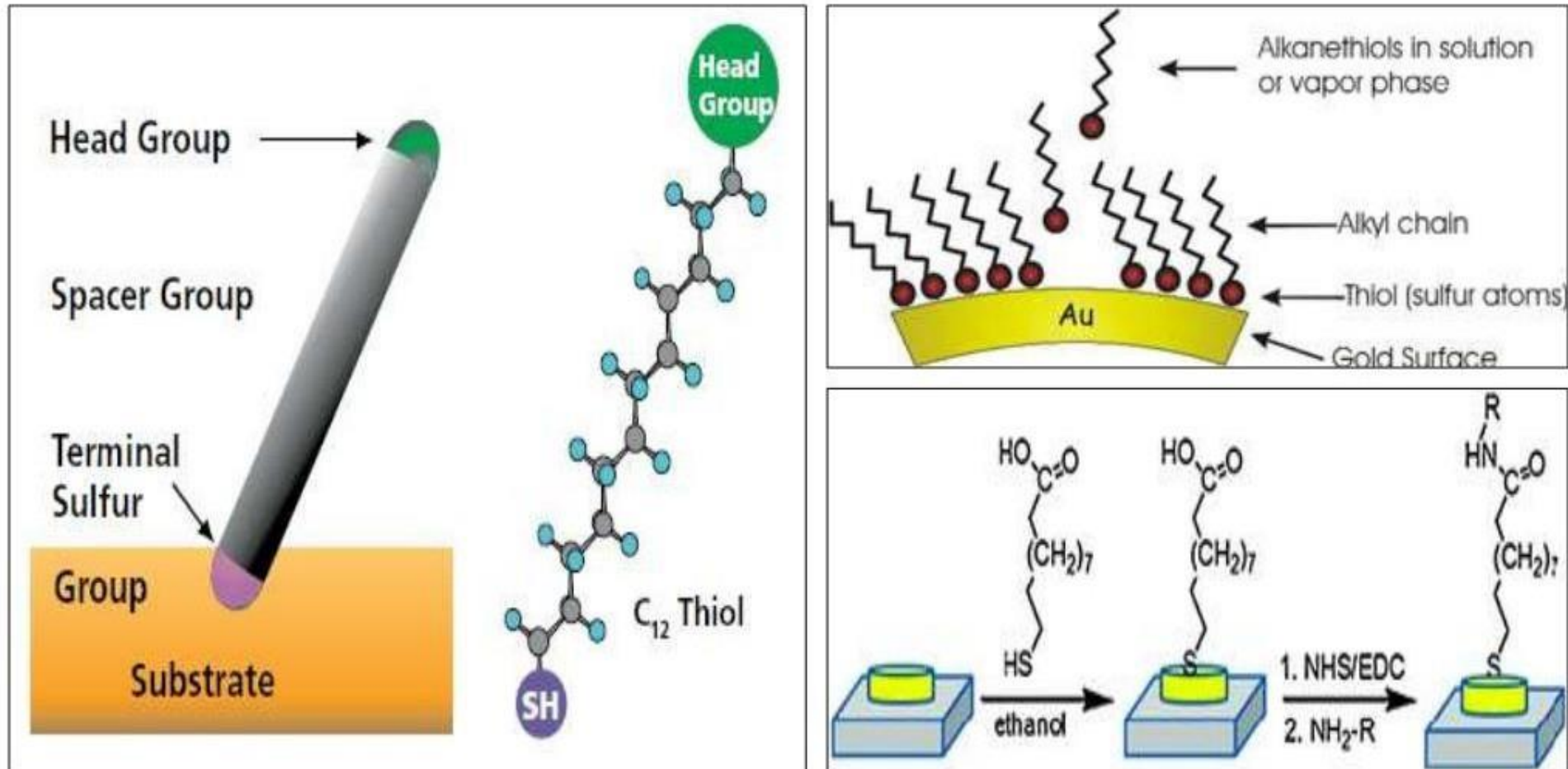
- Thiolated DNA for self assembly onto gold (or platinum) transducers

SAM conjugation

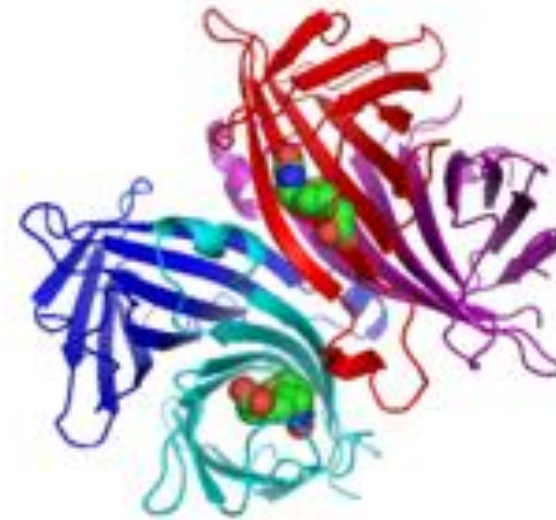
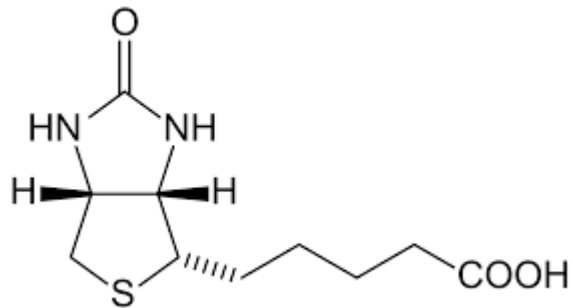
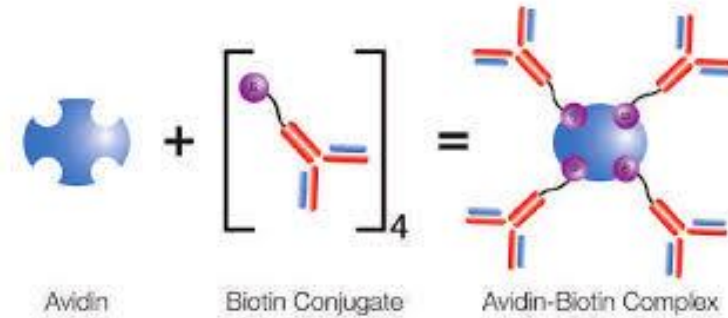
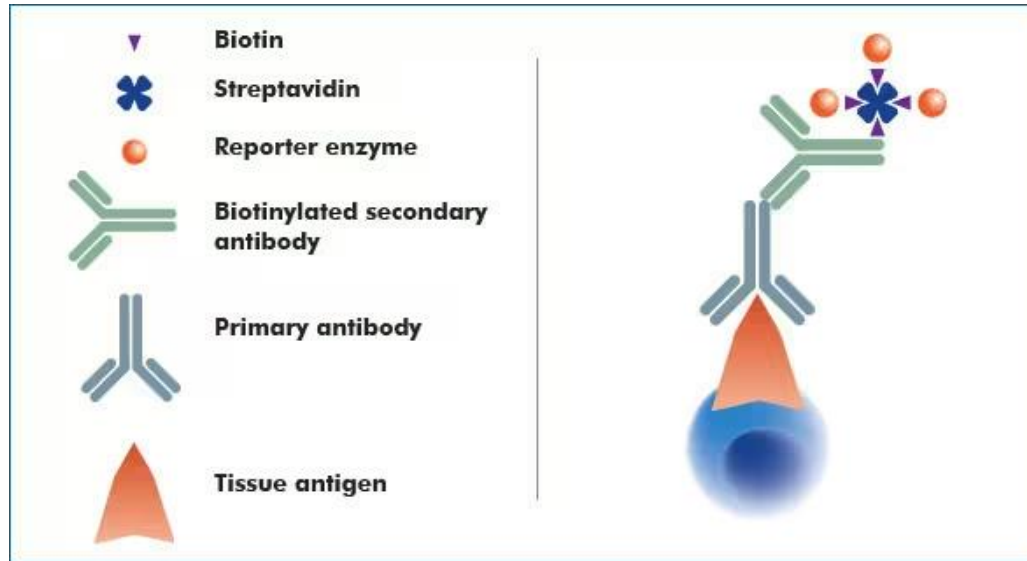


Immobilization of DNA Probe onto Transducer Surface

- Covalent linkage to the gold surface via functional **alkanethiol-based** monolayers

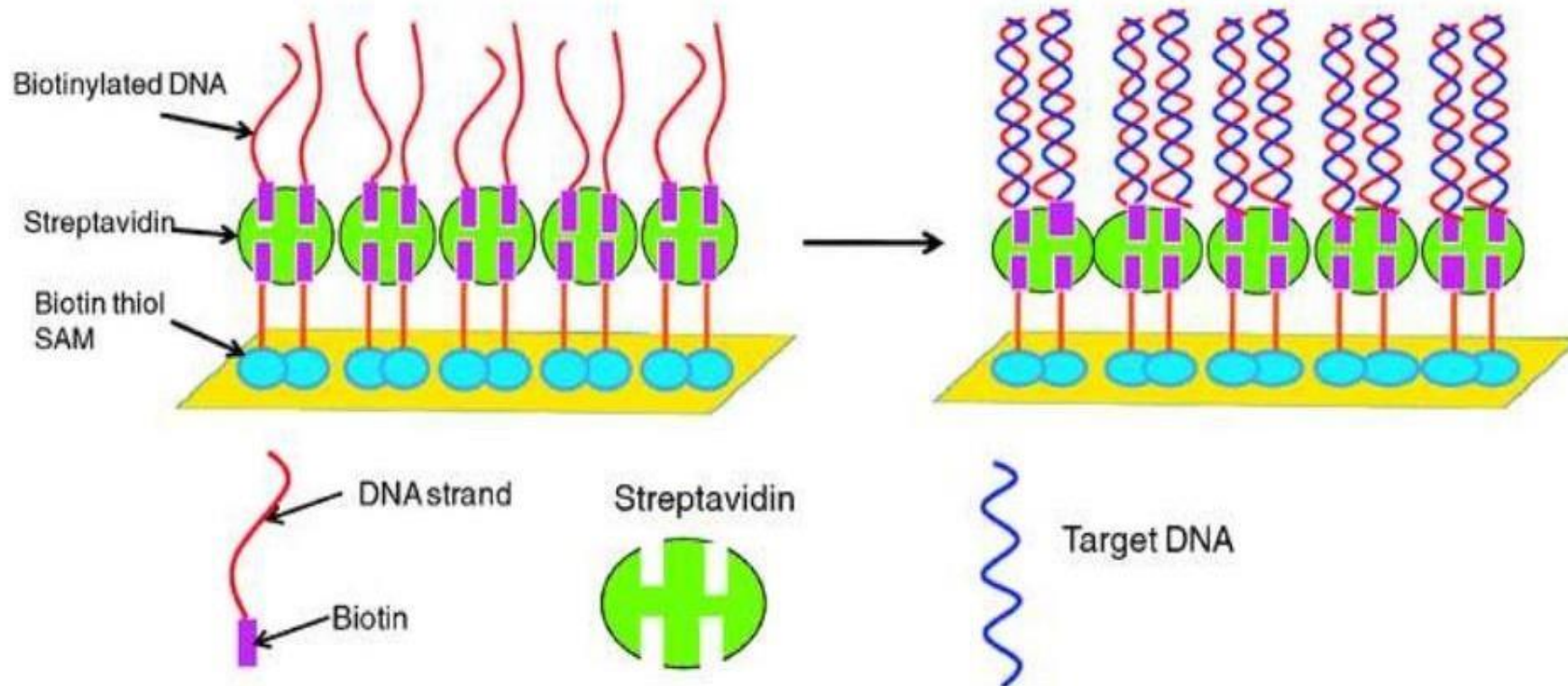


Strept(avidin)- Biotin $K_D = 10^{-15}$

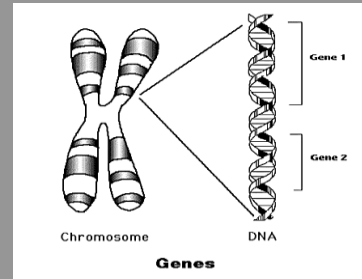


Immobilization of DNA Probe onto Transducer Surface

- Use of biotinylated DNA for complex formation with a surface-confined avidin or streptavidin



- **Development of an *Hybridisation sensor***



**Synthesis of a DNA fragment (probe, bioreceptor)
containing the sequence of interest (**analytical problem**)**

Immobilisation of the probe onto the
solid support of the sensor (**surface**)
(*thiol/dextran/streptavidin/biotinylated probe*)

Extraction of the DNA from the real
sample (blood, water, food) and
amplification of the sequence of
interest (**sample pretreatment**)

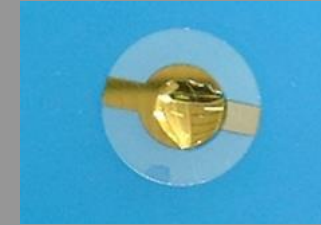
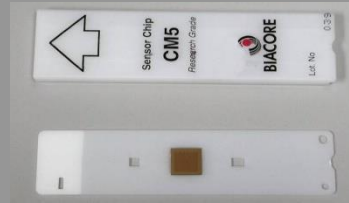
Denaturation of the dsDNA (amplified
fragment or genomic) to obtain a single-
stranded DNA (**sample pretreatment**)

Hybridisation of the obtained ssDNA
with the immobilised probe

Changes in the physicochemical parameters of the layer formed on the
transducer (quartz crystal or gold –glass chip)

Probe immobilisation on gold film

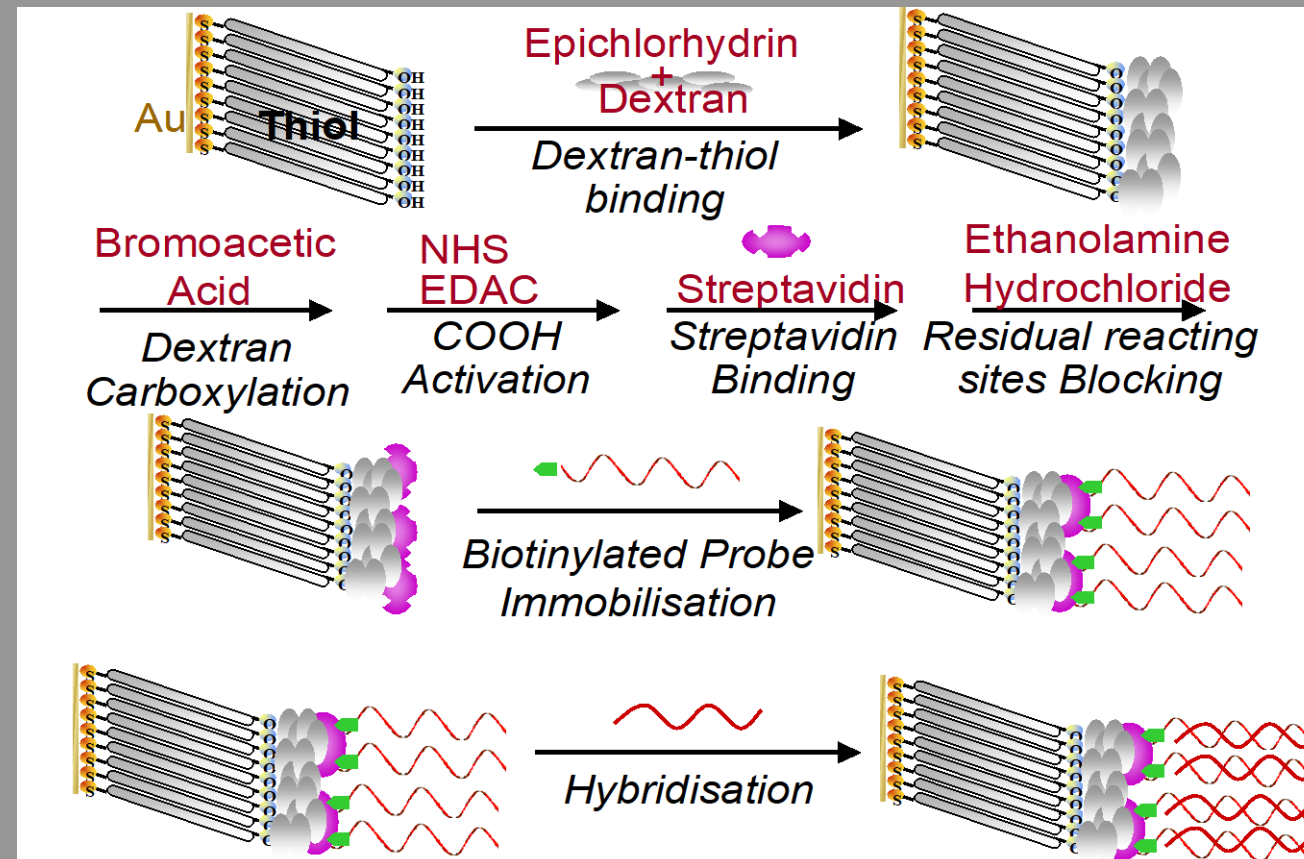
optical



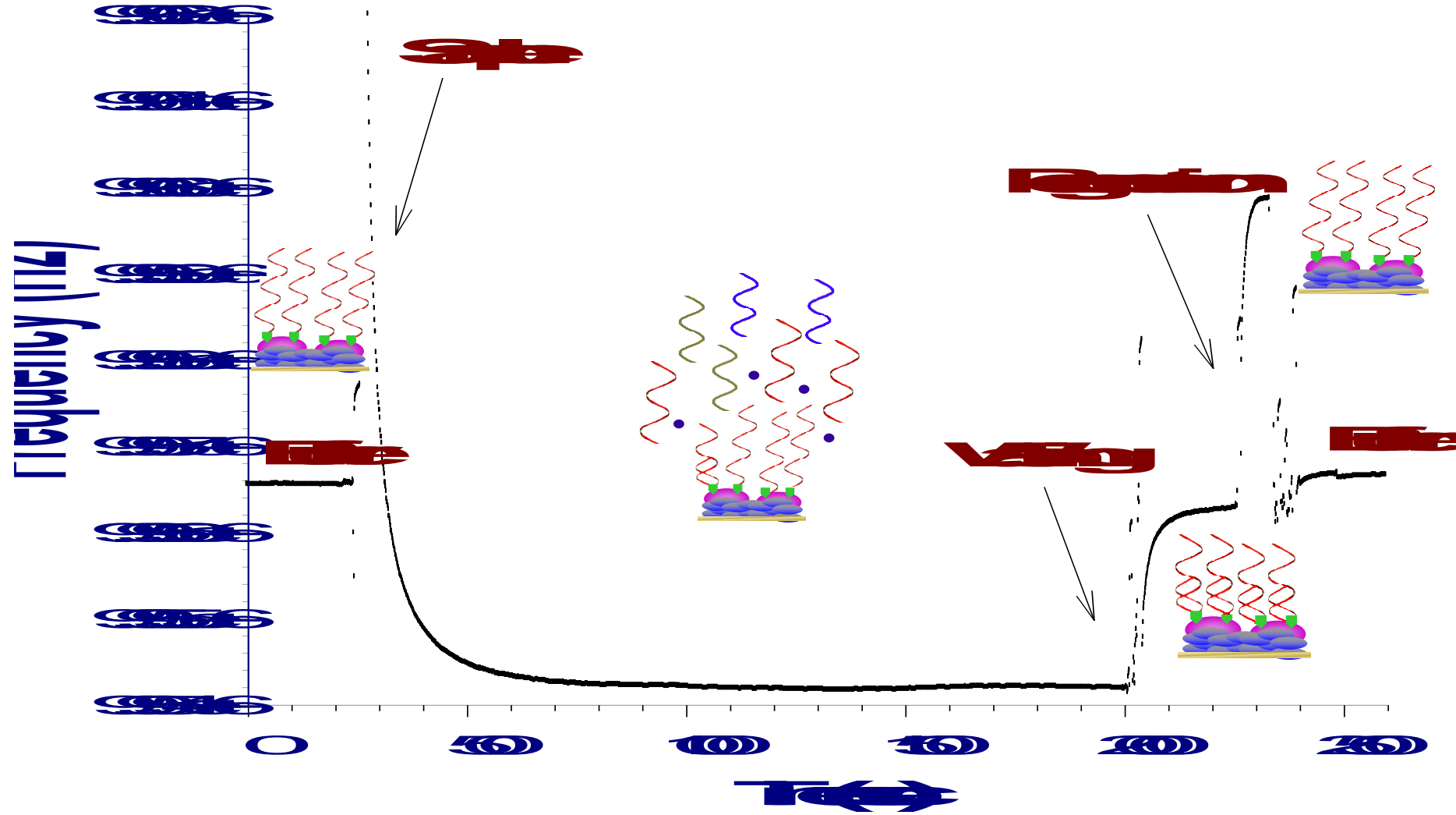
piezoelectric

Performances: specificity, absence of unspecific adsorption, stability, multi-use

thiol/dextran/streptavidin/biotinylated probe



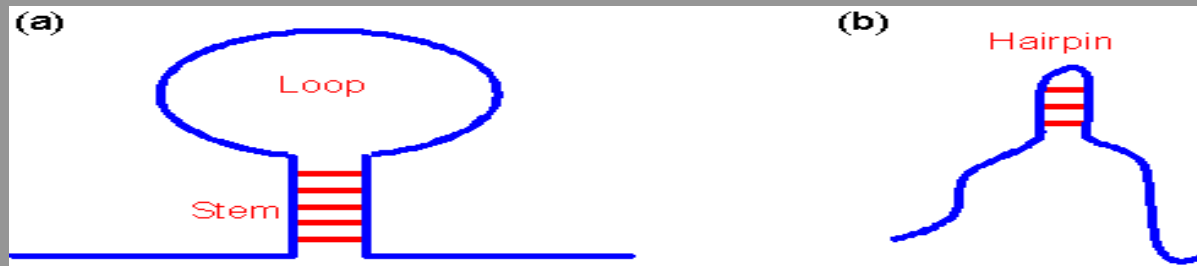
Hybridation-Regeneration Cycle



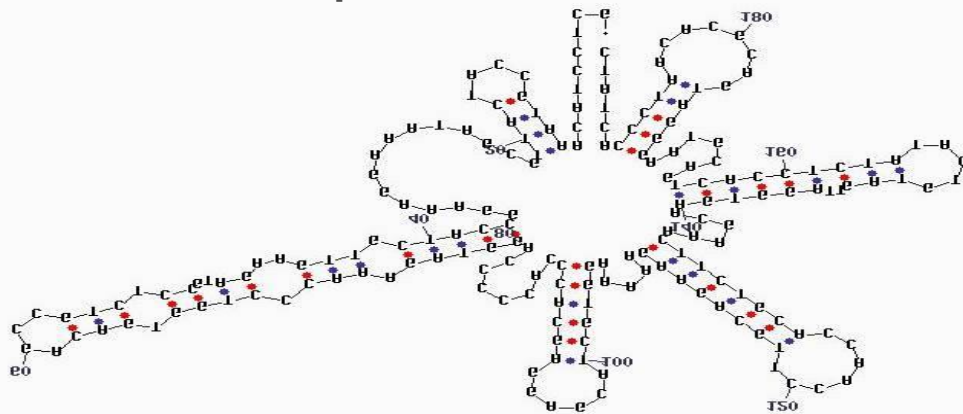
ssDNA strands can form intra-strand base pairs and secondary structures



Limitation of the available ssDNA target for hybridisation with the immobilised probe



Secondary structures of single stranded DNA p35s



To avoid this: proper denaturation!

Aim: prolongate the ssDNA life time as much is possible, preventing dsDNA formation

To allow hybridisation of target sequence with immobilised probe:

1. Thermal

95°C 5 min, 0°C 1 min.

DNA denaturation:

2. Chemical denaturation

- 20% Formamide + NaOH 0.3 M

- 42°C for 30 min.

- HCl 0.3 M

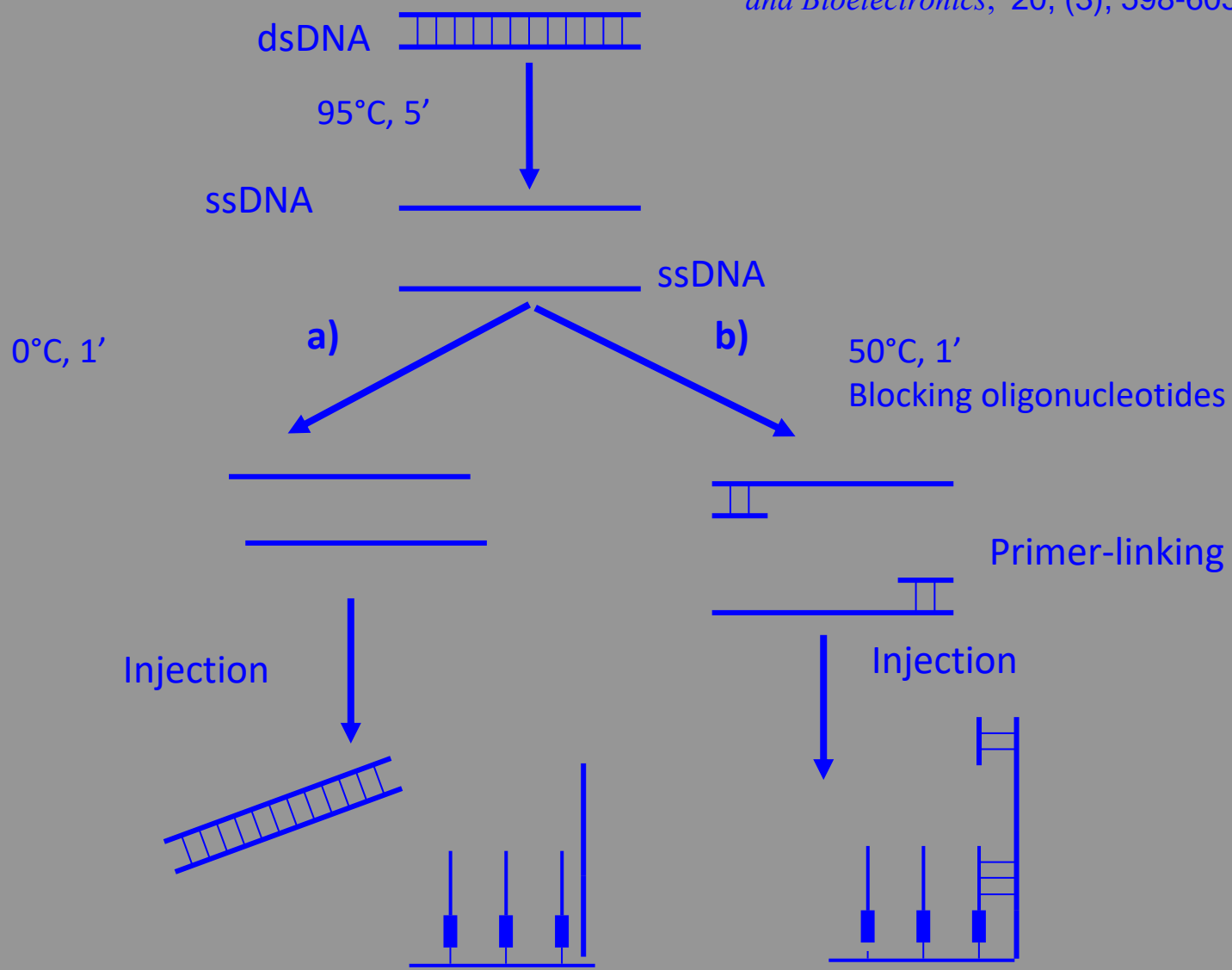
- 0°C for 1 min.

3. Thermal+ blocking oligonucleotides

Denaturation: a) thermal

b) thermal + blocking oligonucleotides

R. Wang, M. Minunni, S. Tombelli, M. Mascini, *Biosensors and Bioelectronics*, 20, (3), 598-605, 2004



Sensori elettrochimici a DNA



Review: Electrochemical DNA sensing – Principles, commercial systems, and applications

Martin Trotter^{a,*}, Nadine Borst^{a,b}, Roland Thewes^c, Felix von Stetten^{a,b,**}

^a Hahn-Schickard, Georges-Koehler-Allee 103, 79110, Freiburg, Germany

^b Laboratory for MEMS Applications, Department of Microsystems Engineering – IMTEK, University of Freiburg, Georges-Koehler-Allee 103, 79110, Freiburg, Germany

^c Faculty of EECS, Chair of Sensor and Actuator Systems, TU Berlin, Einsteinufer 17, 10587, Berlin, Germany

Table 1
Categories of electrochemical NA sensing principles.

	Label-free, reagent-less	Label-free, reagent-dependent	Labeled, reagent-less	Labeled, reagent-dependent
Heterogeneous detection	<ul style="list-style-type: none"> • Change in capacitance • Change in impedance • Field-effect 	<ul style="list-style-type: none"> • Intercalation • Groove-binding • Electrostatic binding • Electrostatic repulsion 	<ul style="list-style-type: none"> • Labeled capture probes • Labeled signaling probes • Labeled nucleotides 	<ul style="list-style-type: none"> • Enzyme labels
Homogeneous detection	<ul style="list-style-type: none"> • Detection of NA amplification by-product with ISFET 	<ul style="list-style-type: none"> • Consumption of electroactive molecules by interaction with NA 	<ul style="list-style-type: none"> • Release of electroactive molecules 	<ul style="list-style-type: none"> • No principle known
Advantages	<ul style="list-style-type: none"> • Cost-effective reagents possible 	<ul style="list-style-type: none"> • Enhanced signals 	<ul style="list-style-type: none"> • Specific signal 	<ul style="list-style-type: none"> • Signal amplification
Drawbacks	<ul style="list-style-type: none"> • Low signals • Risk of unspecific signal changes 	<ul style="list-style-type: none"> • Risk of unspecific signal changes 	<ul style="list-style-type: none"> • Modification of oligonucleotide increases costs 	<ul style="list-style-type: none"> • Additional process steps complicate automation

In electrical engineering, impedance is the opposition to alternating current presented by the combined effect of resistance and reactance in a circuit.

Quantitatively, the impedance of a two-terminal circuit element is the ratio of the complex representation of the sinusoidal voltage between its terminals, to the complex representation of the current flowing through it. In general, it depends upon the frequency of the sinusoidal voltage.

Impedance extends the concept of resistance to alternating current (AC) circuits, and possesses both magnitude and phase, unlike resistance, which has only magnitude.

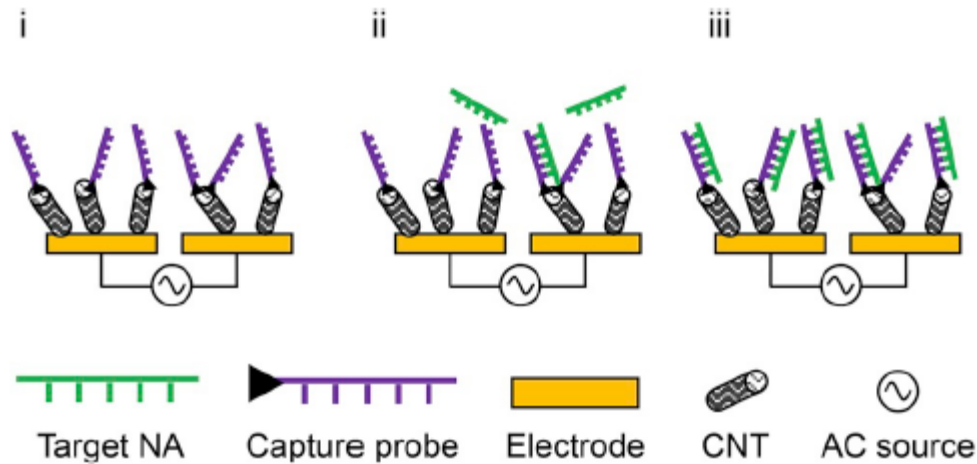


Fig. 2. Heterogeneous, label-free, reagent-less sensing principle. Cubed laboratories use interdigitated electrodes and functionalized CNTs for NA detection. Initially, a baseline impedance measurement is performed (i). Then the single-stranded product of an asymmetric PCR mixed with hybridization buffer is hybridized to the CNT-bound capture probes (ii). After washing with measurement buffer, another impedance measurement is performed (iii). All steps are performed while applying an AC field for dielectrophoresis, which supports specific hybridization.

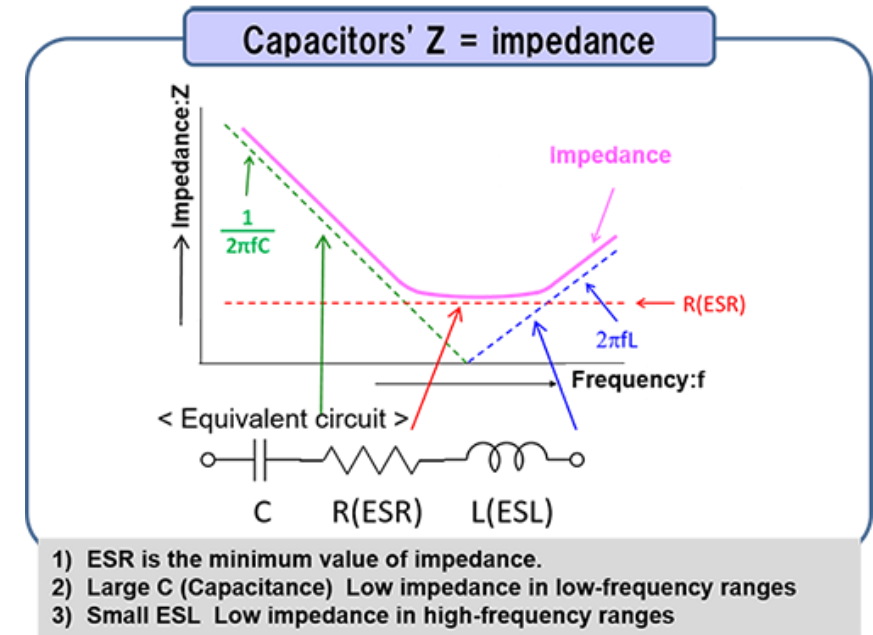




Fig. 1. Images of some of the reviewed commercial electrochemical NA detection systems in the order of their appearance in the text. A: Cubed Laboratories' NESDEP instrument (copyright: Cubed Laboratories) B: Canon's Gelyzer II instrument (copyright: Canon Medical Systems Corp.) C: GenMark's ePlex instrument (four tower version shown – the device can also be equipped with fewer towers, copyright GenMark Diagnostics Inc.) D: Friz Biochem's envisioned Cycle device (copyright: Friz Biochem GmbH) E: CustomArray's ElectraSense reader (copyright: Custom Array Inc.) F: Elice's Leo instrument (copyright: Easy Life Science) G: Binx's io instrument (copyright: Binx Health Inc.). The images are not to scale. All images are published with the permission of the respective companies.

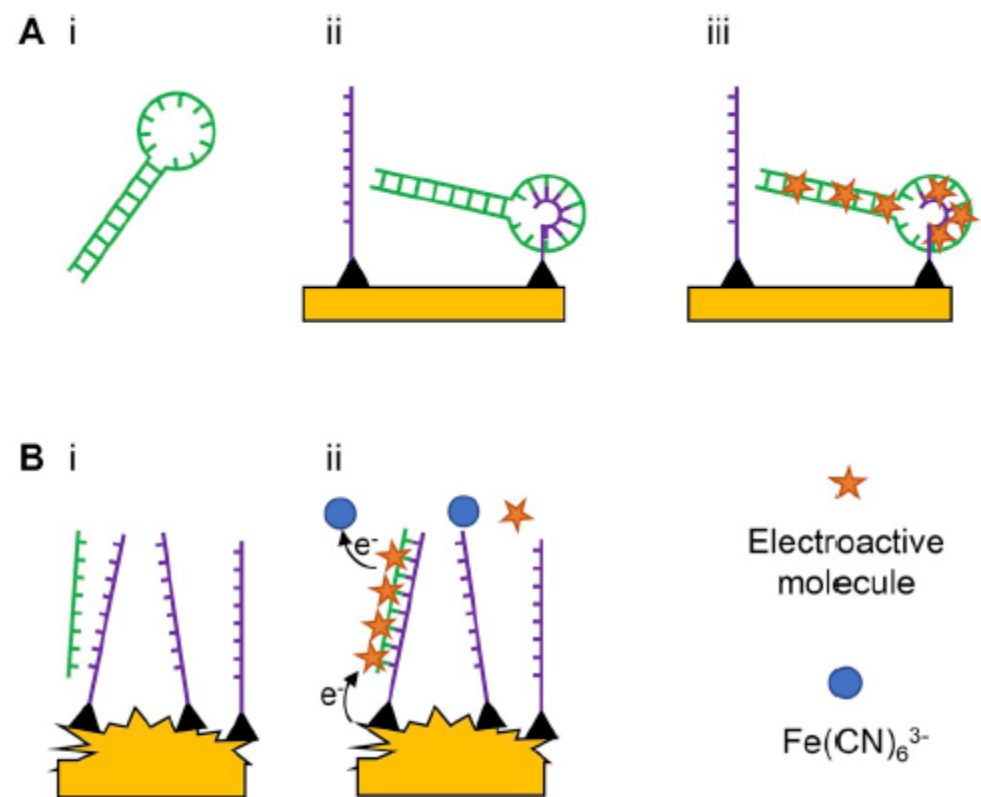


Fig. 3. Heterogeneous, label-free sensing principles that require the addition of electroactive molecules as indicators. A: Canon detects LAMP products (i). Upon mixing with hybridization buffer, the single-stranded loop region of the product can hybridize to the capture probe (ii). After hybridization, the electrodes are washed and then incubated with electroactive molecules, which intercalate into double-stranded DNA (iii). B: Xagenic immobilizes PNA capture probes on nanostructured microelectrodes. Extracted NAs hybridize to the probes (i) and become detectable by their electrostatic interaction with electroactive Ru^{3+} . The reduction signal of Ru^{3+} is electrocatalytically amplified by the presence of $\text{Fe}(\text{CN})_6^{3-}$, which oxidizes the reduced Ru during the measurement procedure (ii).

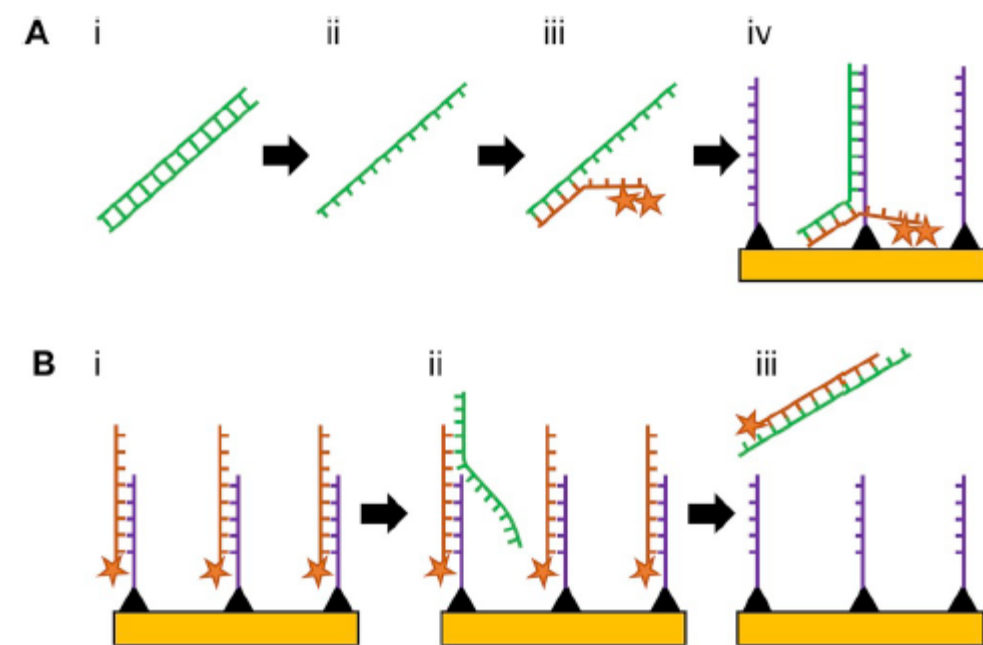


Fig. 4. Heterogeneous sensing principles relying on electroactive labels. A: For GenMark's approach, the double-stranded PCR products (i) become single-stranded via exonuclease digestion (ii). The ssDNA is labeled with a signaling probe (iii) and finally hybridized to the capture probe (iv). B: For FRIZ Biochem's EDDA principle, the signal probe is initially hybridized to the capture probe (i). Since the signal probe's affinity to the target NA is higher, the target NA can displace the signal probe from the capture probe (ii), leading to a decrease in the number of electroactive molecules in the proximity of the electrode surface (iii).

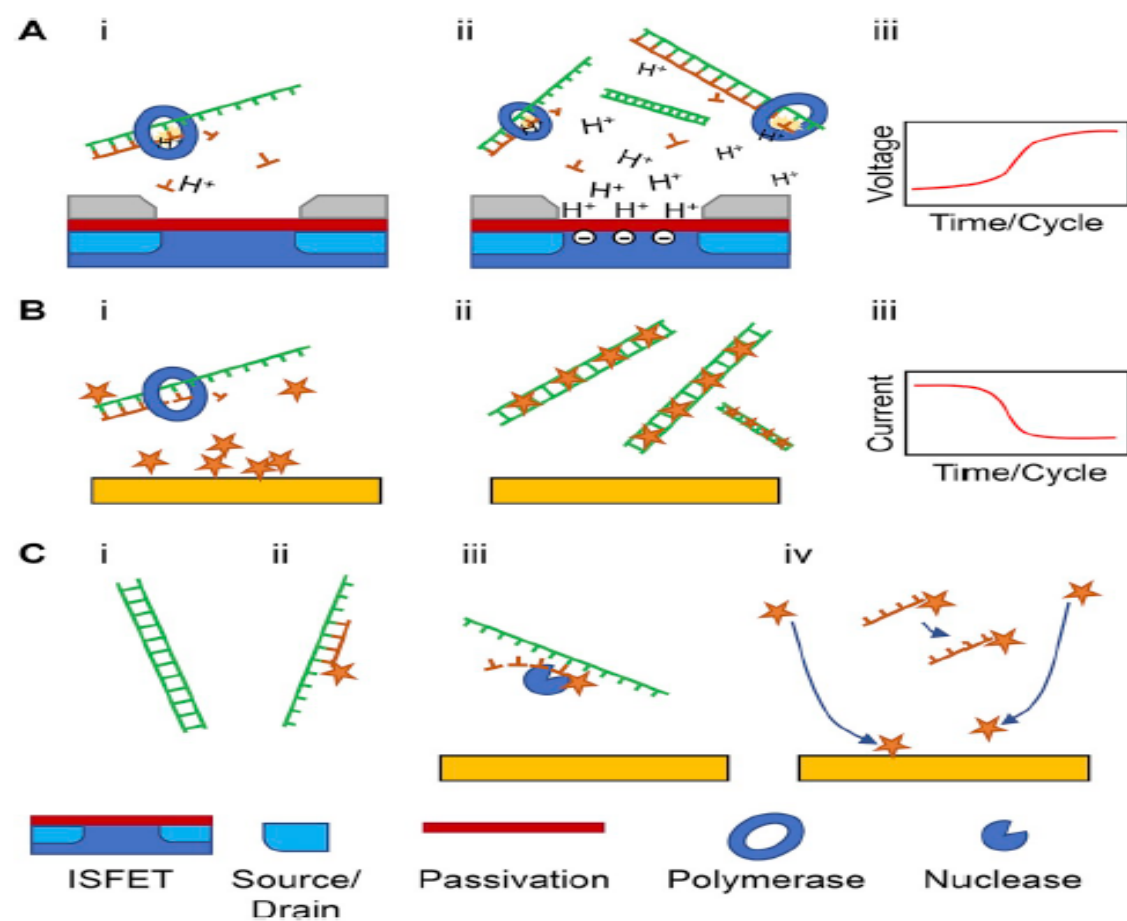
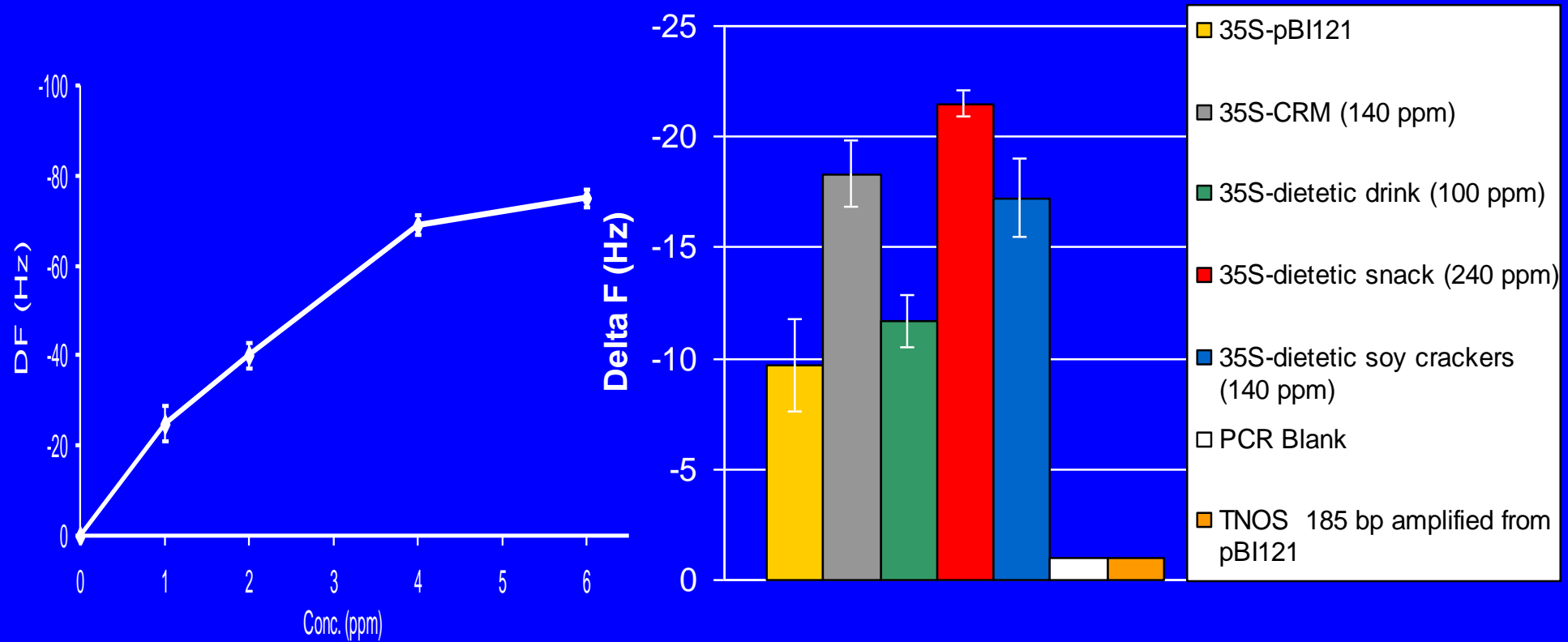


Fig. 6. Homogeneous sensing principles. **A:** DNAe use ISFETs to monitor the amplification reaction by detecting protons (H^+) that are generated during the incorporation of nucleotides (i). With increasing time (isothermal amplification) or cycles (PCR), the concentration of protons increases. The accumulation of protons at the passivation layer attracts negative charges in the semiconductor (blue), which influence the threshold voltage between the source and the drain (ii + iii). For further details, see SI of (Toumazou et al., 2013) **B:** Elice detects NAs by monitoring the consumption of electroactive molecules. The initially high concentration of freely diffusing electroactive molecules (i) decreases when double-stranded DNA is generated, into which the molecules intercalate (ii). The signal decreases if the target is present (iii). **C:** Binx detects double-stranded PCR products (i) by hybridizing a labeled signaling probe to the target (ii), which is then digested by a double-strand-specific nuclease (iii). The released electroactive molecule diffuses faster to the electrode surface than the intact signaling probes (iv). (For interpretation of the references to colour in this figure legend, the reader is referred to the Web version of this article.)

Piezoelectric sensor, CRM 2% samples and processed food samples

Sample pre-treatment:



5'-BIOT-ggc cat cgt tga aga tgc ctc tgc c-3' probe 35S



UNIVERSITÀ
degli STUDI
di CATANIA

DIPARTIMENTO DI SCIENZE CHIMICHE
Viale Andrea Doria, 6 – I-95125 Catania

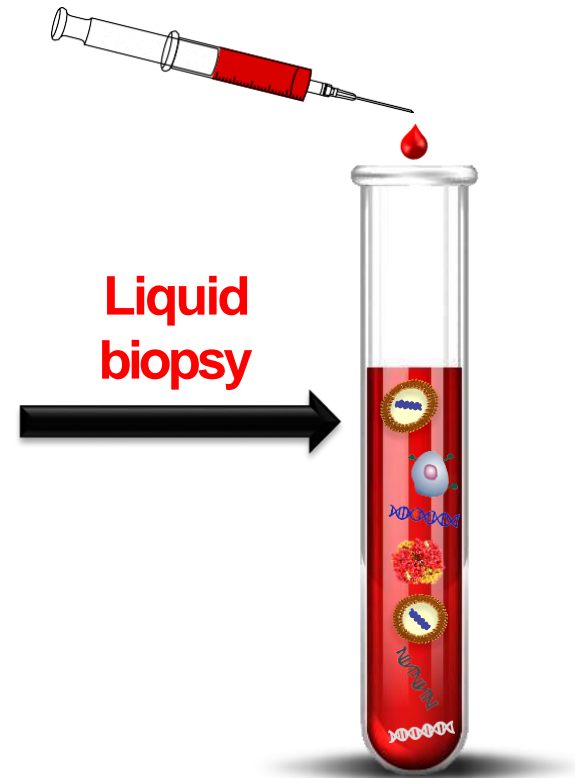
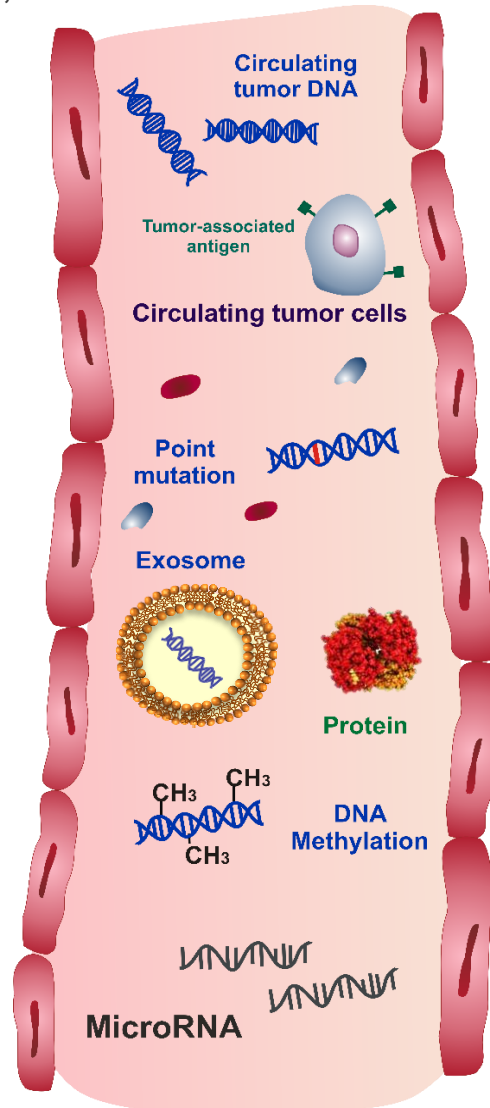
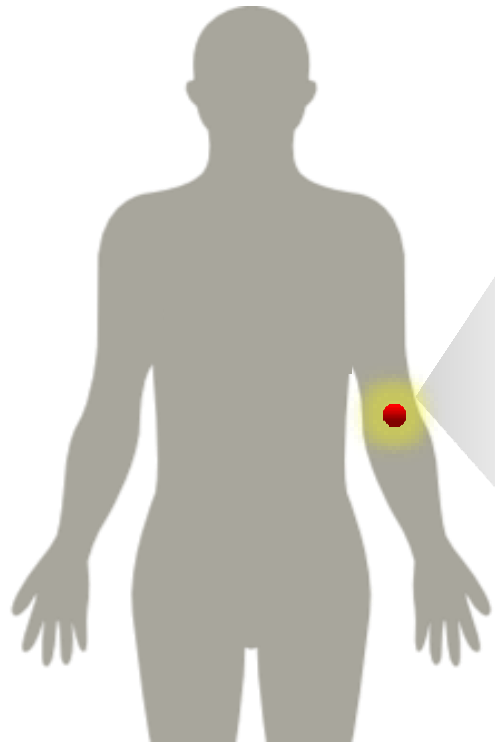
Tecniche innovative ed ultrasensibili PCR-free per la diagnosi precoce di acidi nucleici in biopsia liquida

Noemi Bellassai

Webinar, 28 Aprile 2021

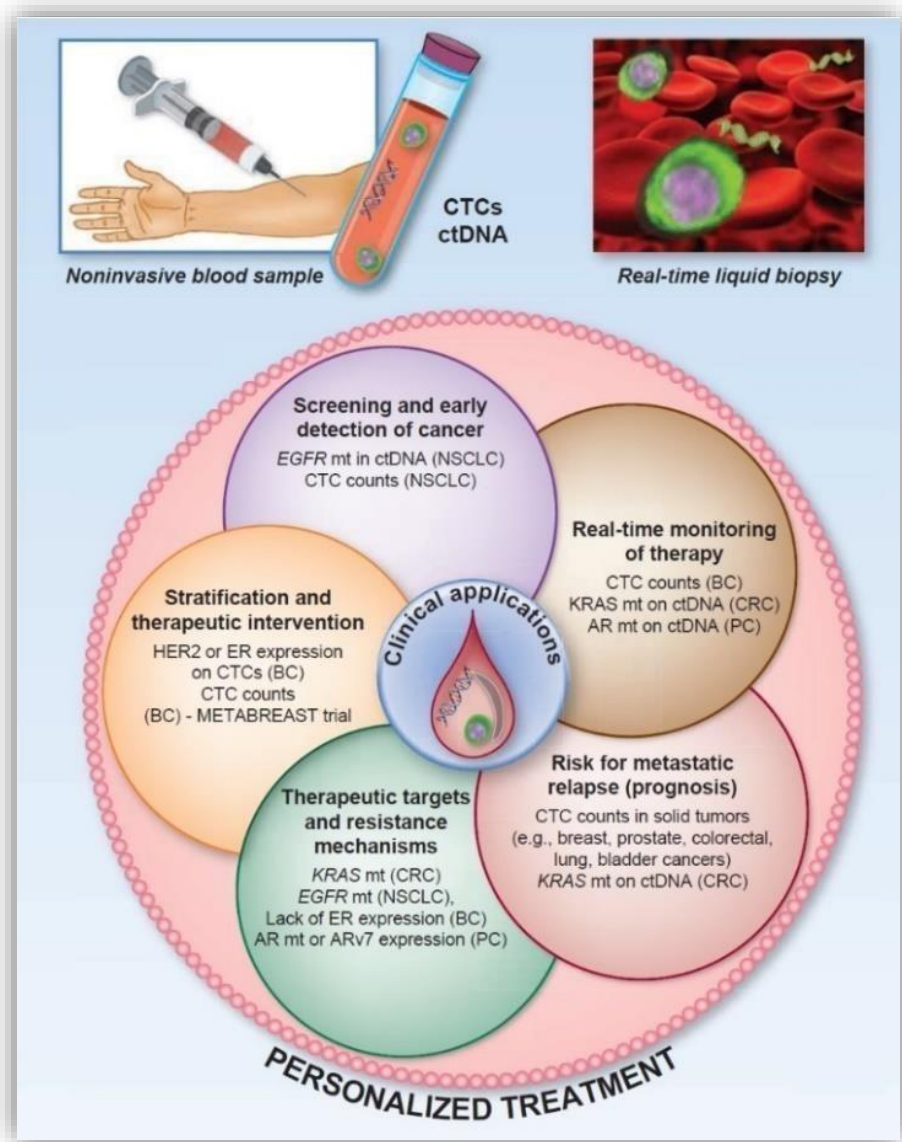
Liquid biopsy

Non-invasive test based on the detection of biomarkers related to specific disease circulating in body fluids (blood, plasma, serum, urine, saliva, synovial fluid etc.).

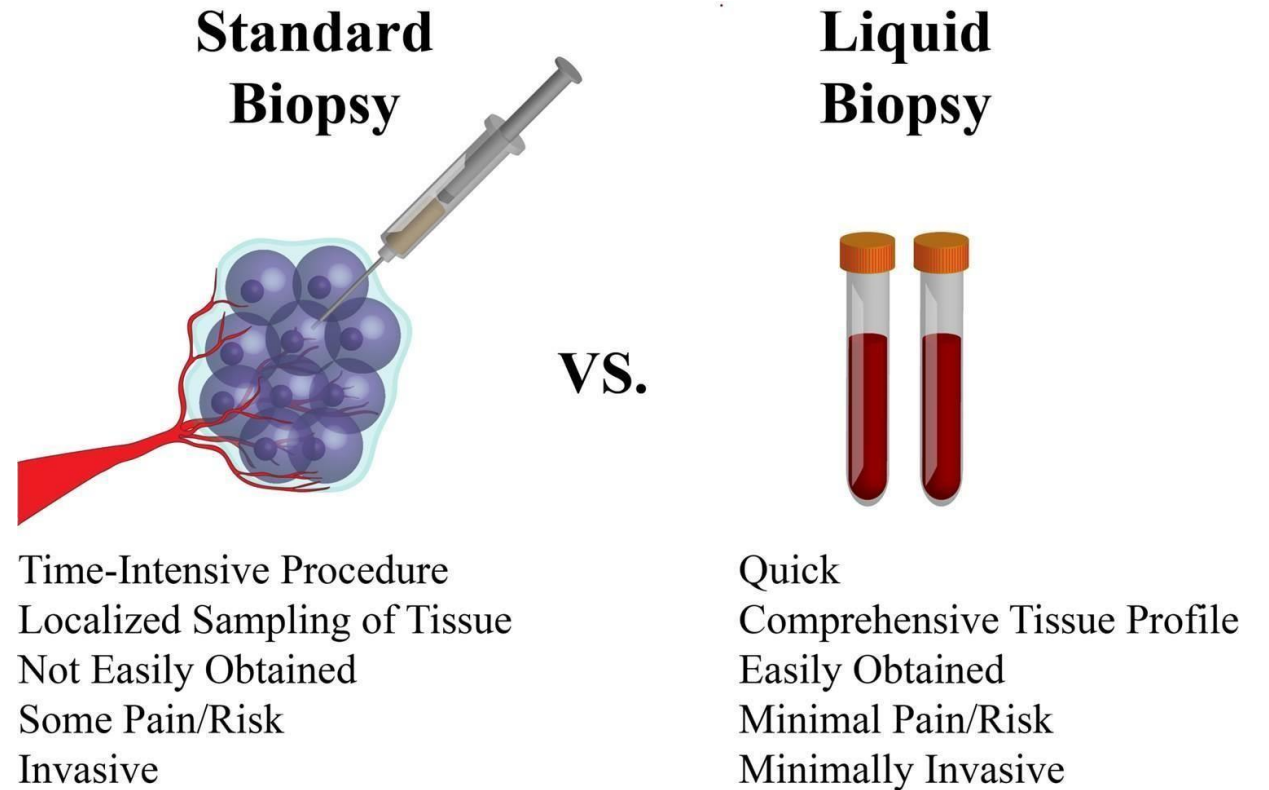


- ctDNA
- miRNA
- Protein
- CTCs

Liquid biopsy



Alix-Panabières et al., Cancer Discov. 2016;6(5), 479



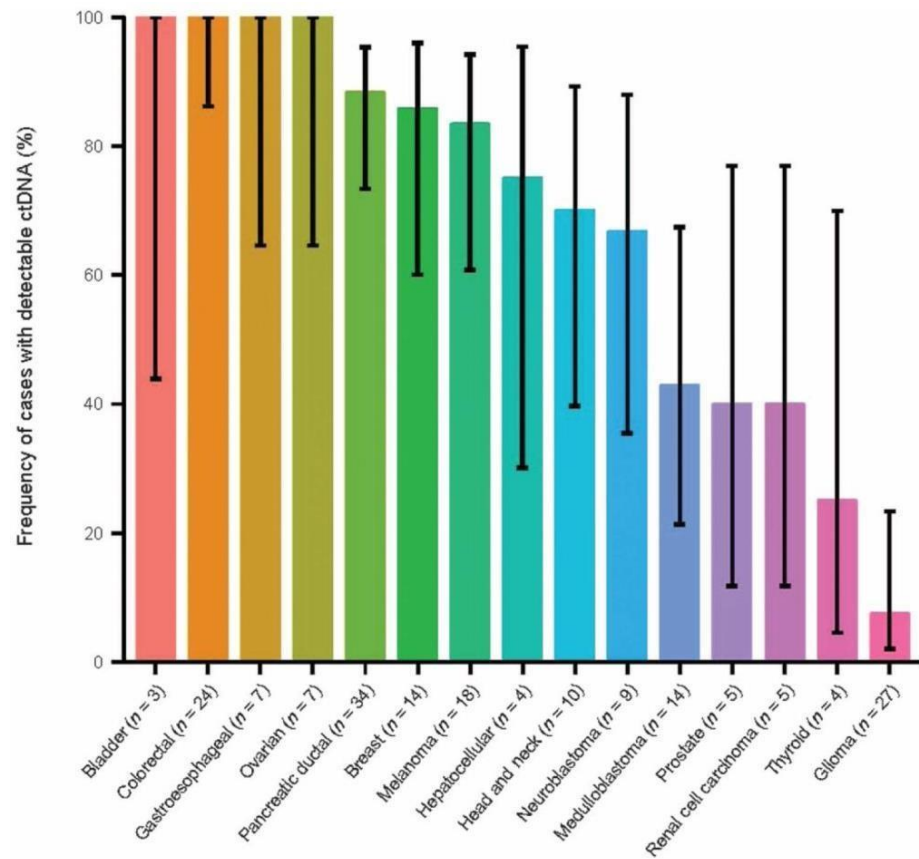
Lovly et al. 2016. Circulating Tumor DNA. My Cancer Genome (Updated February 8).

Sosa et al., Nat. Rev. Cancer. 2014; 14:611-622

Liquid biopsy for early diagnosis disease

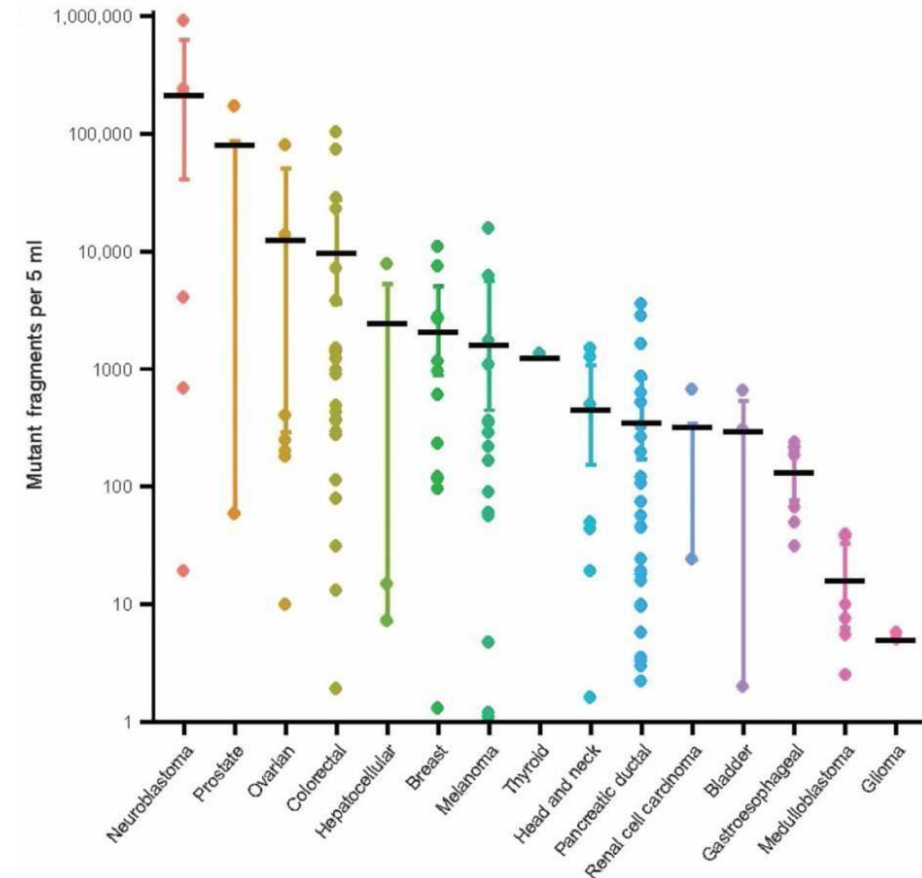
The opportunity

Circulating tumour DNA (ctDNA) is easy accessible and can be detected in most metastatic cancers

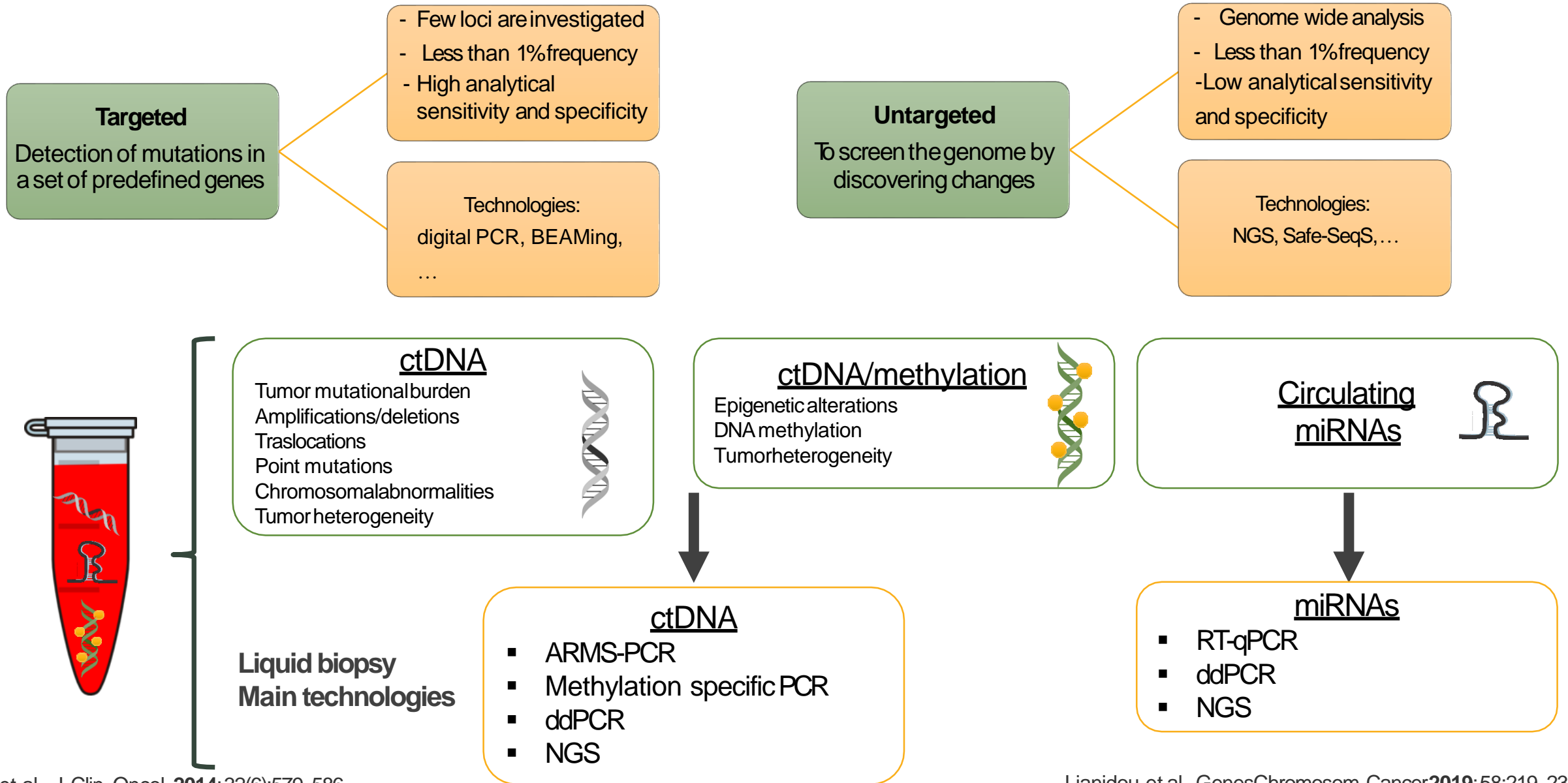


The challenge

ctDNA is often only present at low levels



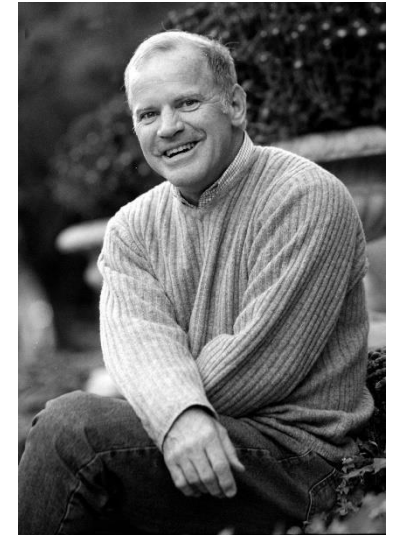
Detection of nucleic acid biomarkers



Target Amplification Methods

- **Polymerase chain reaction (PCR)**
 - **PCR using specific probes**
 - **RT PCR**
 - **Nested PCR-increases sensitivity, uses two sets of amplification primers, one internal to the other**
 - **Multiplex PCR-two or more sets of primers specific for different targets**
 - **Arbitrarily Primed PCR/Random Primer PCR**
- **Isothermal methods**

**Polymerase chain reaction
(PCR) Inventor**



**Kary Banks Mullis
(1944-2019)**

**Nobel Prize in Chemistry
1993**

Beyond PCR ... Isothermal amplification

Nucleic acids amplification operated at a constant temperature

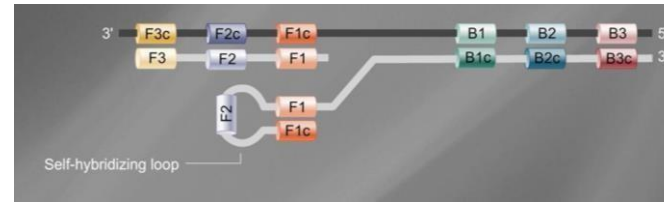
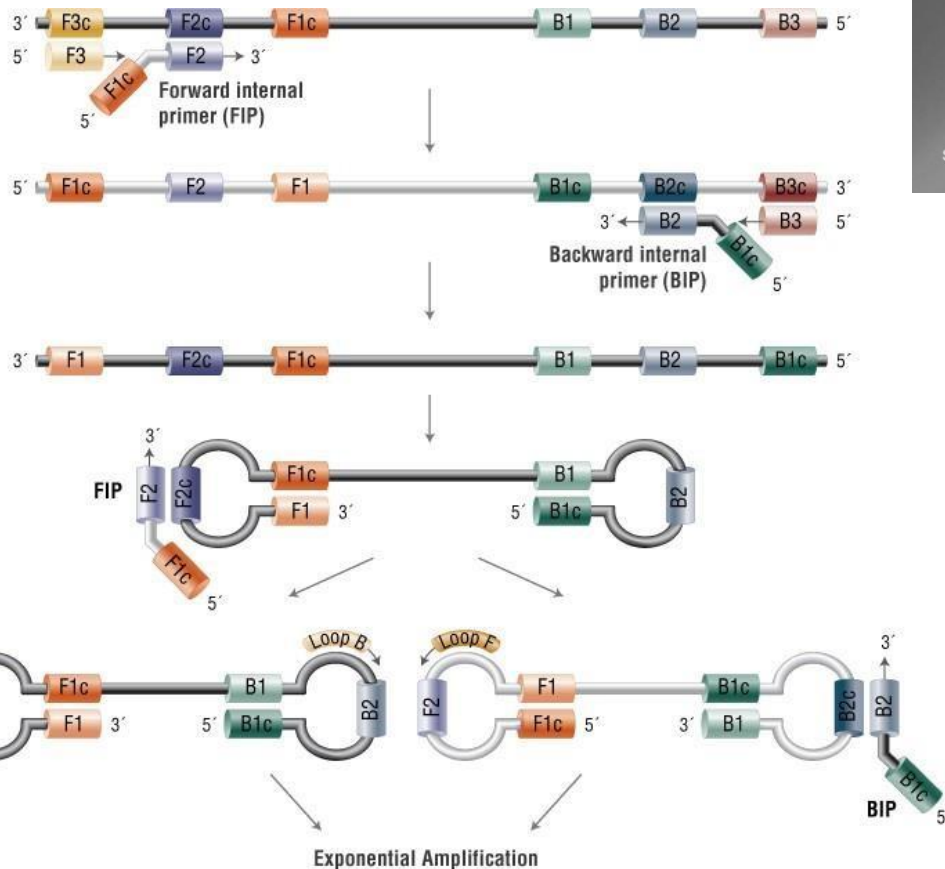
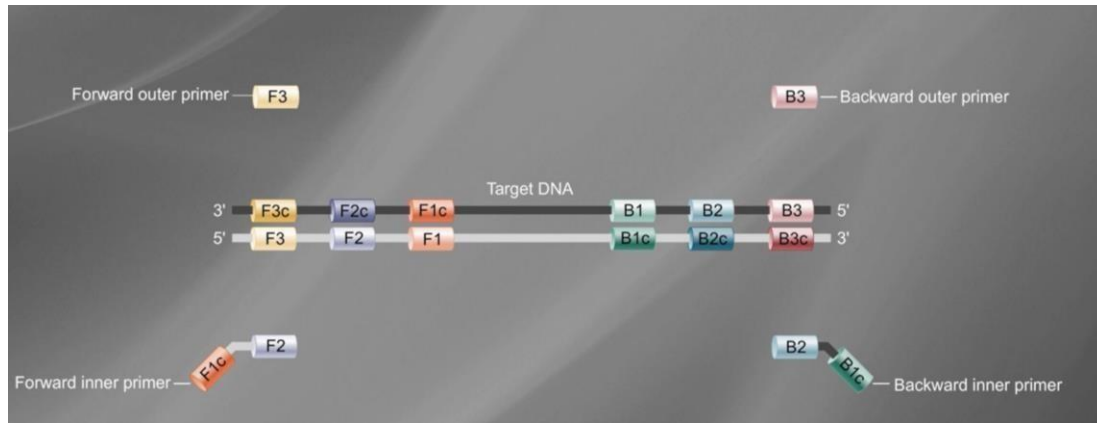
- Implementation in point-of-care devices is simplified
- Can be performed under simple conditions (e.g., water bath)
- Many isothermal amplification methods are available providing exponential or linear amplification
- Enzymatic and enzyme-free isothermal amplification methods are available

Method	Temp (°C)	Reaction time (min)	Amplification	Target	Primers	Main applications
LAMP	60-65	30-60	10^9	dsDNA hundred base- pair long	4-6	Bacteria, Viruses
RPA	25-42	5-20	10^9 - 10^{11}	dsDNA ssDNA RNA	2	Pathogens, Viruses
NASBA	~41	90-120	10^9	RNA	2	Bacteria, Pathogens
RCA	30-65	60-120	10^3 linear 10^9 expon.	ssDNA	1	Plasmid, Viruses
NEEA	54-58	15-30	10^9	dsDNA RNA	2	Viruses, RNA DNA
HDA	37-60	60-120	10^6	dsDNA	2	Biomarkers, Viruses

Loop mediated isothermal amplification (LAMP)

- Amplification takes place at a single temperature (65°C)
(No need of thermal cycler)
- Uses polymerase with high strand displacement activity
(*Bacillus stearothermophilus* Bst DNA Polymerase instead of *Taq*Poly)
- Amplification efficiency is high (up to 10^9)
- Can be also used for RNA templates by addition of reverse transcriptase

Loop mediated isothermal amplification (LAMP)



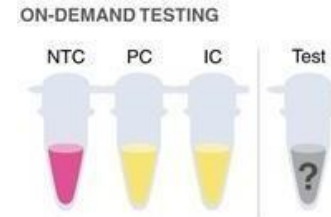
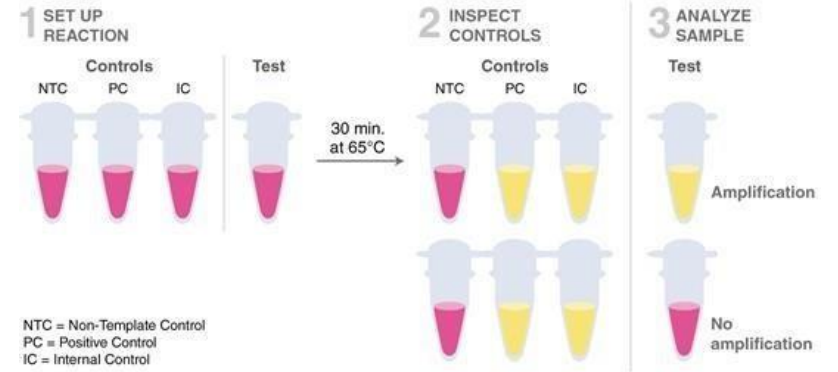
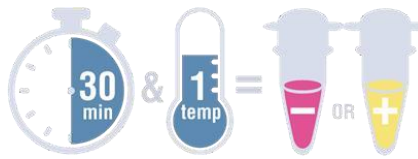
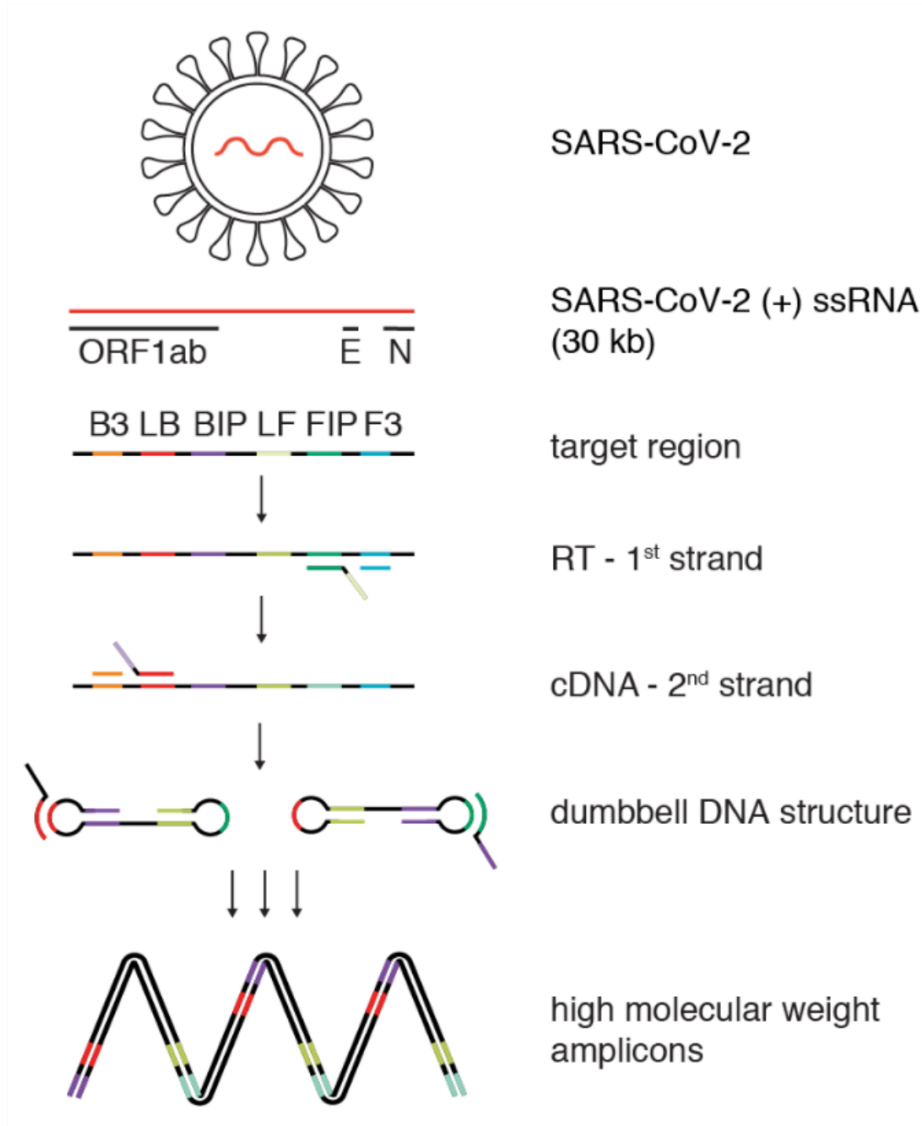
Loop-mediated isothermal amplification (LAMP) uses 4-6 primers recognizing 6-8 distinct regions of target DNA.

A strand-displacing DNA polymerase initiates synthesis and 2 of the primers form loop structures to facilitate subsequent rounds of amplification.

<https://www.youtube.com/watch?v=L5zi2P4lggw>

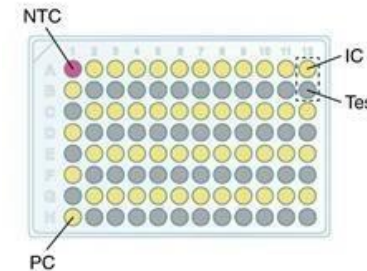
LAMP-Based SARS-CoV-2 Testing Methods

SARS-CoV-2 Rapid Colorimetric LAMP Assay Kit



Reactions/sample	4
Reactions/kit	96
Samples/kit	24

HIGH-THROUGHPUT TESTING



Reactions/sample	2	+1 NTC per plate +1 PC per plate
Reactions/kit	96	
Samples/kit	47	

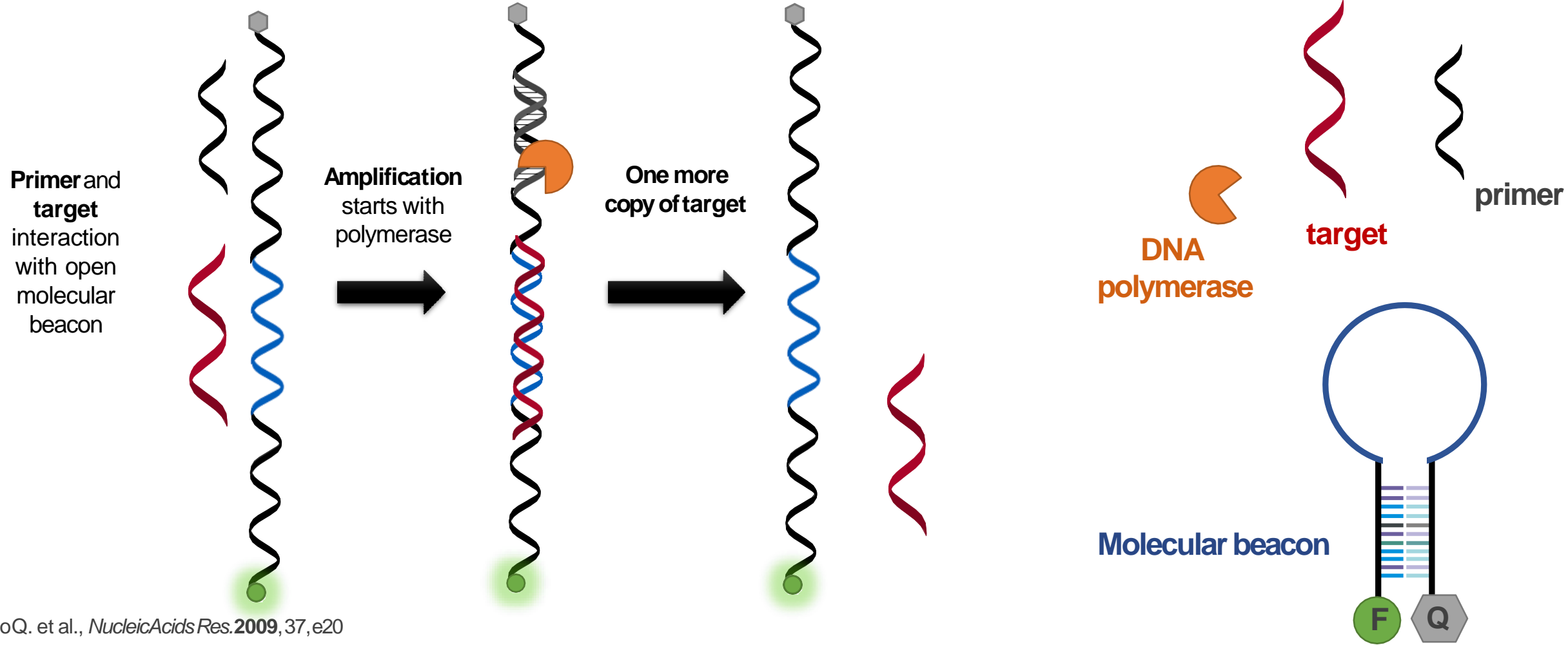
NTC = Non-Template Control PC = Positive Control IC = Internal Control

Molecular beacon-assisted isothermal circular strand displacement polymerization (ICSDP)

Isothermal amplification

Isothermal circular strand displacement polymerization. Displaced target available for a new cycle.

Linear amplification

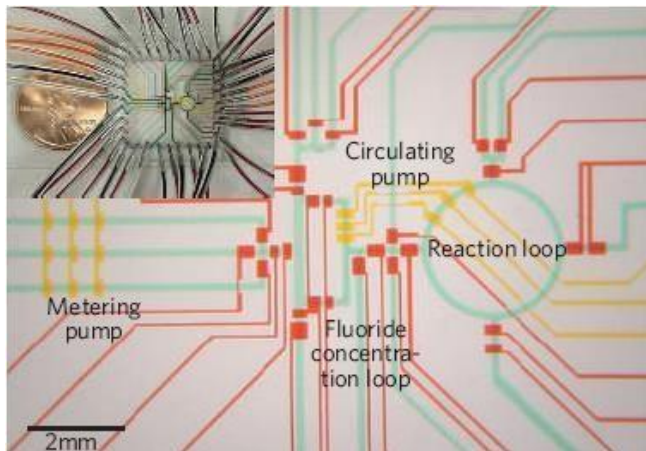
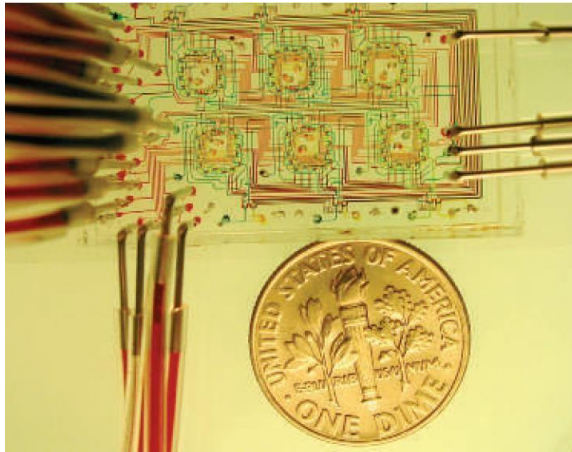


GuoQ. et al., *NucleicAcids Res.* **2009**, 37, e20

Giuffrida M.C. et al., *Anal. Bioanal. Chem.* **2015**, 407, 6, 1533-1543

MICROFLUIDICS

It is the science and technology of systems that process or manipulate small (10^{-9} to 10^{-18} litres) amounts of fluids, using channels with dimensions of tens to hundreds of micrometres.



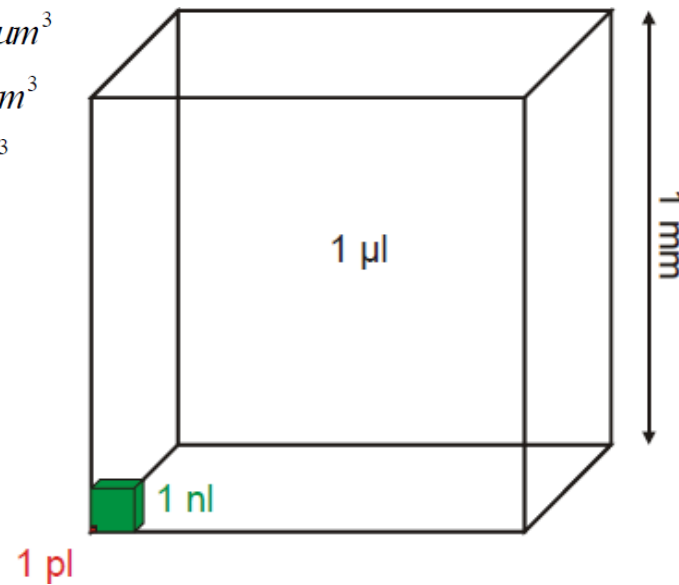
$$1l = 1dm^3$$

$$1\mu l = 1mm^3$$

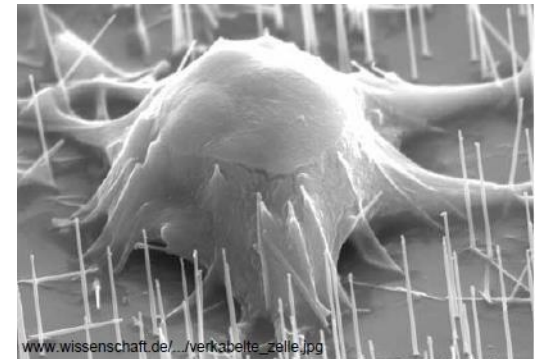
$$1nl = 100\mu m^3$$

$$1pl = 10\mu m^3$$

$$1fl = 1\mu m^3$$



Typical size of a cell 1-30 μm



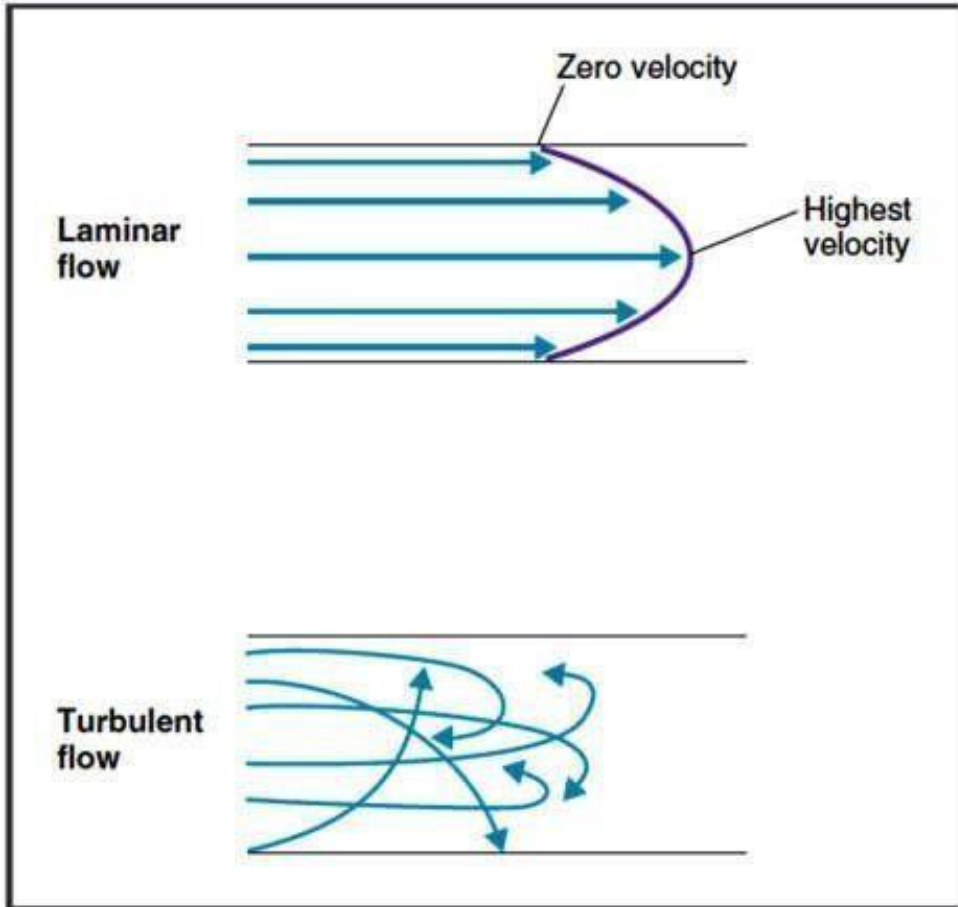
Drug inhaler, Droplet diameter ~ 5 μm



MICROFLUIDICS

Model for the description of the motion of fluids

Newtonian fluid \rightarrow laminar flow



- Non-dimensional Navier-Stokes equation

$$\frac{\rho UL}{\mu} \left(\frac{\partial \mathbf{u}'}{\partial t'} + \mathbf{u}' \nabla \mathbf{u}' \right) = -\nabla p' + \eta \nabla^2 \mathbf{u}' + \mathbf{f}'$$

Reynolds number

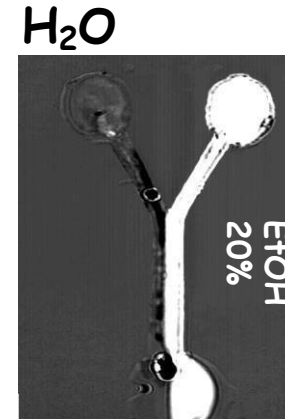
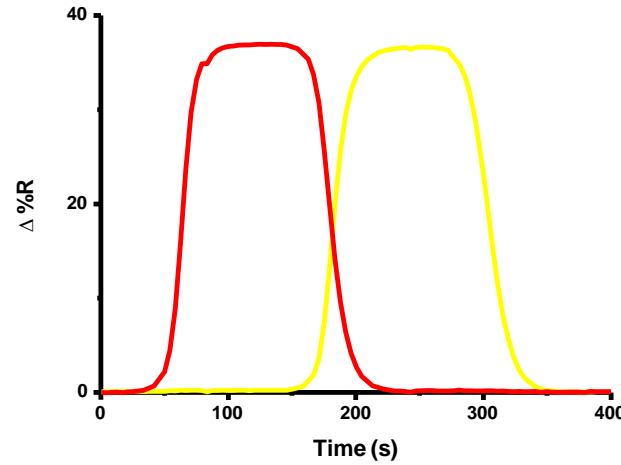
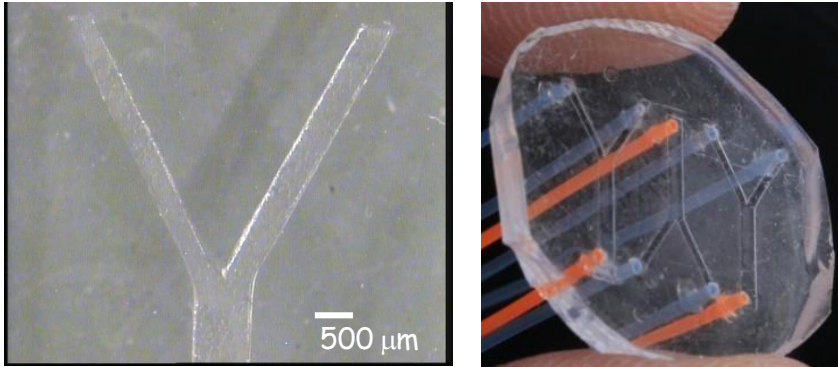
$$Re = \frac{\rho UL}{\mu} \approx \frac{\text{Inertial forces}}{\text{Viscous forces}}$$

$Re > 2000$
Turbulent

$Re < 2000$
Laminar

MICROFLUIDICS: devices fabrication

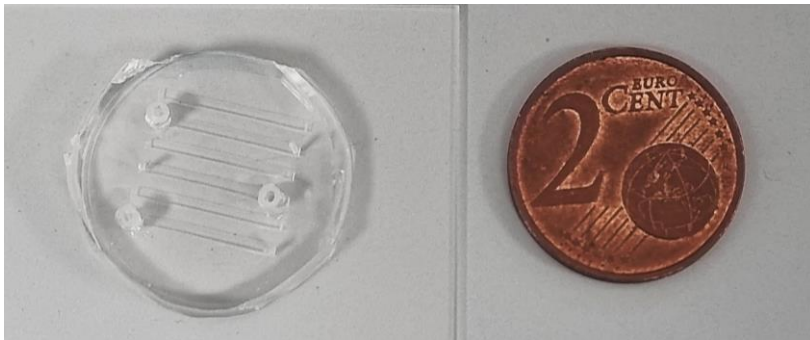
Fabrication of microfluidic device by PDMS replica molding



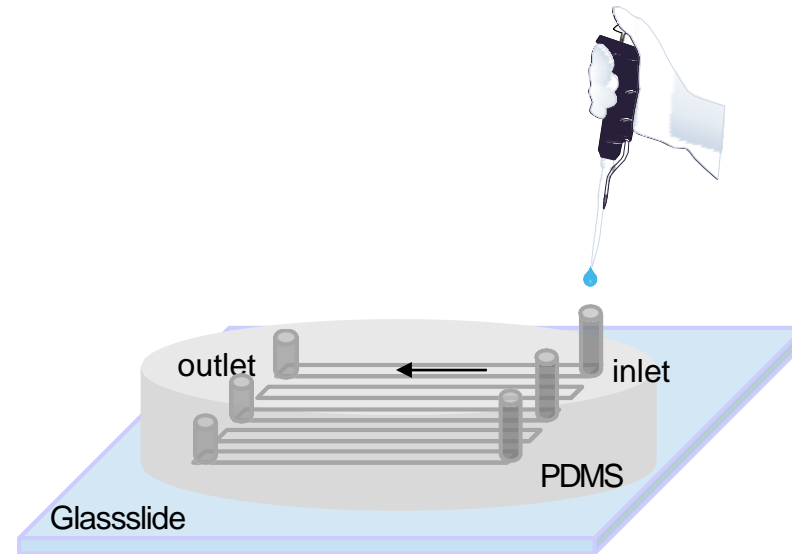
$Re \approx 100$

Laminar flow

Immiscible liquids



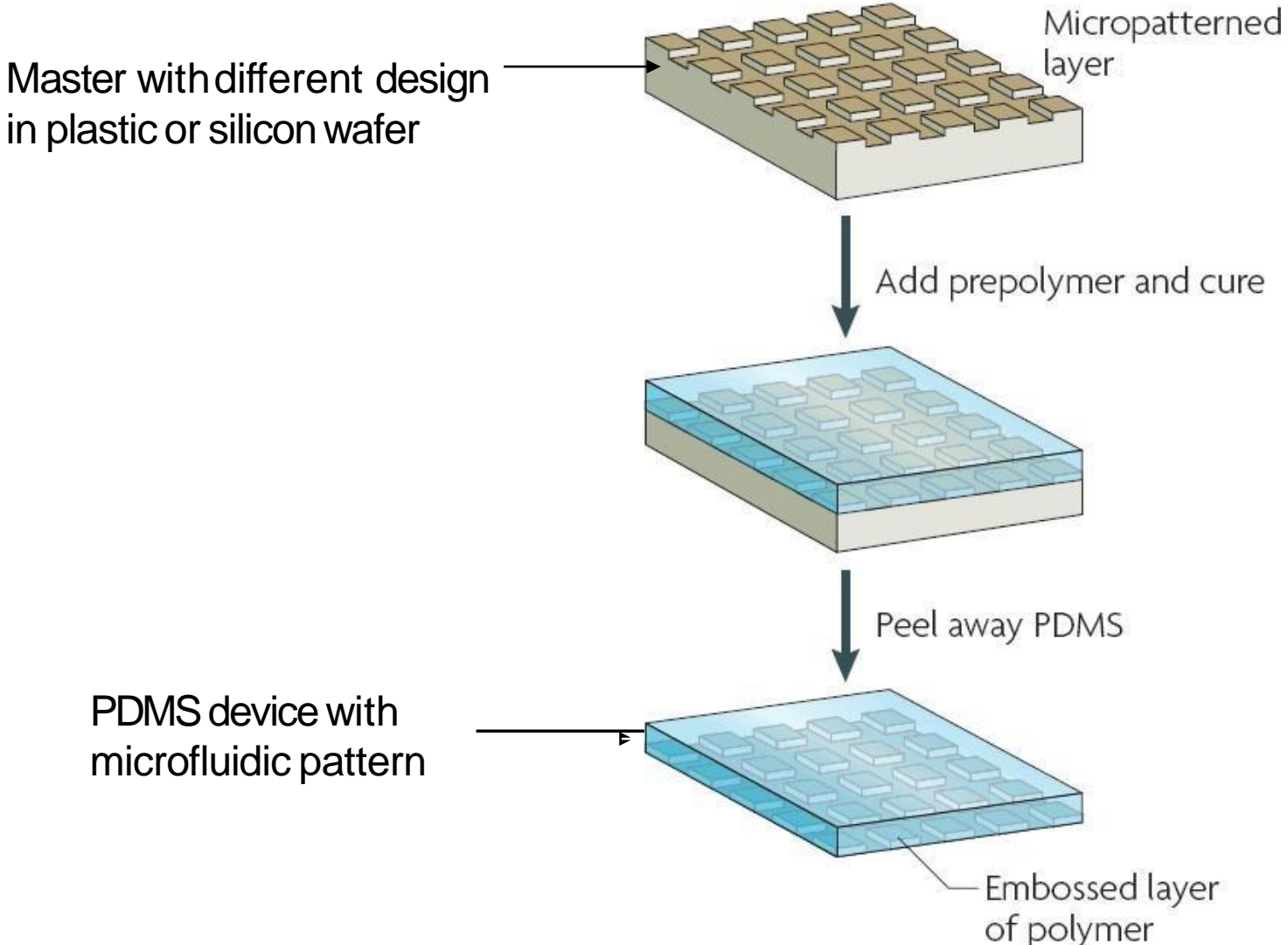
microfluidic channels (14×0.4×0.8mm)



< 1 μL of sample volume

Parallel microchannels
for multiple detection

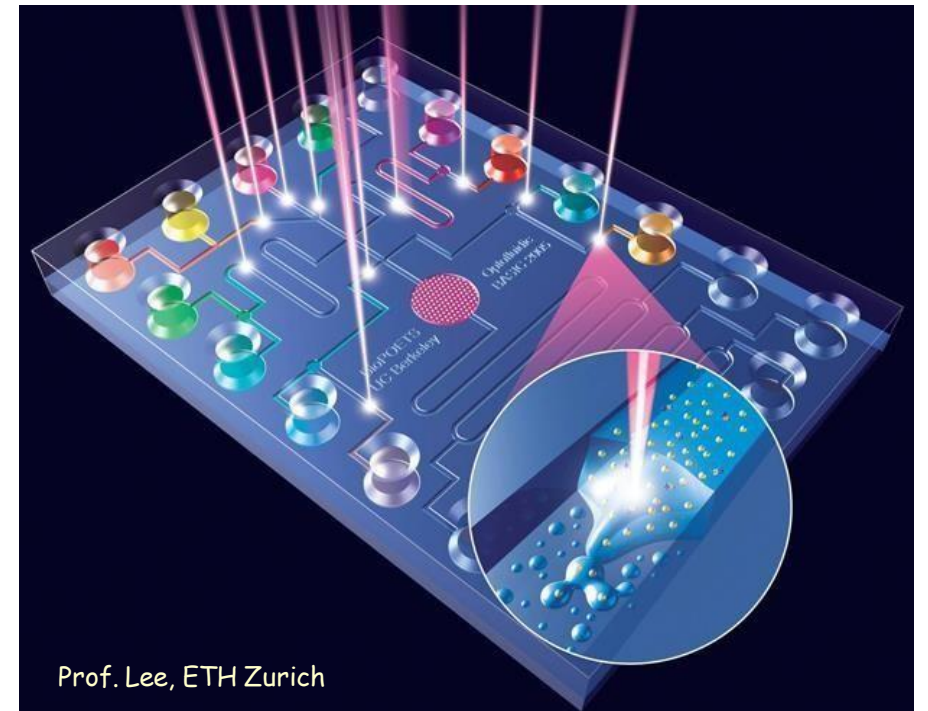
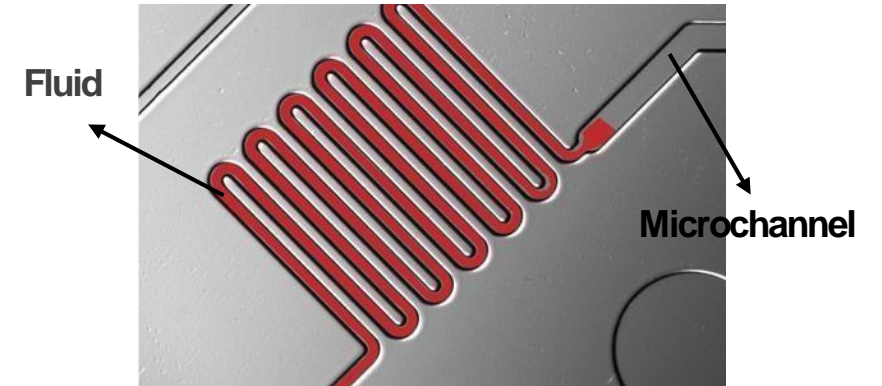
MICROFLUIDICS: devices fabrication Fabrication of microfluidic device by PDMS (polydimethylsiloxane) replica molding



Weibelet al. *Nature Reviews: Microbiology* 2007, 5, 209.

MICROFLUIDICS: Why?

- **Small sample volume**
- **Miniaturization**
- **Reduction of analysis time**
- **Parallel devices and faster processes**
- **High-throughput**
- **Integration and portable devices**
(lab-on-a-chip, micro Total Analysis Systems μ TAS)



Prof. Lee, ETH Zurich

microRNA (miRNA)

- **Single-stranded, non-coding RNA molecules**
- **Key-role in protein expression**
- **mRNA silencing**
- **Remarkable stability when released into biofluids**



Challenges for miRNA detection

- Analytes are present at low concentrations

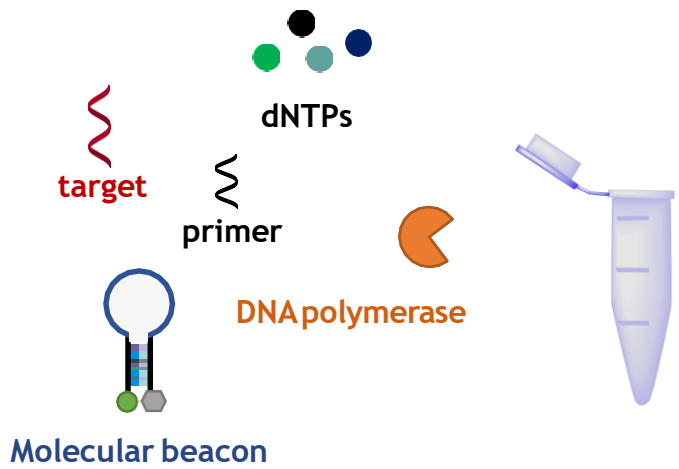
Biomarker levels: fg mL⁻¹ - ng mL⁻¹

- Short length sequence

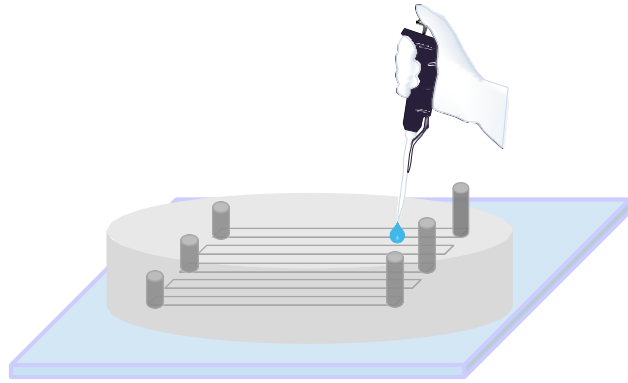
Length: 19-23 nt

- High sequence homology

Microfluidic lab-on-a-chip platform for liquidbiopsy: microRNA

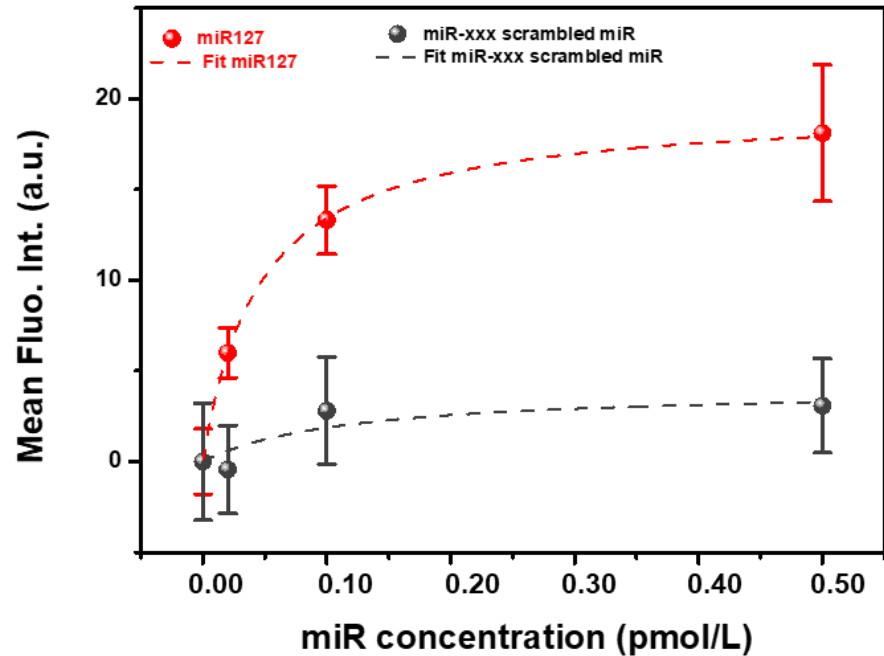
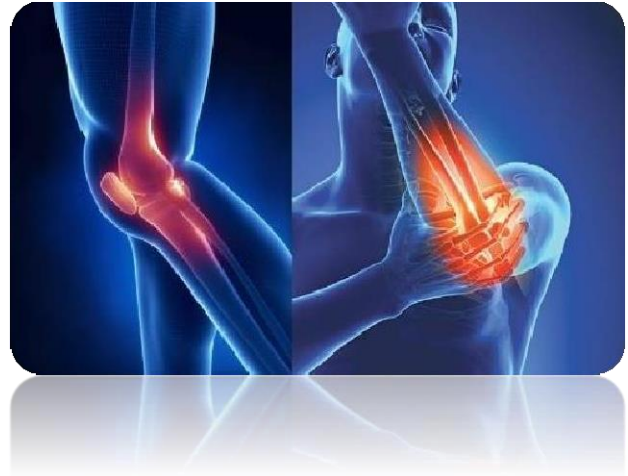


ICSDP
amplification
30° C 2 hr
constant
temperature



Fluorescence
detection

microRNA-127
biomarker for chronic joint disease

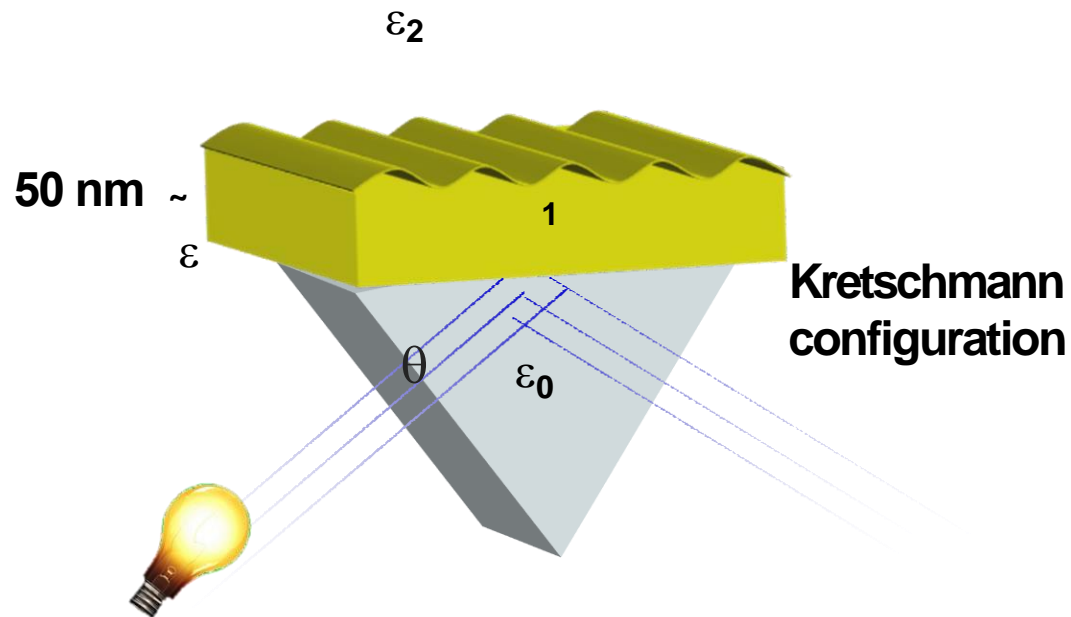


- Low sample volume
- No time consuming
- High selectivity in buffer
- Discrimination in synovial fluid
- Low detection

Optical biosensors: Surface Plasmon Resonance

Electromagnetic radiation in resonance with surface plasmon oscillation.

Surface plasmon polaritons : quasi-particles resulting from the coupling of surface plasmons and photons



Radiation wave vector

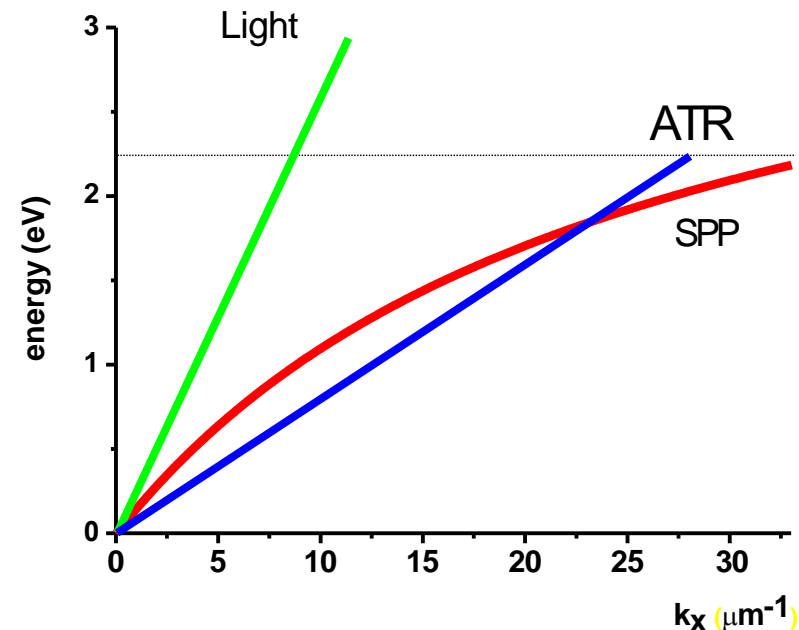
$$k_{light} = \frac{m}{c} \sqrt{\epsilon_0} \sin \theta$$

Snell's Law

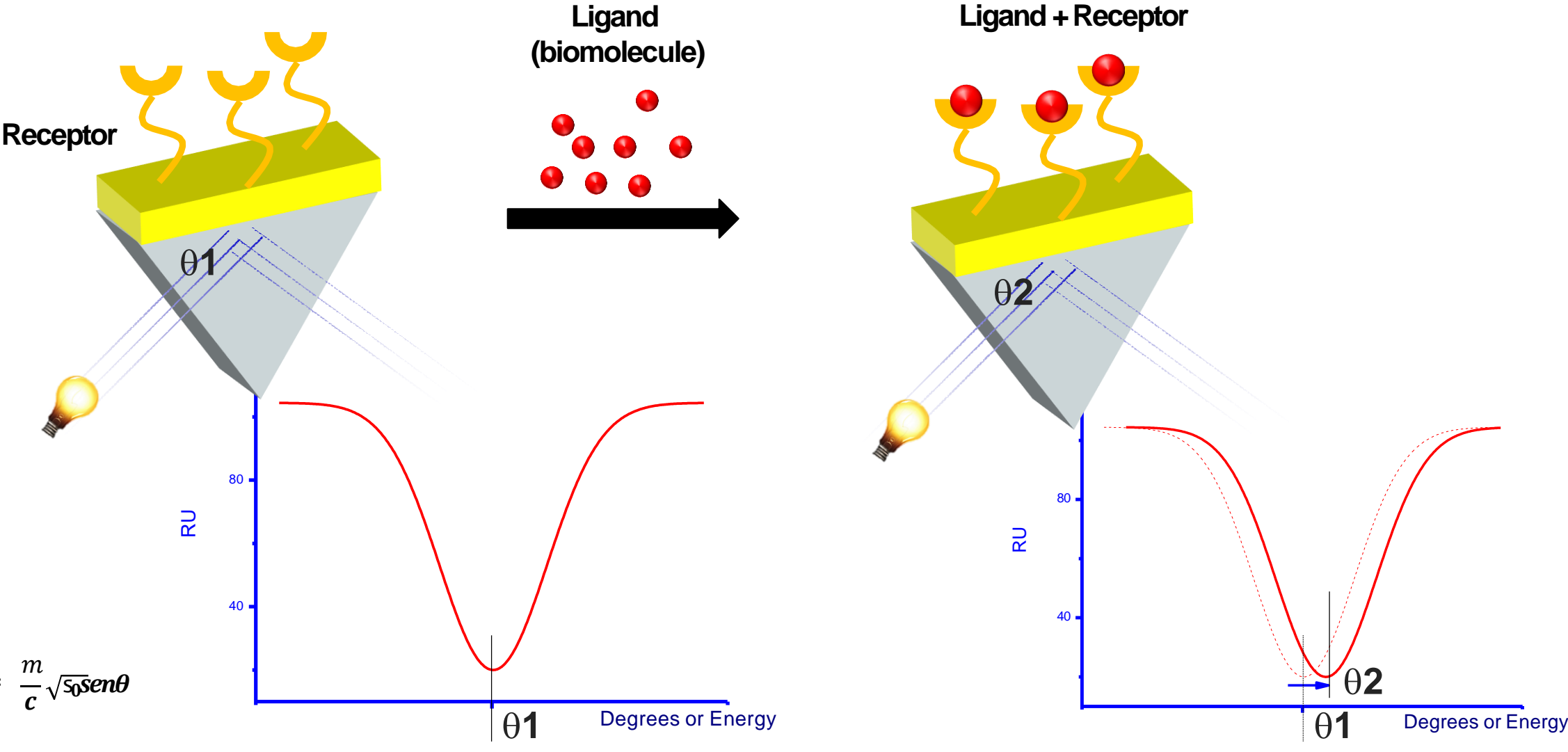
$$\sin \theta = \frac{\epsilon_1}{\epsilon_0}$$

Plasmon wave vector = radiation wave vector

$$K_{SPP} = \frac{\omega}{c} \sqrt{\frac{\epsilon'_1 \epsilon_2}{\epsilon'_1 + \epsilon_2}} = \frac{\omega}{c} \sqrt{\epsilon_0} \sin \theta = K_{Light}$$



Optical biosensors: Surface Plasmon Resonance

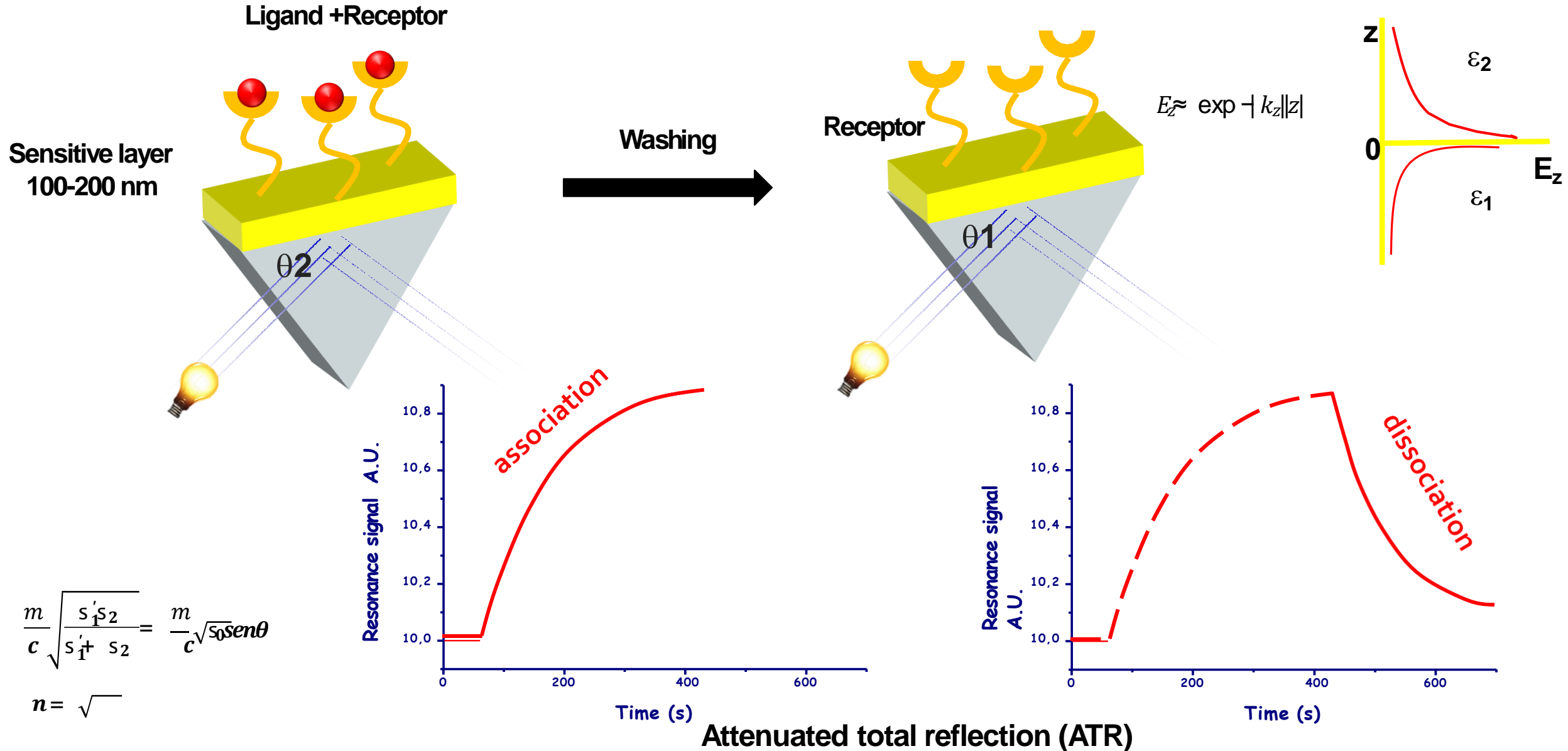


$$\frac{m}{c} \sqrt{\frac{s_1' s_2}{s_1 s_2}} = \frac{m}{c} \sqrt{s_0 \sin \theta}$$

$$n = \sqrt{\quad}$$

Attenuated total reflection (ATR)

Optical biosensors: Surface Plasmon Resonance



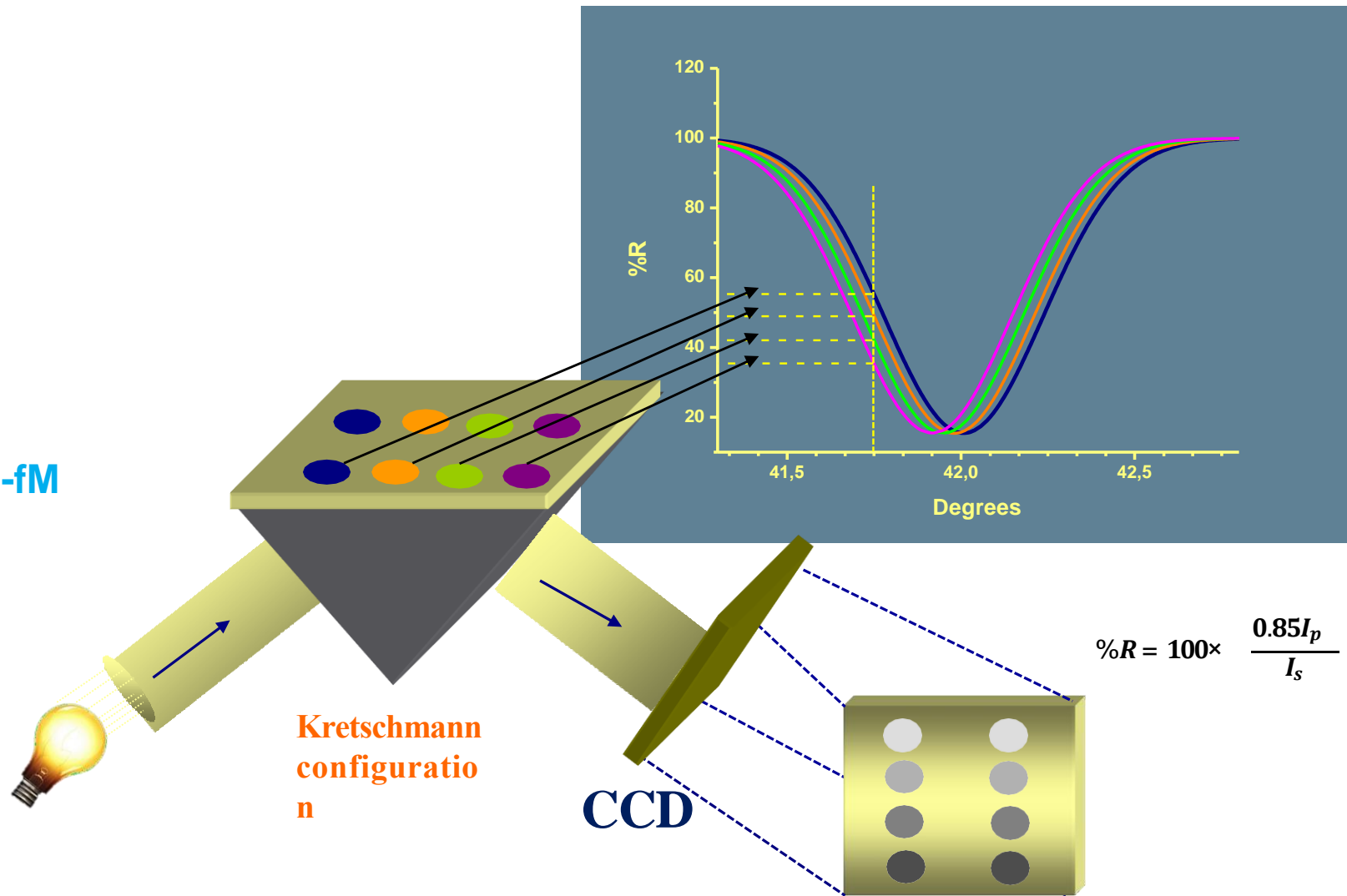
$$\frac{m}{c} \sqrt{\frac{s_1' s_2}{s_1' + s_2}} = \frac{m}{c} \sqrt{s_0} \sin \theta$$

$$n = \sqrt{\quad}$$

Surface Plasmon Resonance Imaging (SPRI)

- Real-time analysis
- Label-free
- High sensitivity
- Multi-analyte monitoring

Sensitivity can be improved up to nM-fM
PCR-free method!



Rothenhäusler et al. Surface-plasmon microscopy. **1988**, Nature 332, 615–617
D'Agata et al. Anal Bioanal Chem. **2013**; 405(2-3):573-84.

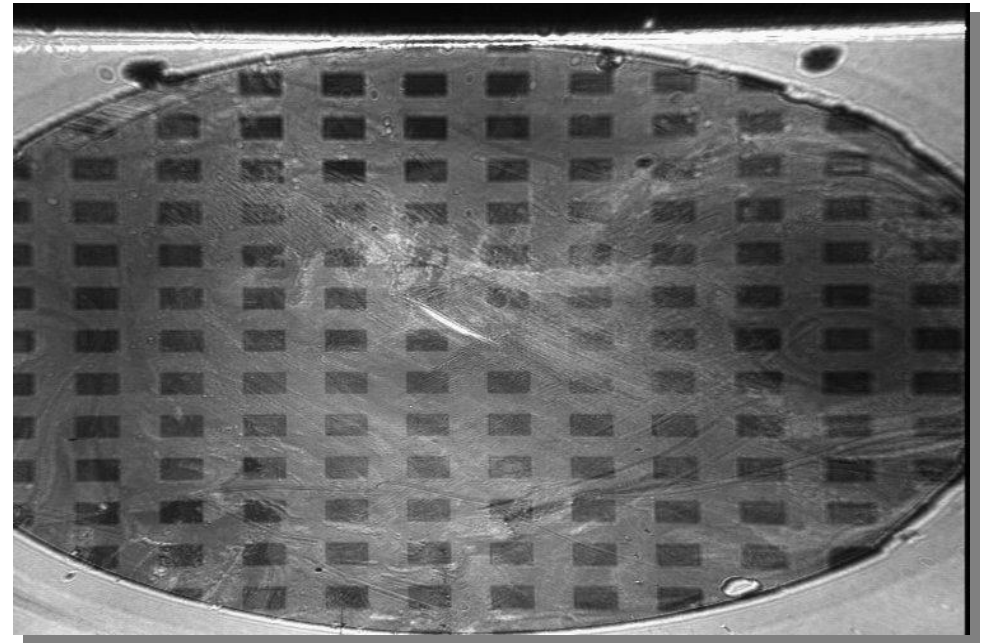
Surface Plasmon Resonance Imaging (SPRI)

The lateral resolution of a SPR image is limited by the surface plasmon decay distance L_x that is the distance on the surface by which the intensity of the field associated to plasmons decreases by a $1/e$ factor.

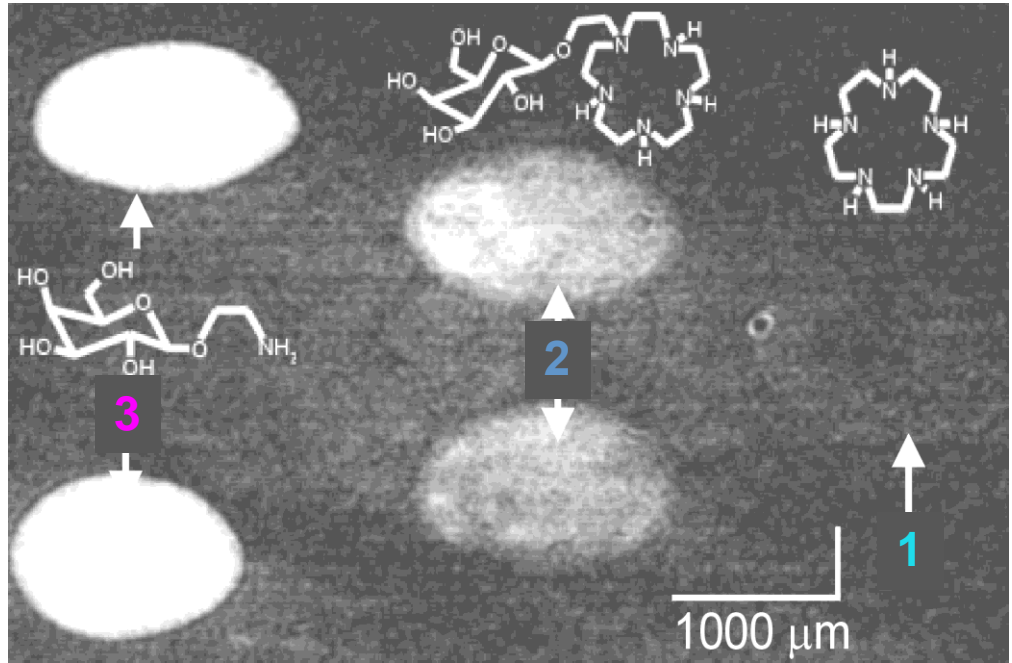
$$L_x = \frac{1}{2k''_x}$$

k''_x is the imaginary part of the x component of the wave-vector

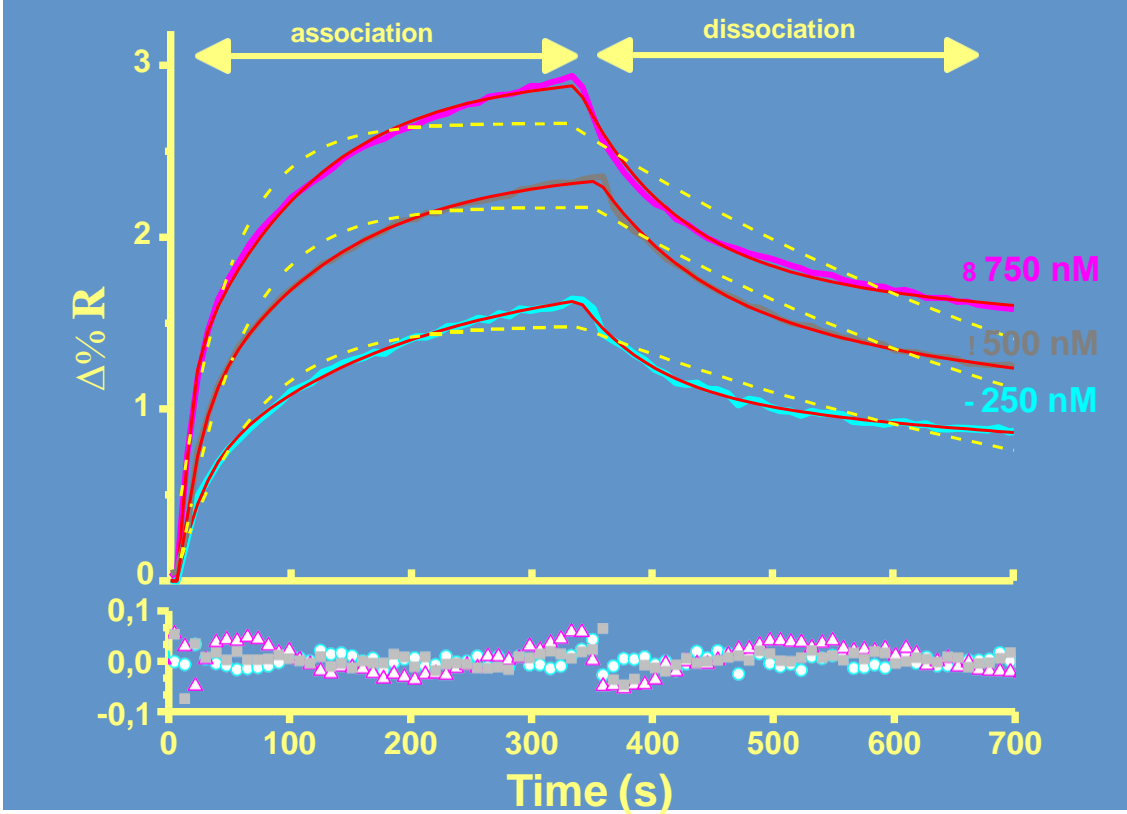
For gold: $L_x=0.1 \mu\text{m}$ at $\lambda=488 \text{ nm}$, $L_x=10 \mu\text{m}$ at $\lambda=647 \text{ nm}$



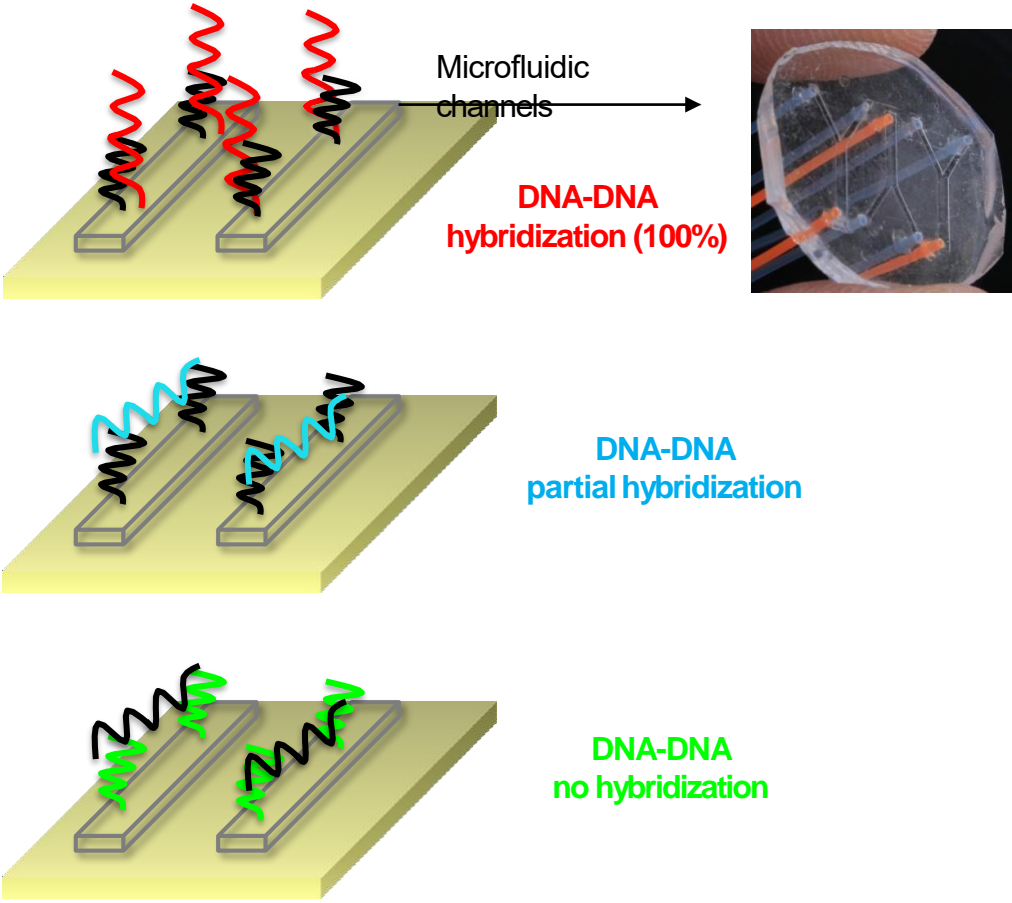
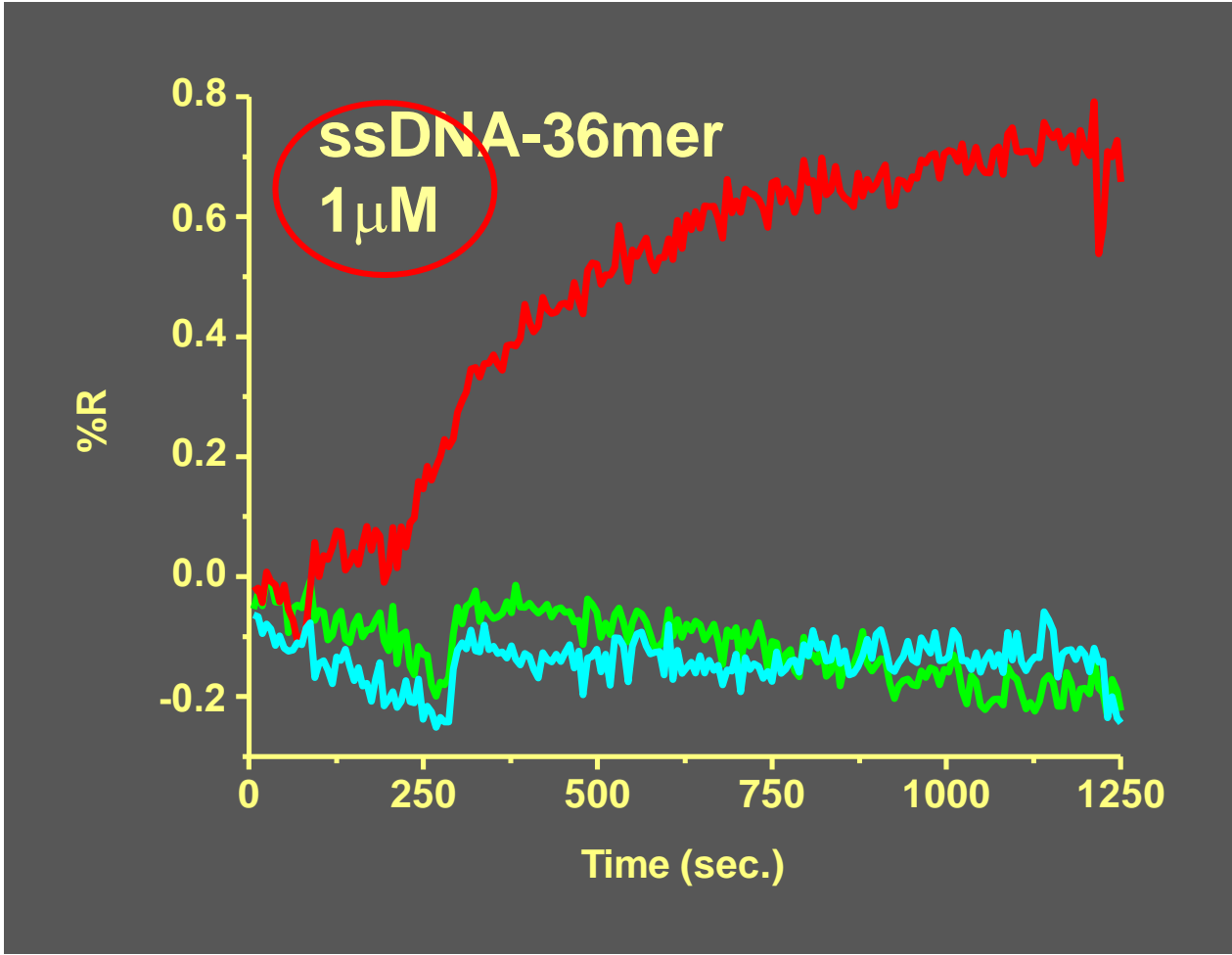
Surface Plasmon Resonance Imaging (SPRI)



Example of SPRI image

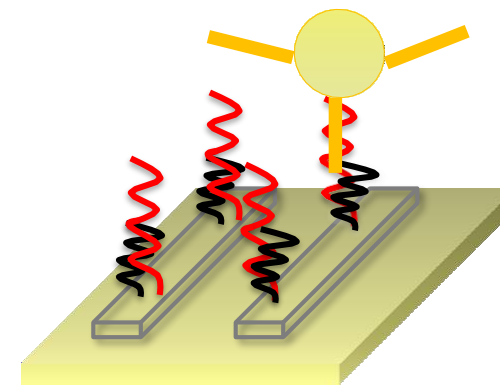
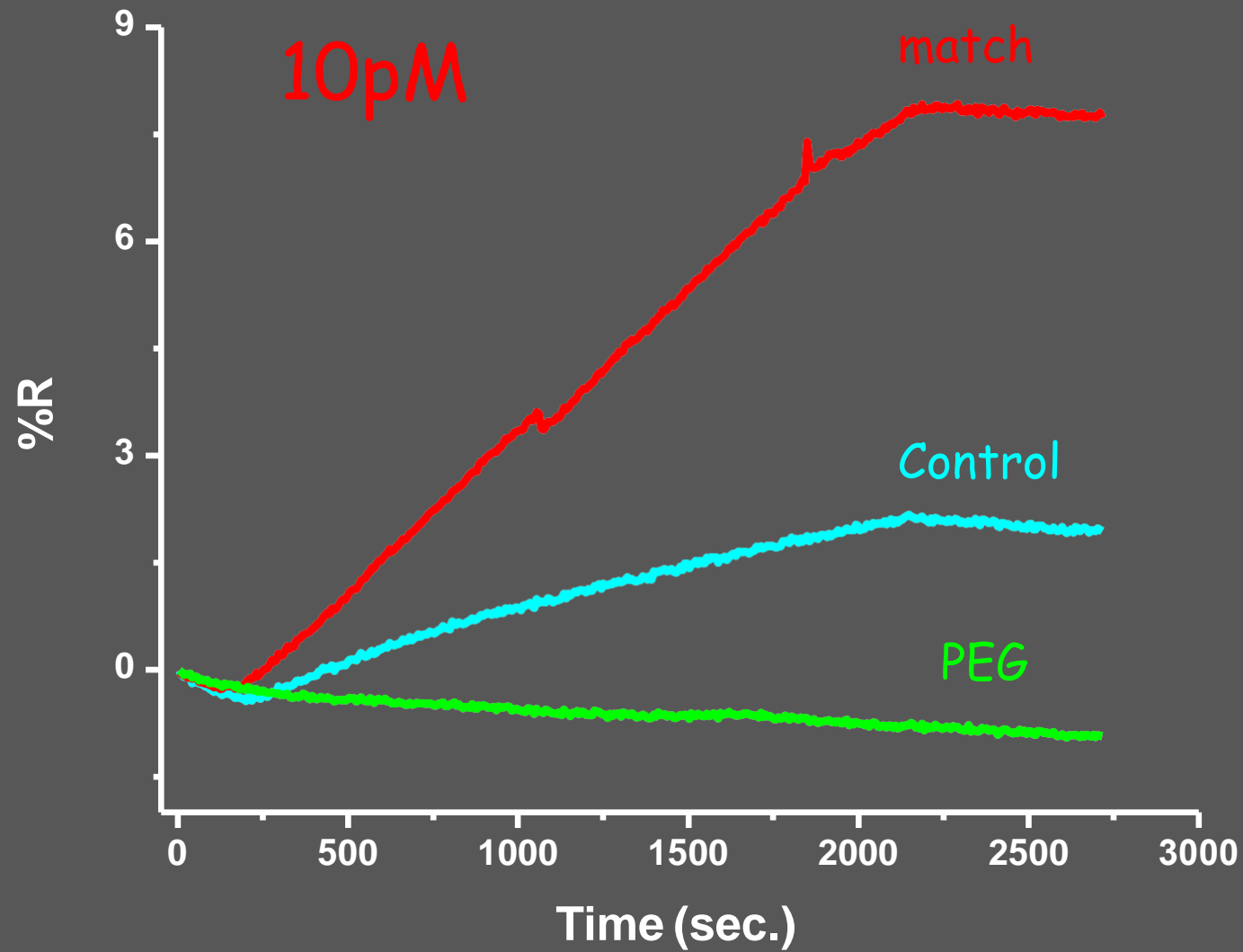


Microfluidic lab-on-a-chip plasmonic platform: detection of DNA

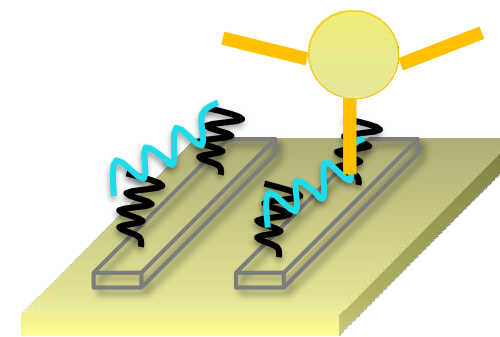


5'-LL-AAACCCTTAATCCCA-3' PROBE

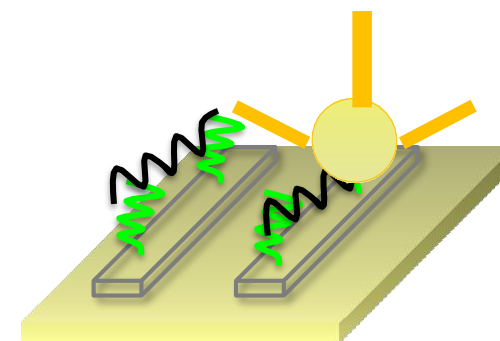
3'-TTTGGGAATTAGGGTTTTTTTTTTTCGTCGAATAGCA-5'
ssDNA-36mer-match



DNA-DNA
hybridization (100%)

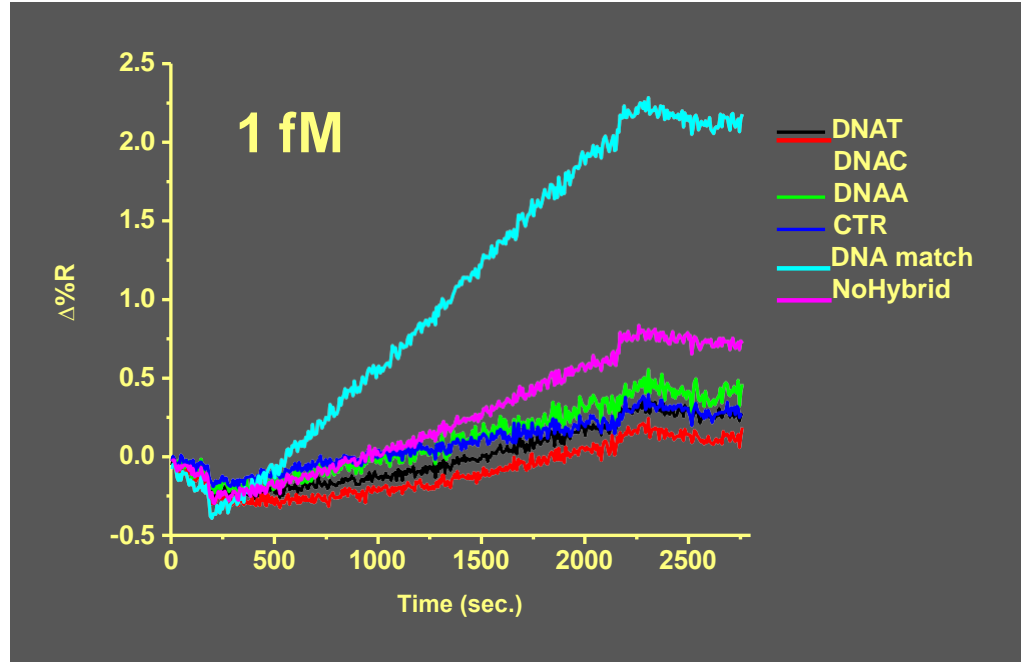
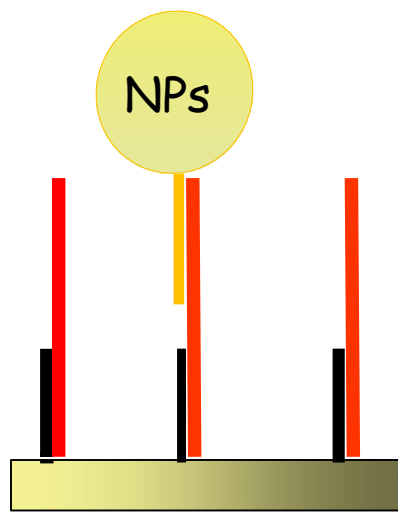
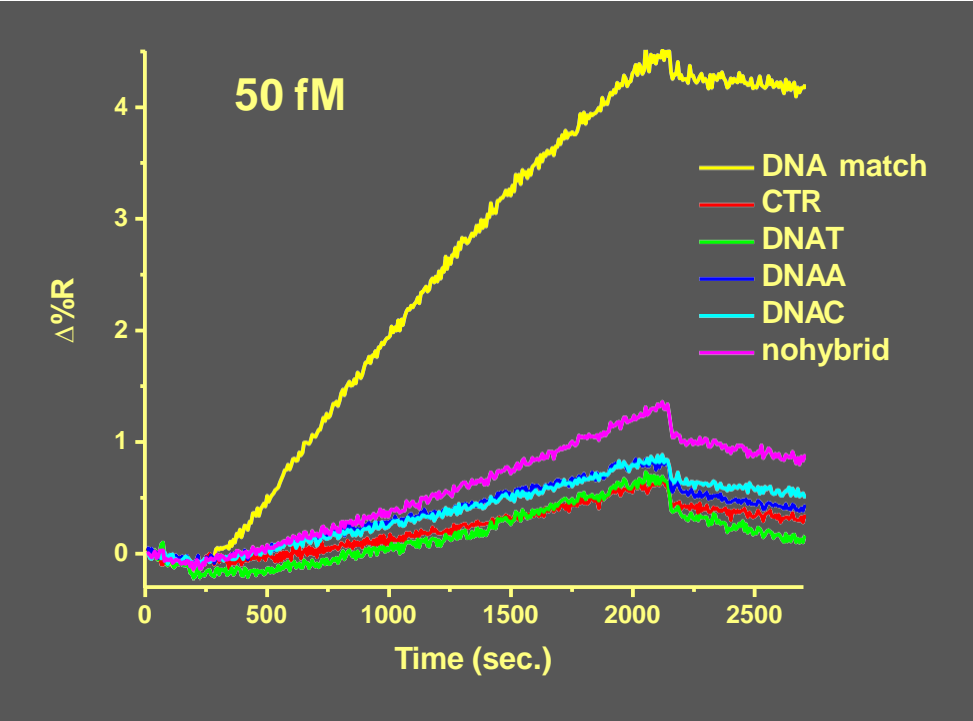


DNA-DNA
partial hybridization



DNA-DNA
no hybridization

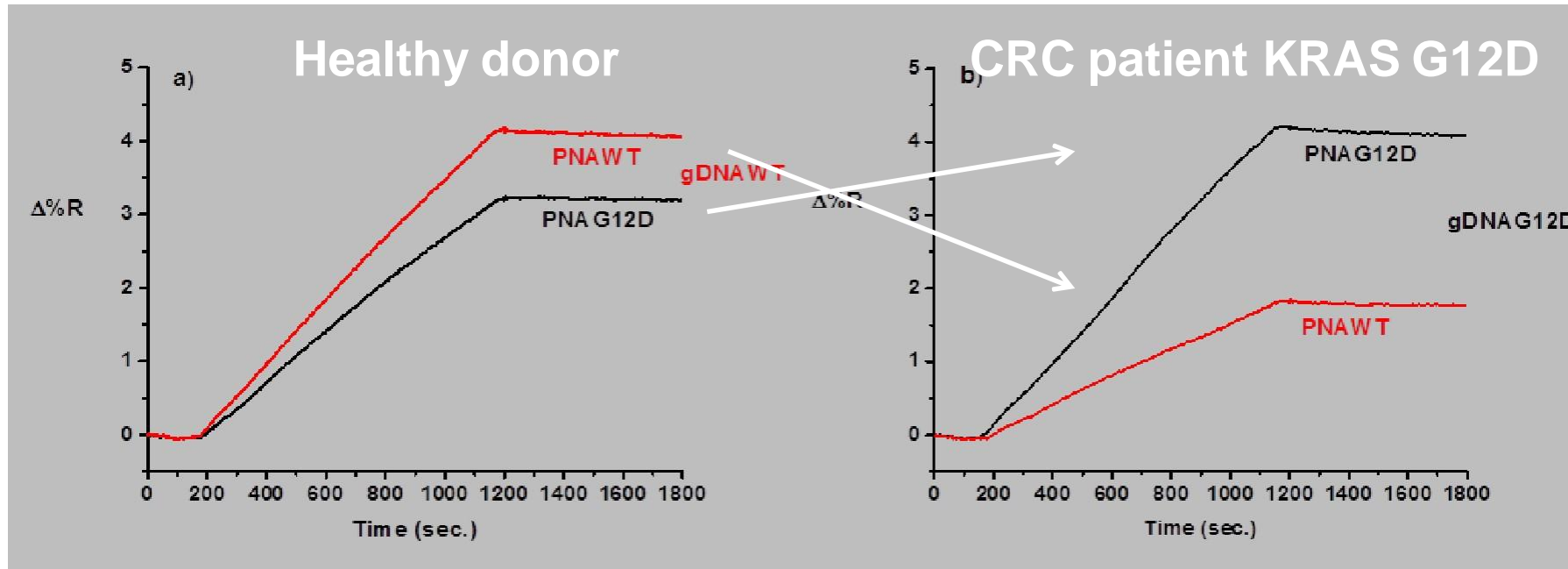
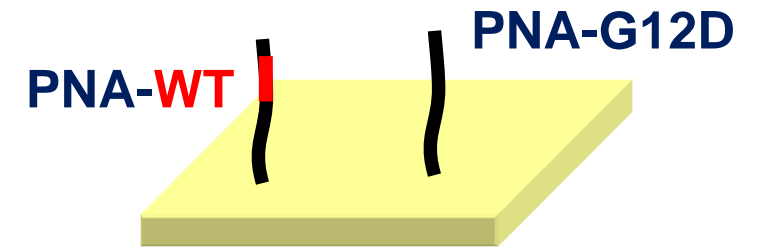
Nanoparticle amplification-SPRI: SNPs detection

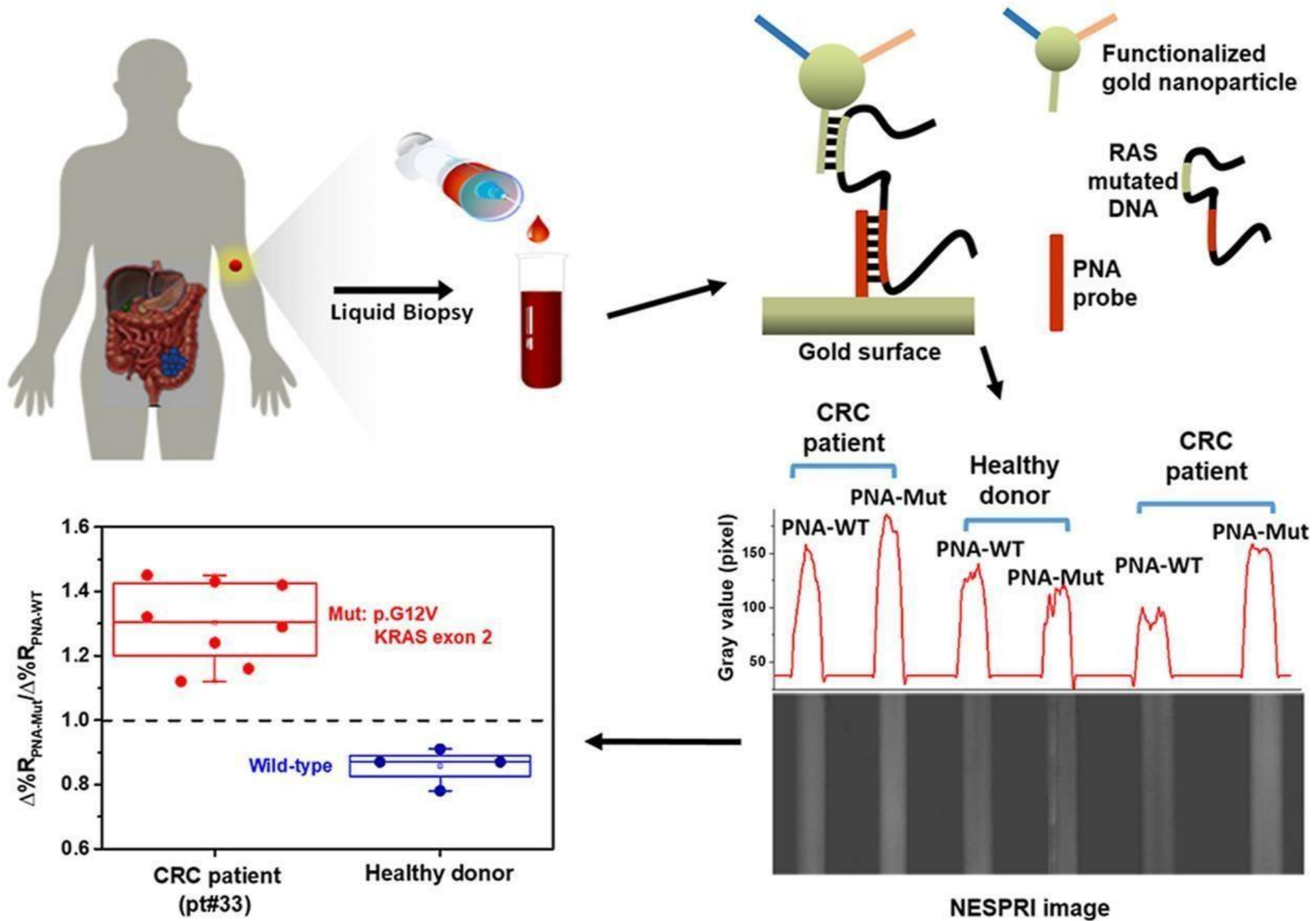




PCR-free detection of KRAS mutations (Plasma from colorectal cancer patients)

YouTube <https://youtu.be/88n3IRsWTm8>





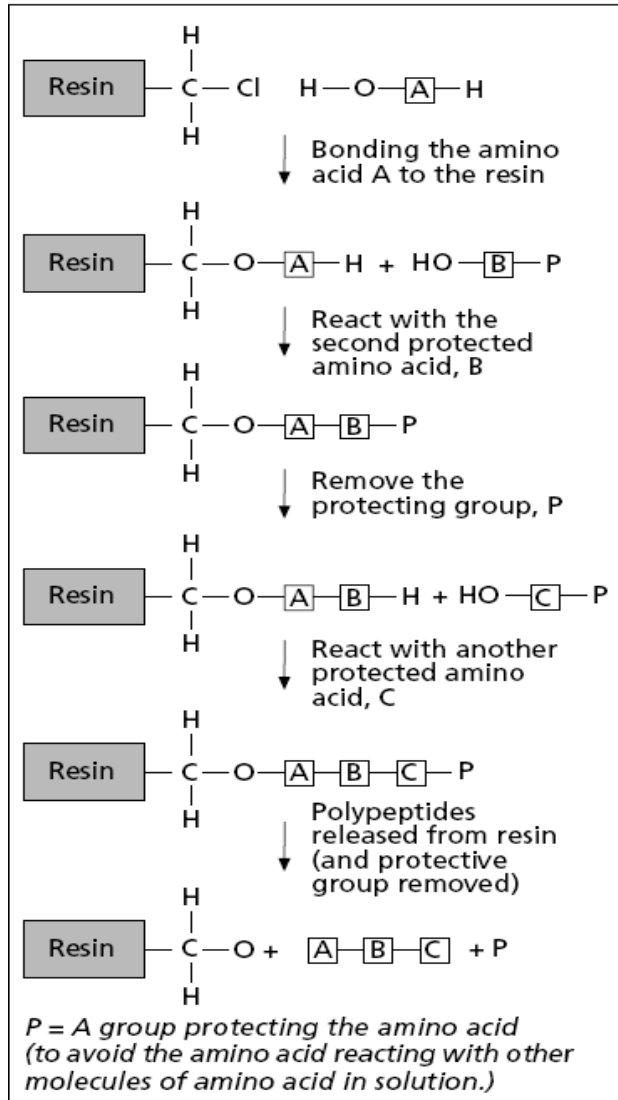
Biomimetic receptors

Used for biosensors or for sample preparation/purification

Obtained via combinatorial chemistry and/or molecular modelling

- Peptides
- Aptamers
- MIP (Molecularly Imprinted Polymers)

Combinatorial chemistry approach: Synthesis of amino acids via split and mix



Split synthesis

Stage	Reaction vessel 1 (A)	Reaction vessel 1 (B)	Reaction vessel 1 (C)	
1	Resin + A	Resin + B	Resin + C	3 compounds
	MIX			
2	Resin-A+A Resin-B+A Resin-C+A	Resin-A+B Resin-B+B Resin-C+B	?	9 compounds
	MIX			
3	Resin-A-A+A Resin-B-A+A Resin-C-A+A Resin-A-B+A Resin-B-B+A Resin-C-B+A Resin-A-C+A Resin-B-C+A Resin-C-C+A	Resin-A-A+B Resin-B-A+B Resin-C-A+B Resin-A-B+B Resin-B-B+B Resin-C-B+B Resin-A-C+B Resin-B-C+B Resin-C-C+B	Resin-A-A+C Resin-B-A+C Resin-C-A+C Resin-A-B+C Resin-B-B+C Resin-C-B+C Resin-A-C+C Resin-B-C+C Resin-C-C+C	27 compounds
	MIX			

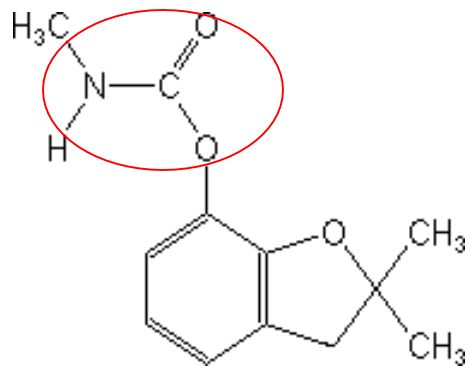
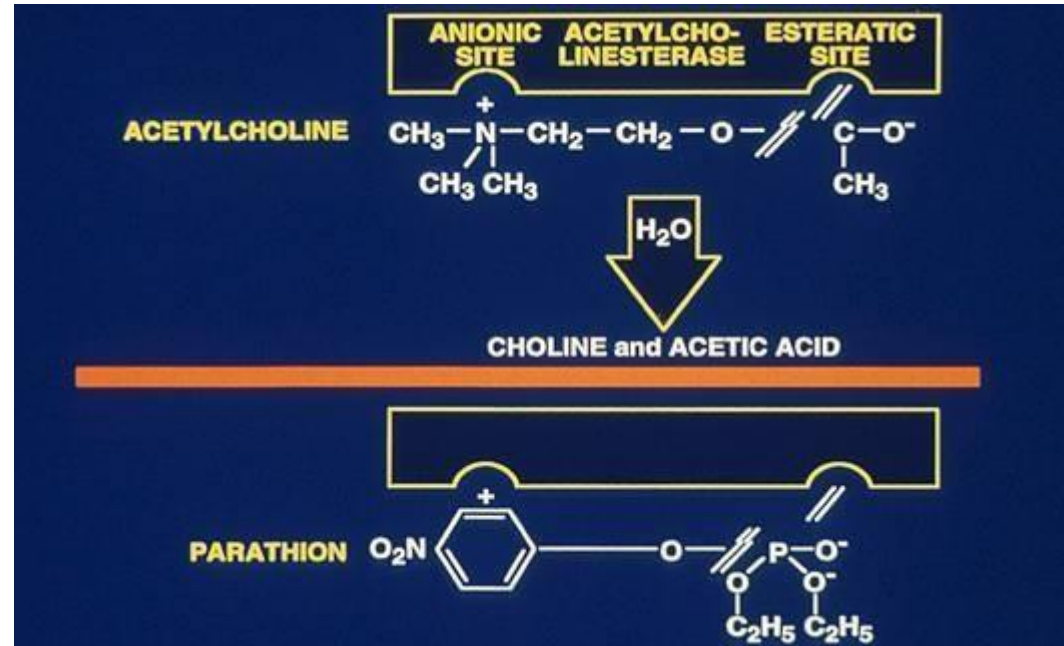
Biomimetic Approach

- Starting from the biological structure it is possible to reproduce with natural amino acids the proper shape of binding dock
- The biomimetic approach relies on the design and development of artificial oligopeptides as a mimic of the biological binding site by using molecular modeling

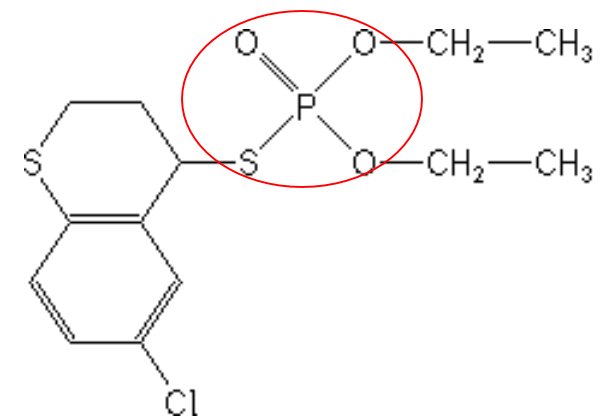
✓ Why oligopeptides?

- Nature exploited aminoacids structures to obtain the most of receptors
- Oligopeptides have the advantage of informatics help from the point of the crystallographic informations from native proteins
- Great number of combinations using 20 aminoacids which can do any binding traps

BIOMIMETIC RECEPTORS FOR PESTICIDES



Carbamate



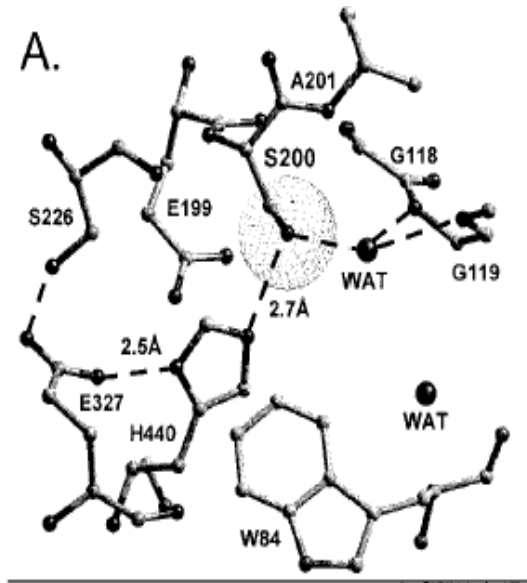
organophosphate

✓ Mechanism of AChE inhibition

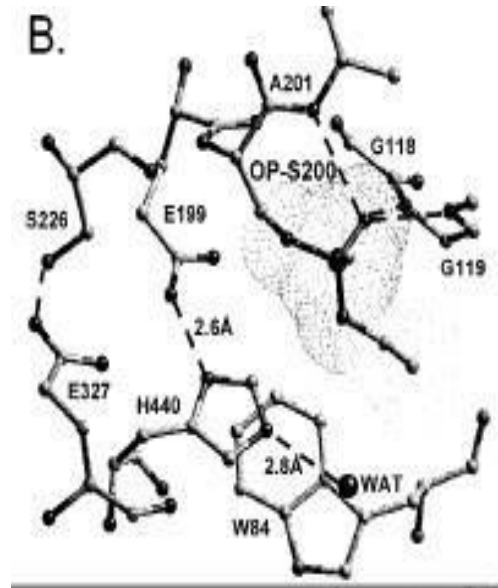
AChE, the target enzyme of pesticides, **is an efficient serine hydrolase** that catalyzes the breakdown of acetylcholine (ACh)



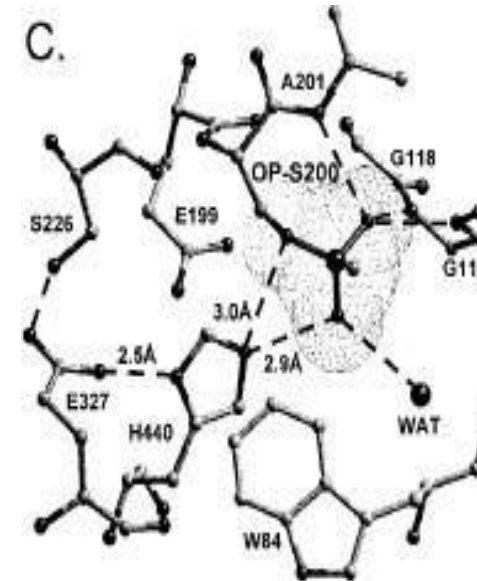
How pesticides work



Native structure: the active site, including the catalytic triad (S200-H440-E327) and the oxanyon hole (-NH of G118, G119, and A201)



Pro-aged structure: Phosphorylation triggers a conformational change for H440 that disrupts the H-bond to E327



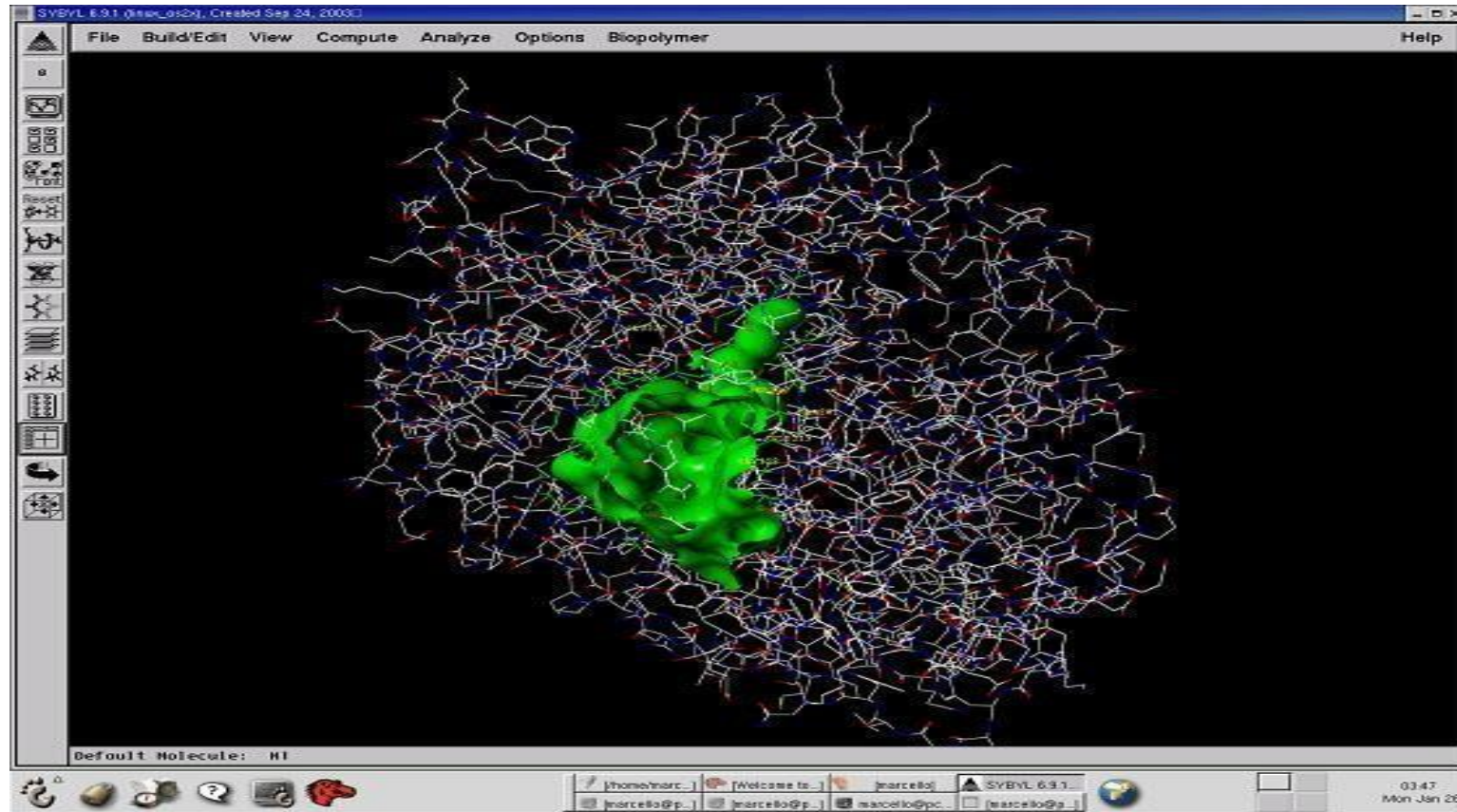
Aged structure: For reaction of AChE with VX and most phosphonates, aging predominates, and dealkylation results in movement of H440 to the negatively charged pocket formed by E327, S200, and one anionic oxygen of the dealkylated OP

From Millard *et al J. Am. Chem. Soc.* 121, (1999)

❖ Computational screening

✓ AChE-OP crystallographic structure (PDB ID: 1VXO)

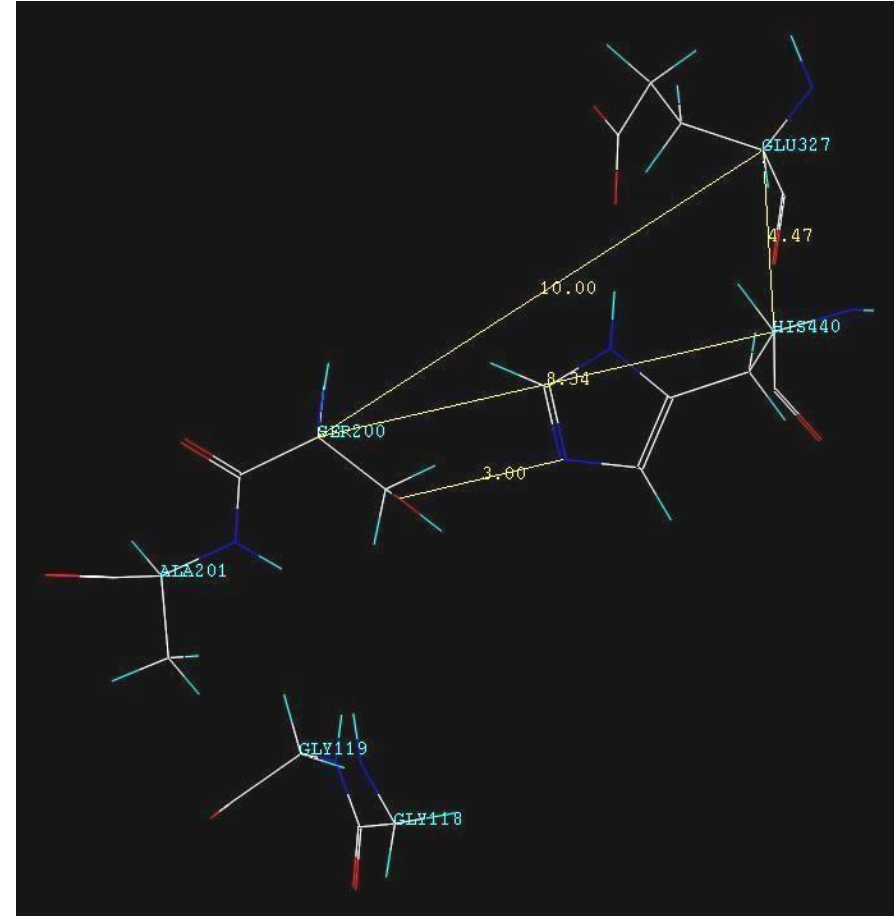
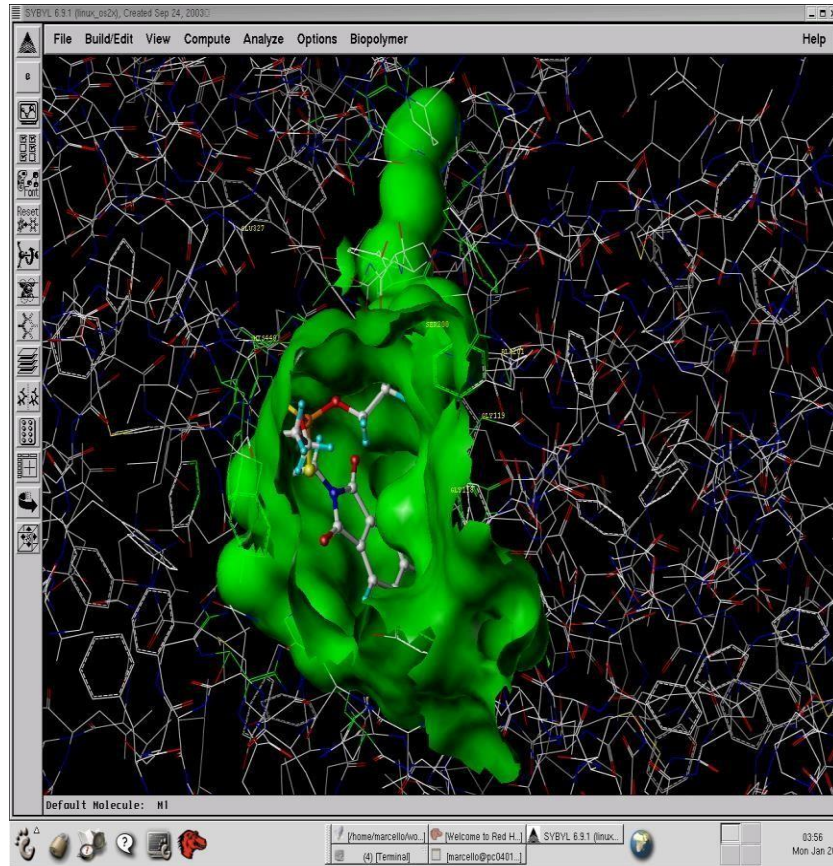
Methylphosphonylated Acetylcholinesterase (Aged) Obtained By Reaction With O-Ethyl-S-[2-[Bis(1-Methylethyl) Amino]Ethyl] Methylphosphonothioate (Vx) conventional X-ray crystallography resolution [\AA]: 2.40



In green the molecular electrostatic potential distribution on the surface of the enzyme binding pocket

✓ Design of the oligopeptides library as possible receptors

The geometry of the binding pocket was investigated to create oligopeptides library



Three dimensional coordinates of the asymmetric carbon ($C\alpha$) of each aminoacid involved in the binding pocket were calculated in order to reproduce the geometry observed

✓ Tetrapeptides library

➤ easy to synthesise

➤ more possibility to preserve in solution the secondary structure predicted

•A series of tetrapeptides, containing the possible combinations of the catalytic triad (SER 200, HIS 440, GLU 327) and the catalytic oxyanion hole (GLY 118 GLY 119 ALA201) was drawn

•The proper geometry of binding pocket was achieved using alternatively a GLY or a PRO residue

Library (24 tetrapeptides)

Ser-Gly-His-Glu	Glu-Gly-Ser-Ala
Ser-Gly-Glu-His	His-Gly-Ser-Ala
His-Glu-Gly-Ser	Gly-Pro-Ser-Ala
Glu-His-Gly-Ser	Ser-Ala-Pro-Glu
Ser-Pro-His-Glu	Ser-Ala-Pro-His
Ser-Pro-Glu-His	Ser-Ala-Pro-Gly
His-Glu-Pro-Ser	Glu-Pro-Ser-Ala
Glu-His-Pro-Ser	His-Pro-Ser-Ala
Gly-Gly-Ser-Ala	Gly-Ser-Gly-Ala
Ser-Ala-Gly-Glu	Ala-Gly-Ser-Gly
Ser-Ala-Gly-His	Ser-Gly-Pro-Ala
Ser-Ala-Gly-Gly	Ala-Pro-Gly-Ser

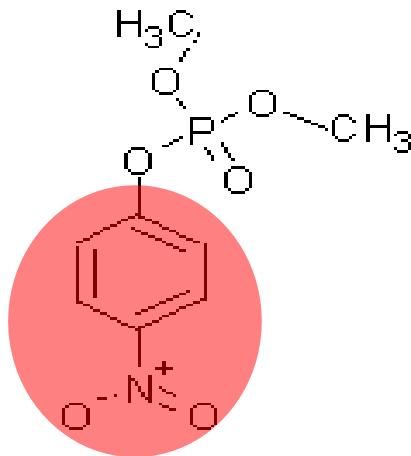
✓ Simulated binding results vs paraoxon of the tetrapeptides selected for experimental screening

	A	B	C	D
	Ser-Ala-Gly-Glu	His-Gly-Ser-Ala	Glu-Pro-Ser-Ala	His-Glu-Pro-Ser
Binding Score (KJ/mol)	38	73	21	93

Negative control (NC): Glu-His-Ser-Gly

Primary sequence of AChE catalytic triad

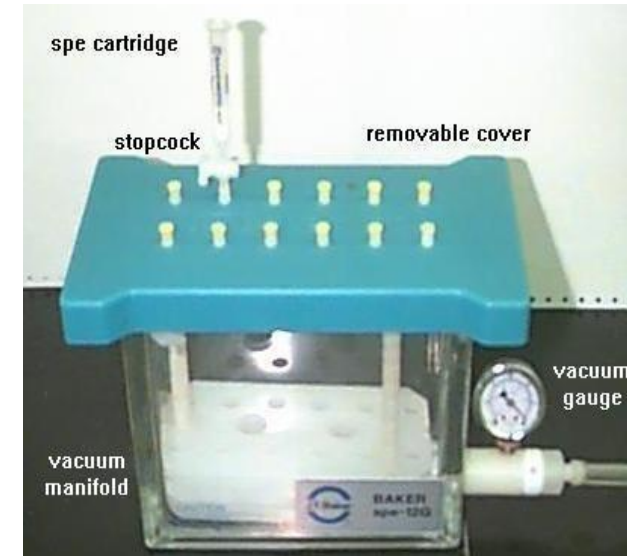
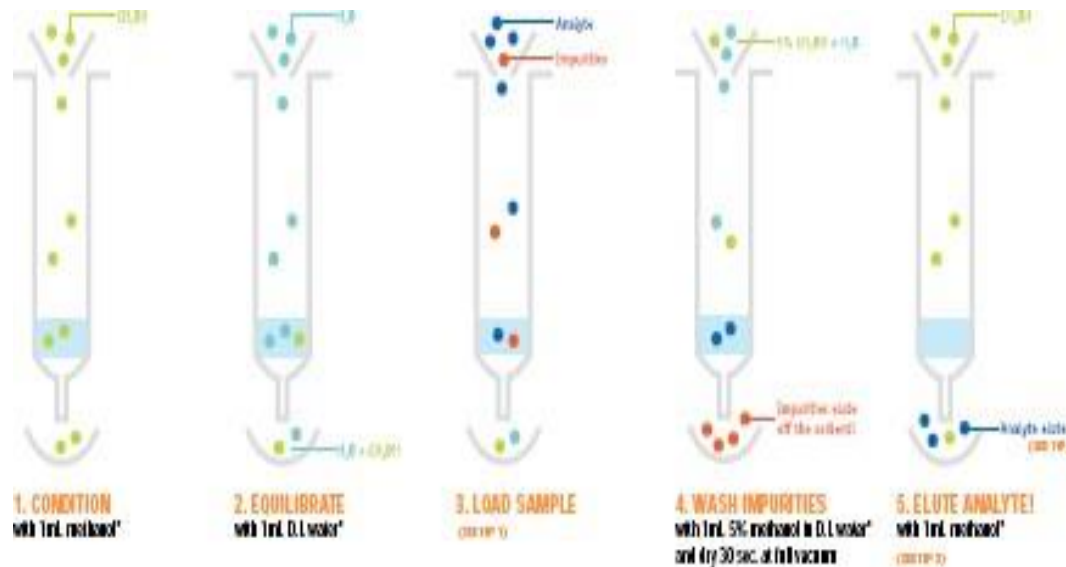
PARAOXON



- A Ser-Ala-Gly-Glu
- B His-Gly-Ser-Ala
- C Glu-Pro-Ser-Ala
- D His-Glu-Pro-Ser
- NC Glu-His-Ser-Gly

✓ Pre-analytical applications: selective affinity columns



(Extraction or purification)



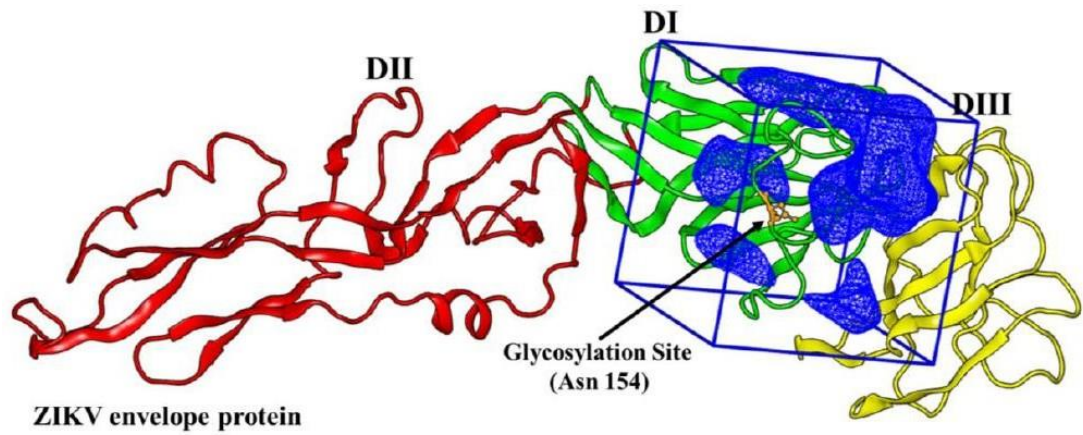
is a technique enabling purification of a biomolecule with respect to biological function or individual chemical structure. The **substance to be purified** is specifically and **reversibly adsorbed** to a **ligand** (binding substance), **immobilized by a covalent bond** to a **chromatographic bed material** (matrix). Samples are applied under favourable conditions for their specific binding to the ligand. Substances of interest are consequently bound to the ligand while unbound substances are washed away. **Recovery of molecules of interest can be achieved by changing experimental conditions** to favour desorption.

Article

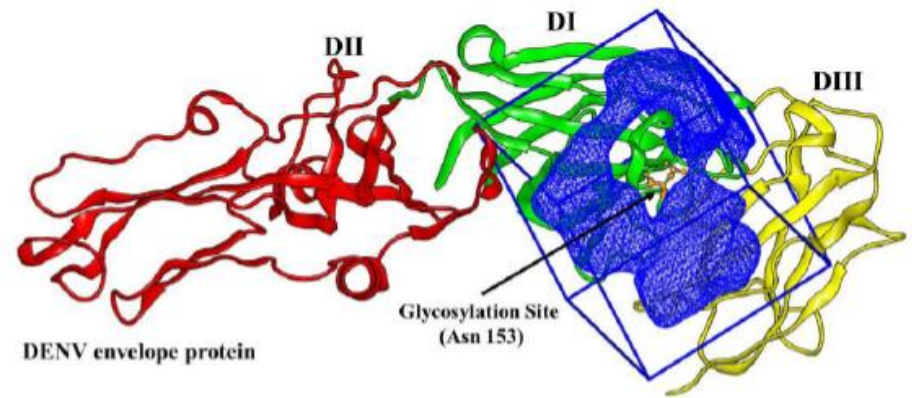
Computationally Designed Peptides for Zika Virus Detection: An Incremental Construction Approach

Marcello Mascini ^{1,2,*} , Emre Dikici ^{3,4}, Marta Robles Mañueco ³, Julio A. Perez-Erviti ⁵, Sapna K. Deo ^{3,4}, Dario Compagnone ² , Joseph Wang ⁶, José M. Pingarrón ¹ and Sylvia Daunert ^{3,4,7,*}

- Zika infection is known to cause neurological problems to pregnant women and potentially cause microcephaly and other congenital malformations and diseases to the unborn child. Zika affects, both male and females and it has been reported that the virus can be transmitted sexually through semen and vaginal fluids.
- The Zika virus is a mosquito-borne flavivirus, and due to the lack of specific antibodies/binders that can be used in immunoassays for diagnosis of the disease, these immunoassays present cross-reactivity with other flaviviruses and arboviruses. It is well established that ZIKV has many common genetic sequences and protein structures with other flaviviruses, like DENV, West Nile virus or Chikungunya. This limits the use of immunoassays for the detection of human pathogens within the flavivirus genus.
- The flavivirus envelope protein is responsible for virus entry and represents a major target for neutralizing antibodies. The Zika virus structure is similar to other known flaviviruses structures except for the ~10 amino acids that surround the Asn-154 glycosylation site found in each of the 180 envelope glycoproteins that make up the icosahedral shell

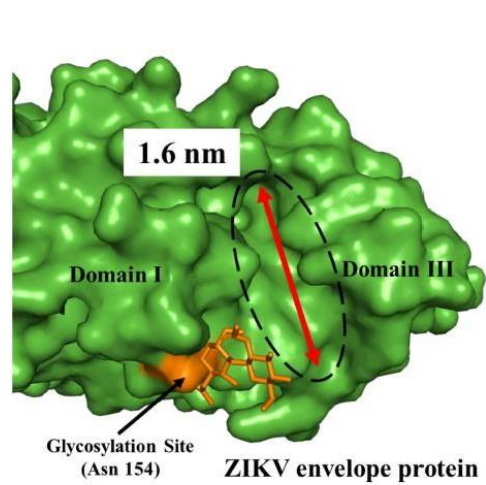


(a)

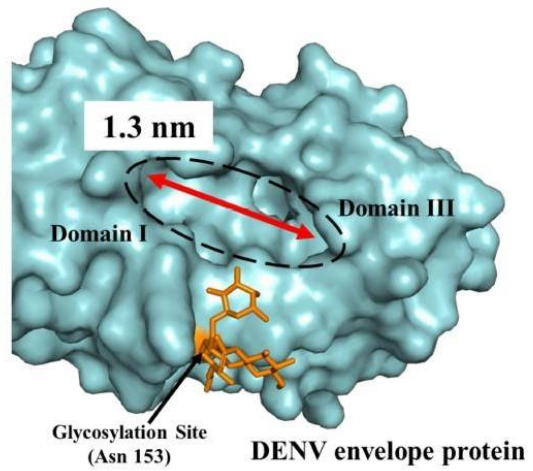


(b)

Glycosylation site



(a)



(b)

Figure 4. *Cont.*

Molecular docking

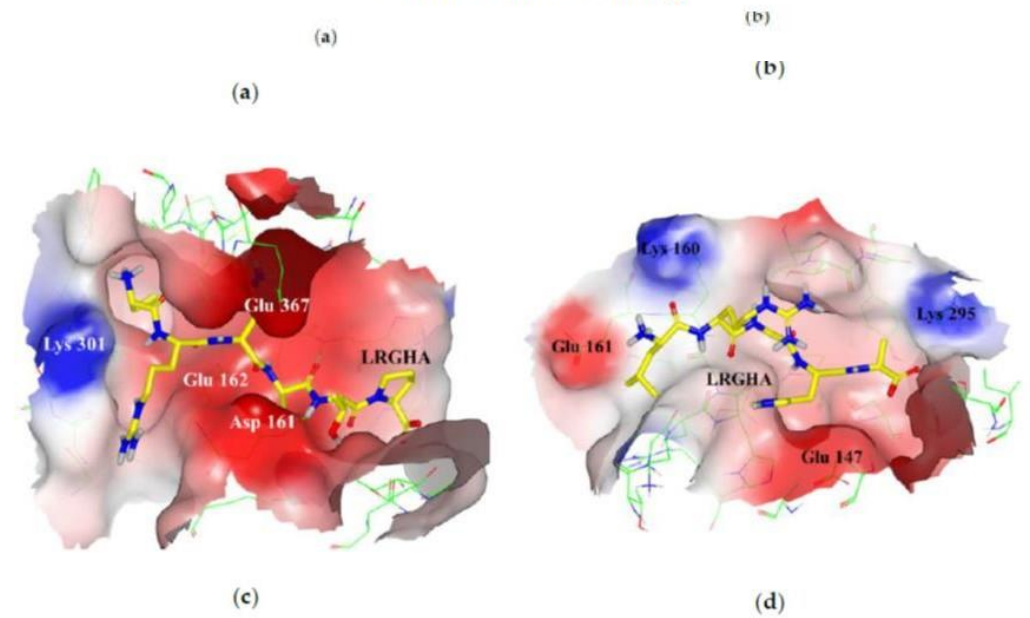


Figure 5. *Cont.*

8 different peptides selected, synthesized, biotinylated and tested with direct ELISA test using Avidin-HRP

i.e. inactivated virus onto ELISA microwells, reaction with peptides, incubation with Avidin-HRP

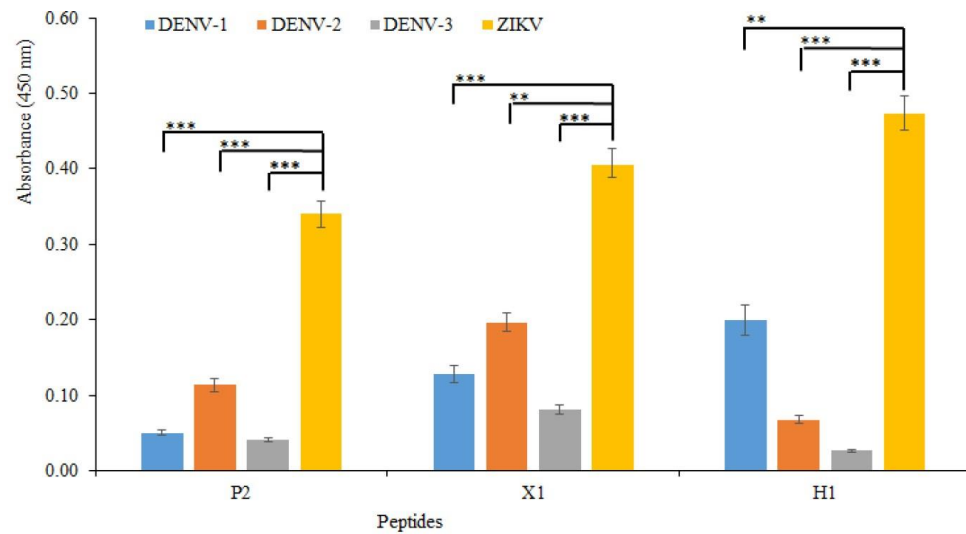


Figure 7. Cross-reactivity study. In the ELISA direct assay, the spectrophotometric absorbance signals were obtained by using the best three peptides (P2, X1, and H1) binding the ZIKV and three serotypes of DENV (DENV-1, -2, and -3) at the concentration of 10^6 copies/mL. Statistical significance between ZIKV and DENV serotypes (1–3) was calculated using two-way analysis of variance. Different p values were indicated by $** (p < 10^{-3})$ or $*** (p < 10^{-4})$.

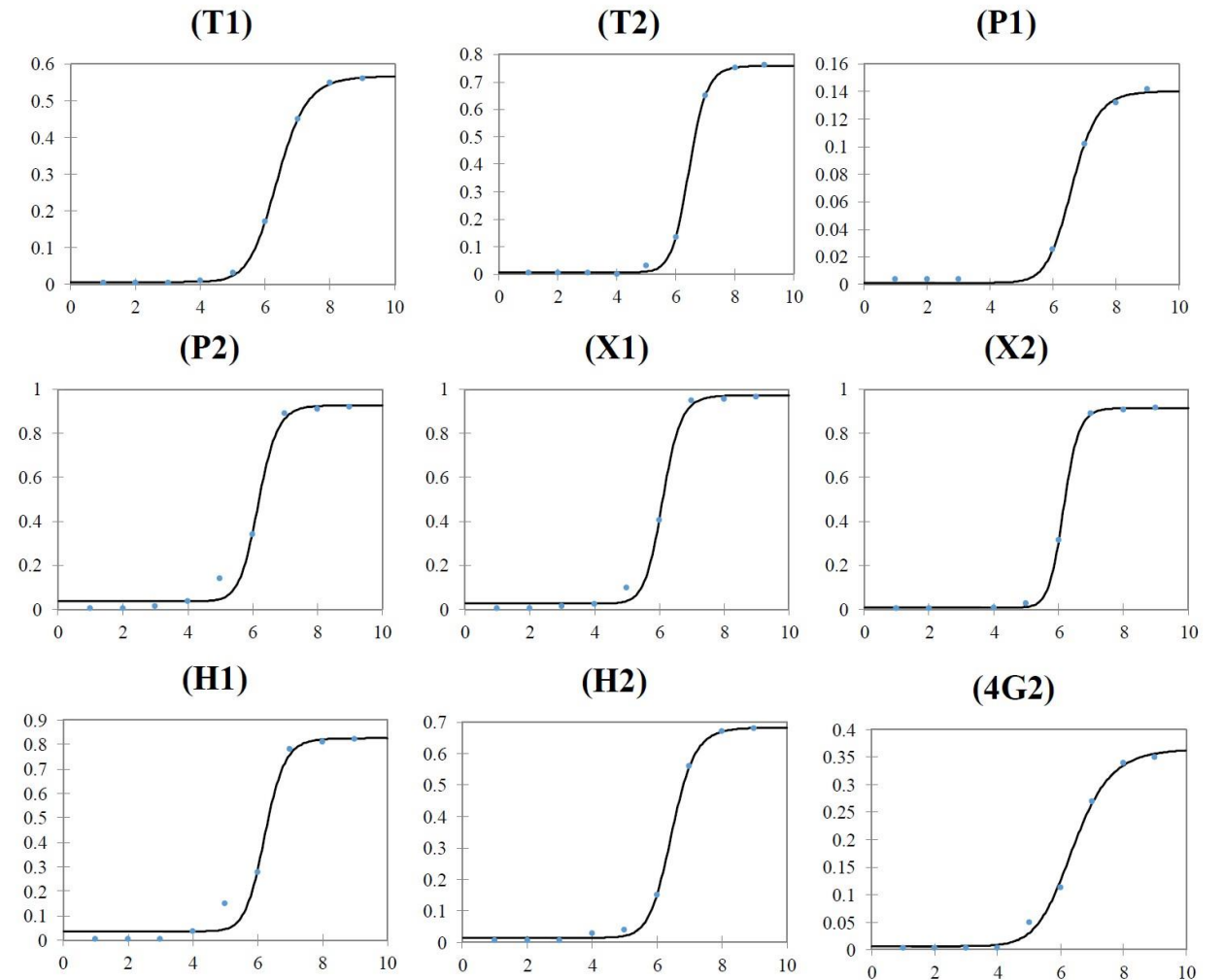


Figure 6. Sigmoidal ZIKV particles concentration response trend of the ELISA assay obtained using the eight peptides and antibody 4G2. Y-axis = absorbance (450nm); X-axis = log [ZIKV], copies/mL.



Contents lists available at [ScienceDirect](#)

Sensors and Actuators: B. Chemical

journal homepage: www.elsevier.com/locate/snb



Biomimetic isolation of affinity peptides for electrochemical detection of influenza virus antigen



Ji Hong Kim^a, Chae Hwan Cho^a, Jae Hwan Shin^a, Moon Seop Hyun^b, Eunha Hwang^c,
Tae Jung Park^{d,*}, Jong Pil Park^{a,*}

^a Department of Food Science and Technology, Chung-Ang University, Anseong, 17546, Republic of Korea

^b National NanoFab Center (NNFC), 291 Daehangno, Daejeon, 34141, Republic of Korea

^c Center for Research Equipment, Korea Basic Science Institute, Cheongju, 28119, Republic of Korea

^d Department of Chemistry, Institute of Interdisciplinary Convergence Research, Research Institute of Chem-Bio Diagnostic Technology, Chung-Ang University, 84 Heukseok-ro, Dongjak-gu, Seoul, 06974, Republic of Korea



Biomimetic isolation of affinity peptides for electrochemical detection of influenza virus antigen

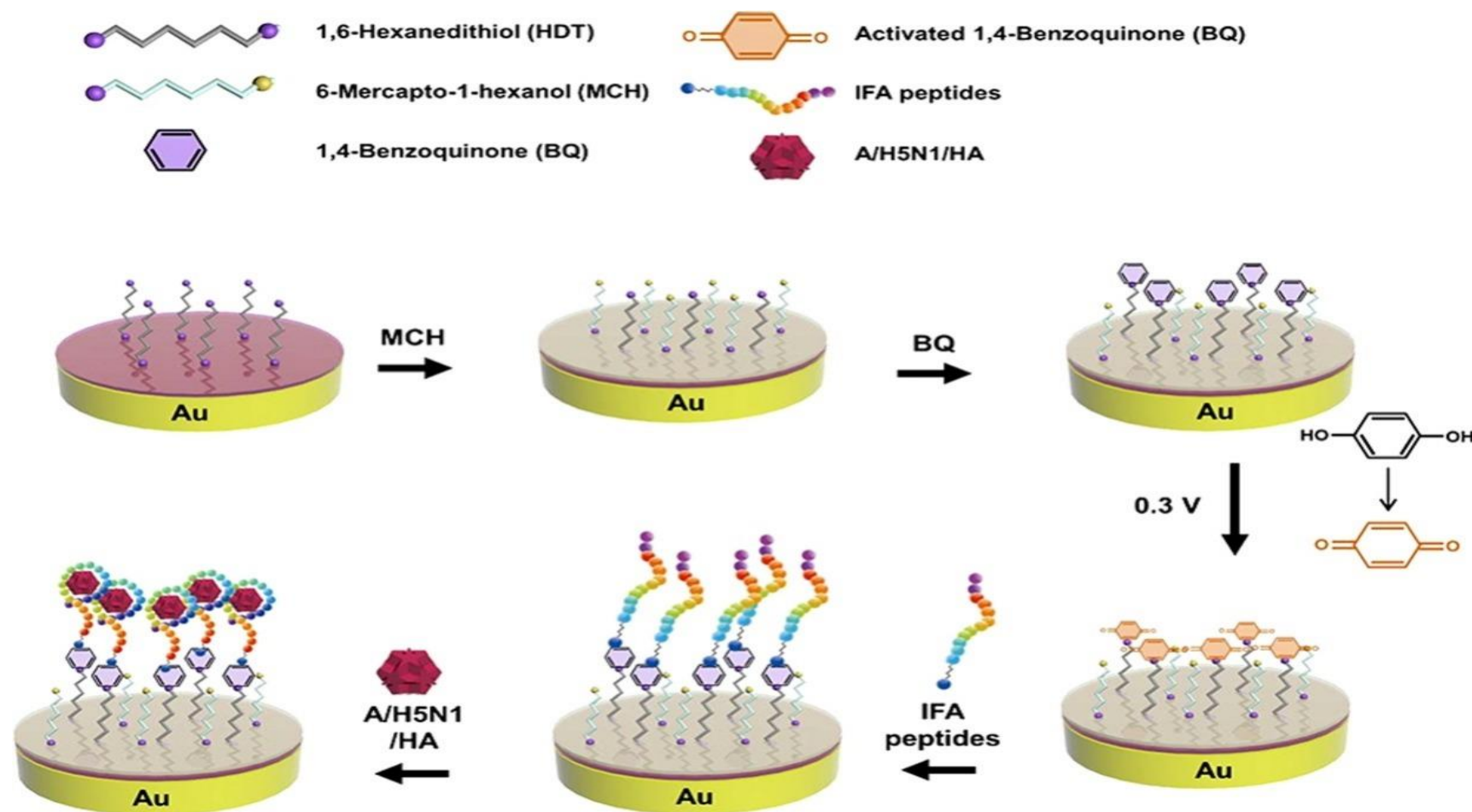
Ji Hong Kim^a, Chae Hwan Cho^a, Jae Hwan Shin^a, Moon Seop Hyun^b, Eunha Hwang^c,
Tae Jung Park^{d,*}, Jong Pil Park^{a,*}

^a Department of Food Science and Technology, Chung-Ang University, Anseong, 17546, Republic of Korea

^b National NanoFab Center (NNFC), 291 Daehangno, Daejeon, 34141, Republic of Korea

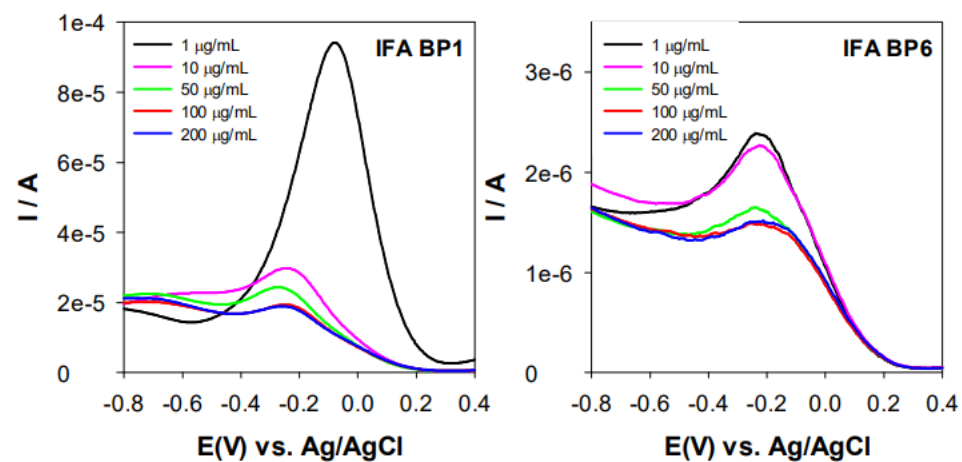
^c Center for Research Equipment, Korea Basic Science Institute, Cheongju, 28119, Republic of Korea

^d Department of Chemistry, Institute of Interdisciplinary Convergence Research, Research Institute of Chem-Bio Diagnostic Technology, Chung-Ang University, 34 Heukseok-ro, Dongjak-gu, Seoul, 06974, Republic of Korea



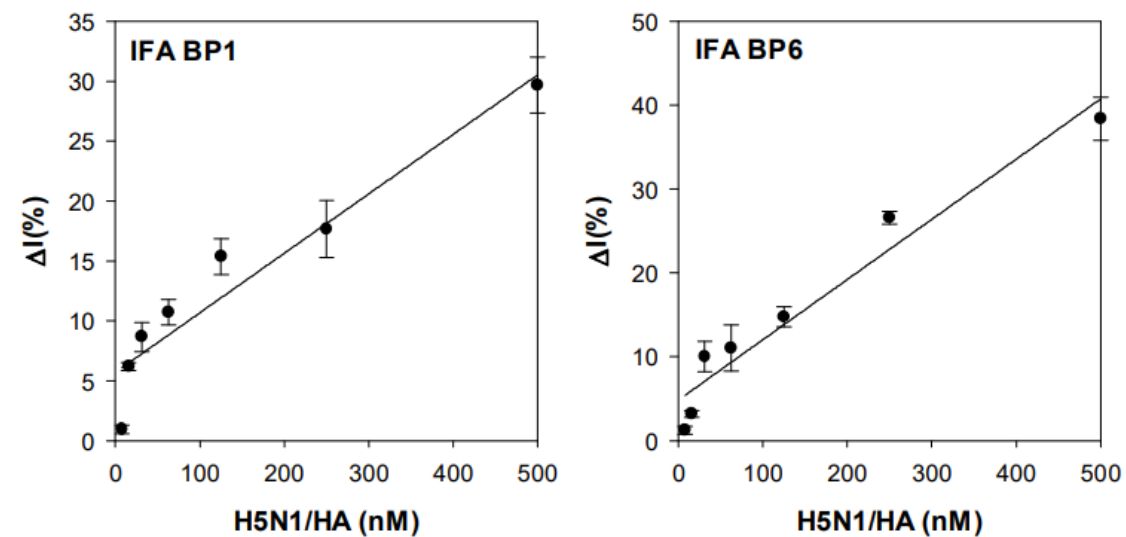
Detection con
Voltammetria
differenziale ad
impulsi in presenza di
ferricianuro

Figure S1. Optimization of IFA BP1 and BP6 peptides concentration



The current decreased with increasing concentration of IFA BP1 and BP6 up to 200 µg/mL and reached saturation at 100 µg/mL. Therefore, IFA BP1 and BP6 peptide concentration of 100 µg/mL was selected as the optimum concentration.

Figure S2. Comparison of limit of detection (LOD) of IFA BP1 and IFA BP6

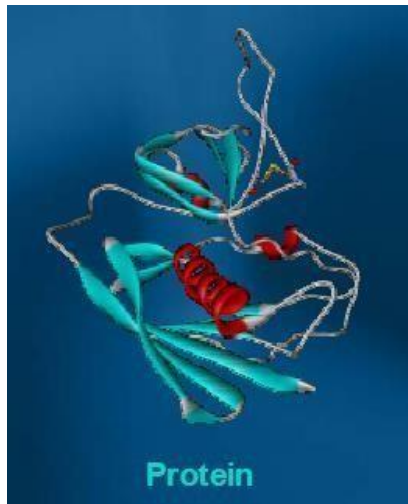


Aptamers are oligonucleotides (DNA or RNA molecules) that can bind with high affinity and specificity to a wide range of target molecules (proteins, peptides, drugs, vitamins and other organic or inorganic compounds).

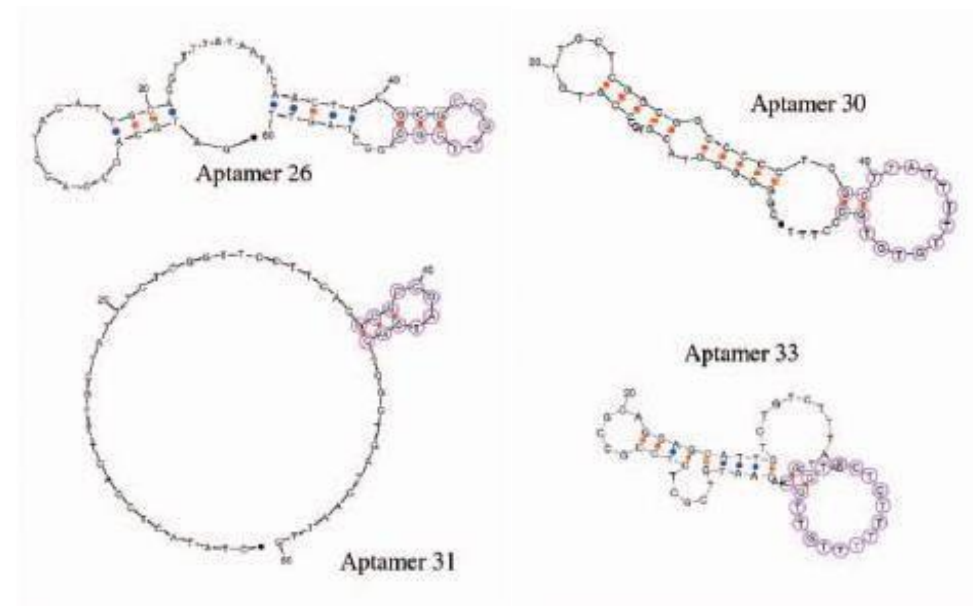
They were “discovered” in 1990 by the development of an in vitro selection and amplification technique, known as SELEX (Systematic Evolution of Ligands by Exponential enrichment).

(Ellington et al., **Nature** 346, 818; Tuerk and Gold, **Science** 249, 505)

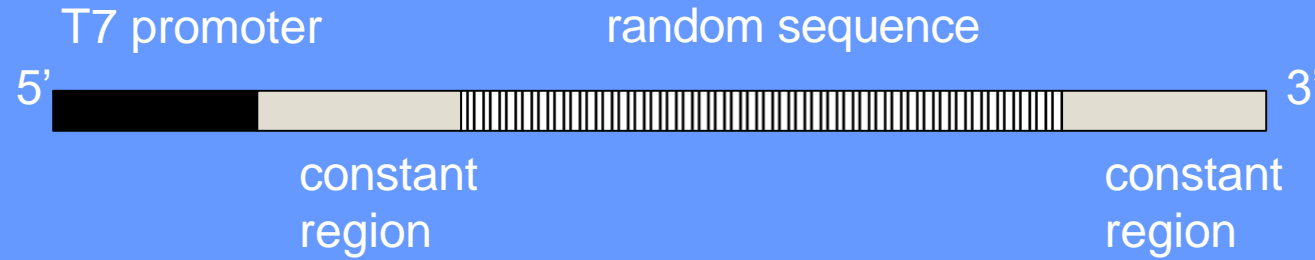
Their name is derived from the Latin word “**aptus**” which means “to fit”.



Similar to proteins short oligonucleotides can adopt complex three-dimensional structures



Starting point: Combinatorial oligonucleotide library



A library containing a 25-nucleotide random region is represented by 4^{25} ($\sim 10^{15}$) individual sequences available for partitioning.
Normally, the starting round contains **10^{14} - 10^{15} individual sequences.**

A, G, C, U(T)

$$4^1 = 4$$

$$4^2 = 16$$

$$4^3 = 64$$

$$4^4 = 256$$

$$4^5 = 1024$$

.....

.....

.....

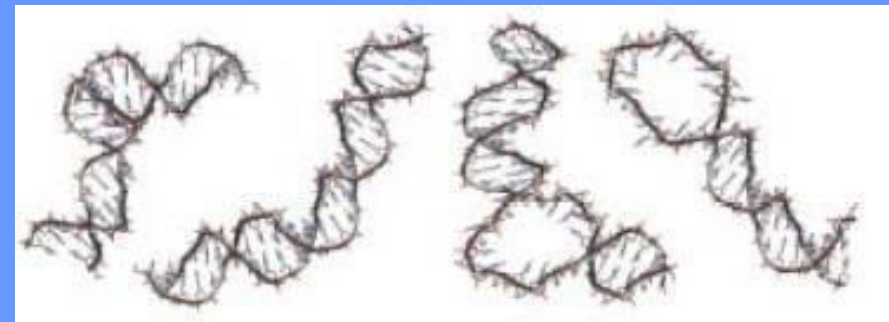
$$4^{25} = 1125899906842624$$

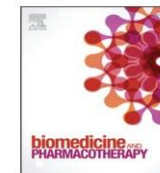


Pool of randomized DNA or RNA



10^{15} different sequences!!!!



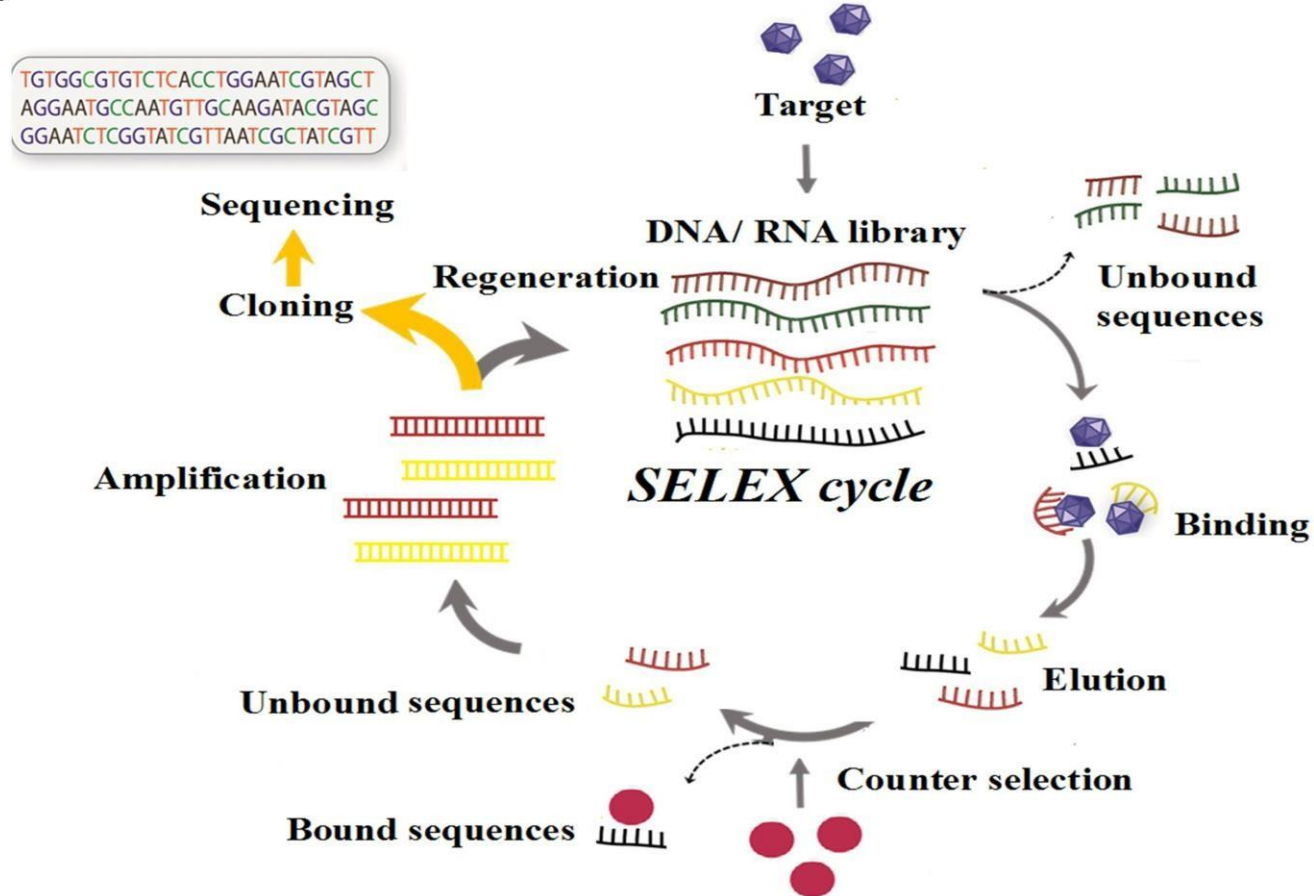


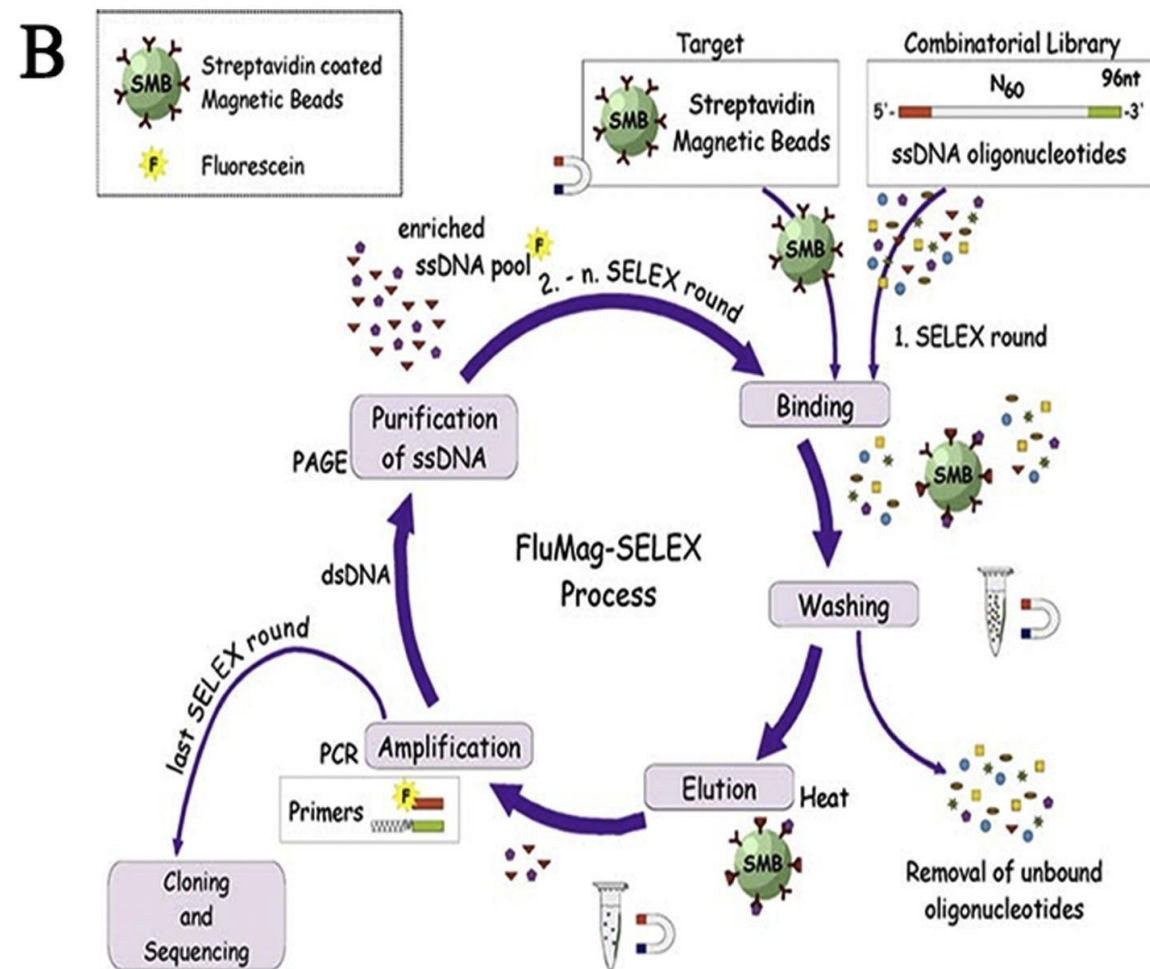
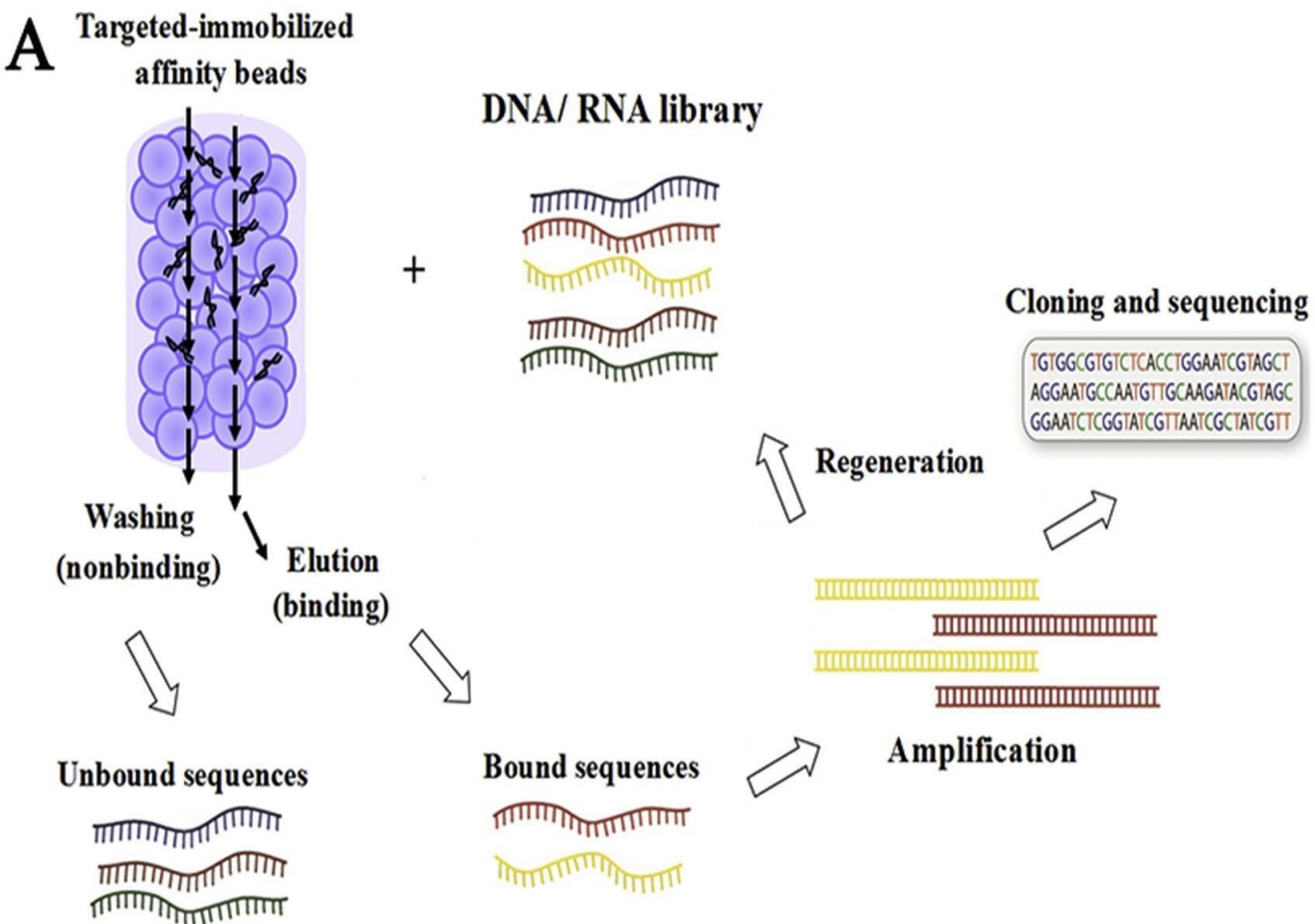
Review

Aptamers used for biosensors and targeted therapy

Yi Ning, Jue Hu, Fangguo Lu *

Department of Microbiology, The Medicine School of Hunan University of Chinese Medicine, Changsha, Hunan, 410208, PR China





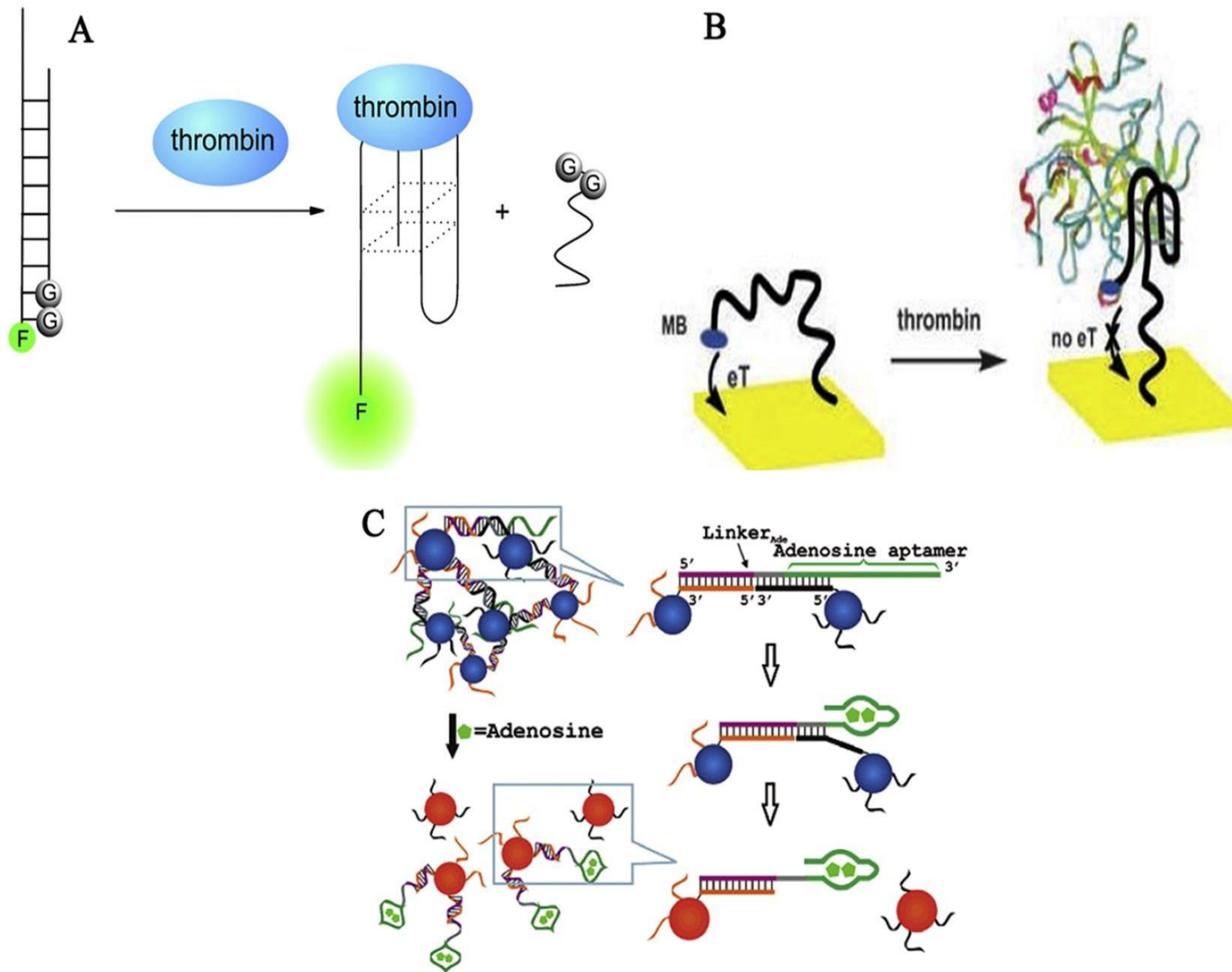


Fig. 5. Various signals generated by aptasensor based on structure-switching designs. (A) A schematic representation of the fluorescent aptasensor for thrombin assay. Thrombin-induced structure change of the aptamer from quenching-state into G-quartet structure could lead to fluorescence enhancement. Fig. 5A adapted from ref. [100]; (B) A schematic representation of the electrochemical aptasensor for thrombin assay. Before adding the thrombin, MB covalently labeled onto aptamer could transfer electron with the electrode surface due to the flexible conformation of the aptamer. Upon adding the thrombin a G-quadruplex structure was formed and the MB moiety was far away from the electrode surface, resulting in the electrochemical signal-off. Fig. 5B adapted from ref. [105]; (C) A schematic representation of the colorimetric aptasensor for adenosine assay. Gold nanoparticles are functionalized with aptamer. Addition of the adenosine results in nanoparticles linking together and aggregating, thus causing the change in color. Fig. 5C adapted from ref. [107]. Copyright (2007) American Chemical Society.

REVIEW


[View Article Online](#)

[View Journal](#) | [View Issue](#)



Cite this: *Mater. Adv.*, 2020,
1, 2663

Detection and beyond: challenges and advances in aptamer-based biosensors

Hyebin Yoo,^{†a} Hyesung Jo^{†a} and Seung Soo Oh *^{ab}

Beyond traditional needs of biosensors such as high sensitivity and selectivity for analyte detection, newly emerging requirements including a real-time detection ability and in-field applicability have been gradually emphasized to address clinical and environmental availability. Highly programmable, synthetic aptamers that can specifically recognize a broad range of targets have the potential to fulfill these requirements; cooperative binding to target molecules achieves a significant increase in sensitivity, and binding-induced structure-switching enables target detection even in complex mixtures. Due to the availability of chemical synthesis and functional modifications, these artificial ligand materials are easily installed in many devices, and the amenability to modularization allows the aptamer-based biosensors to diversify detectable targets and signaling processes. In this review, we highlight current progress in the development of aptamer-based, next-generation biosensors including new types of field-effect transistors, electrochemical detectors, and microfluidic devices. As the nucleic acid aptamers have been rapidly generated by various *in vitro* selection techniques, the use of the versatile nanostructures is expected to expand further to include in-field and real-time biosensors.

Received 24th August 2020,
Accepted 19th October 2020

DOI: 10.1039/d0ma00639d

rsc.li/materials-advances

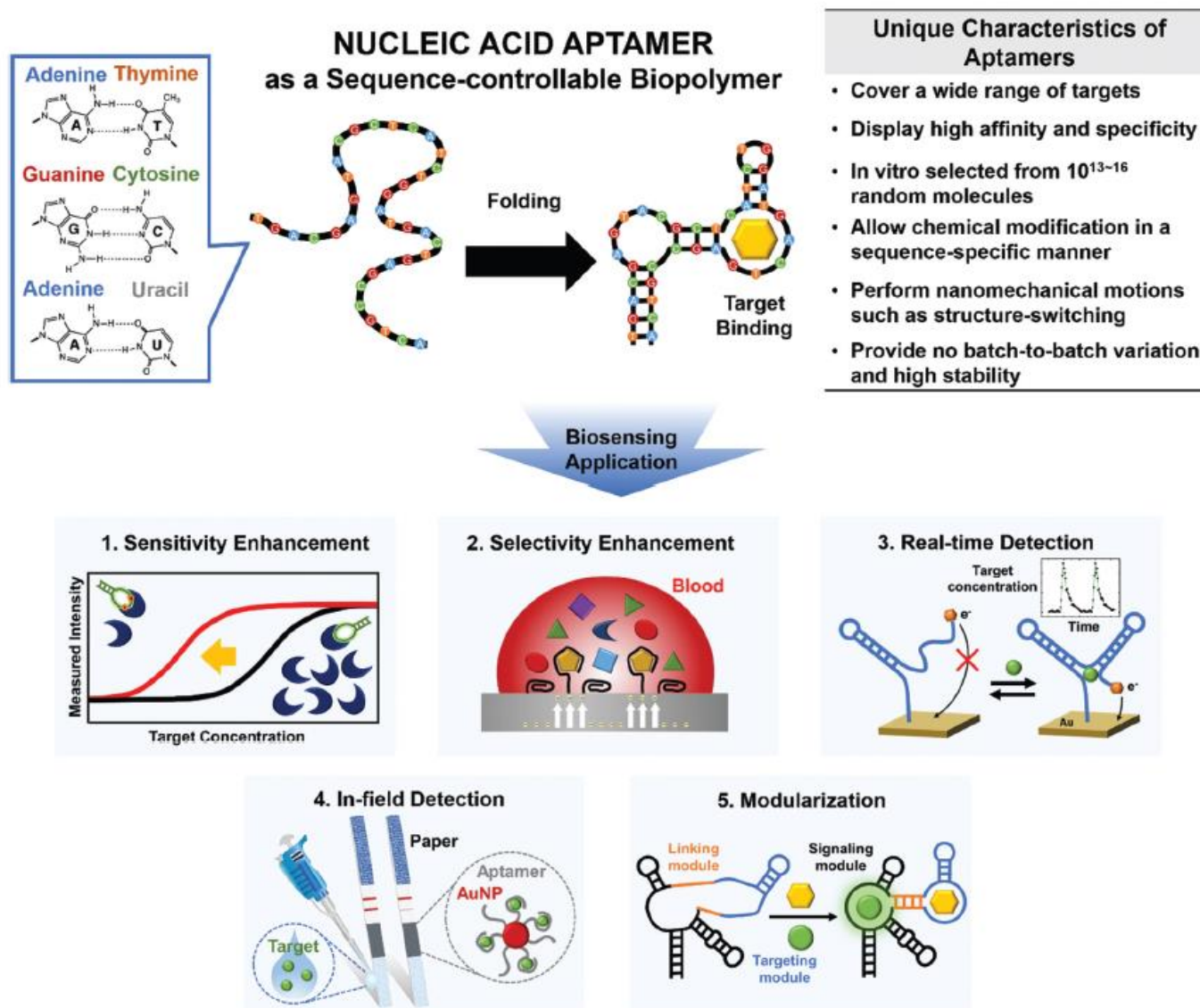


Fig. 1 Main characteristics and functionalities of nucleic acid aptamers to overcome various limitations of conventional biosensors. Specific base pairing (top, left) folds the sequence-controllable biopolymers into thermodynamically-favored 3D nanostructures that enable molecular recognition (top, middle). The synthetic aptamers have unique features that can facilitate the development of next-generation biosensors (top, right). Here, we review technical advances in the development of aptamer-based biosensors, such as increases in sensitivity and selectivity, and actualization of newly emerging real-time and in-field detection applications, along with aptameric biosensors' interesting properties, such as amenability to modularization (bottom).

La sensibilità e selettività può essere aumentata con diverse strategie

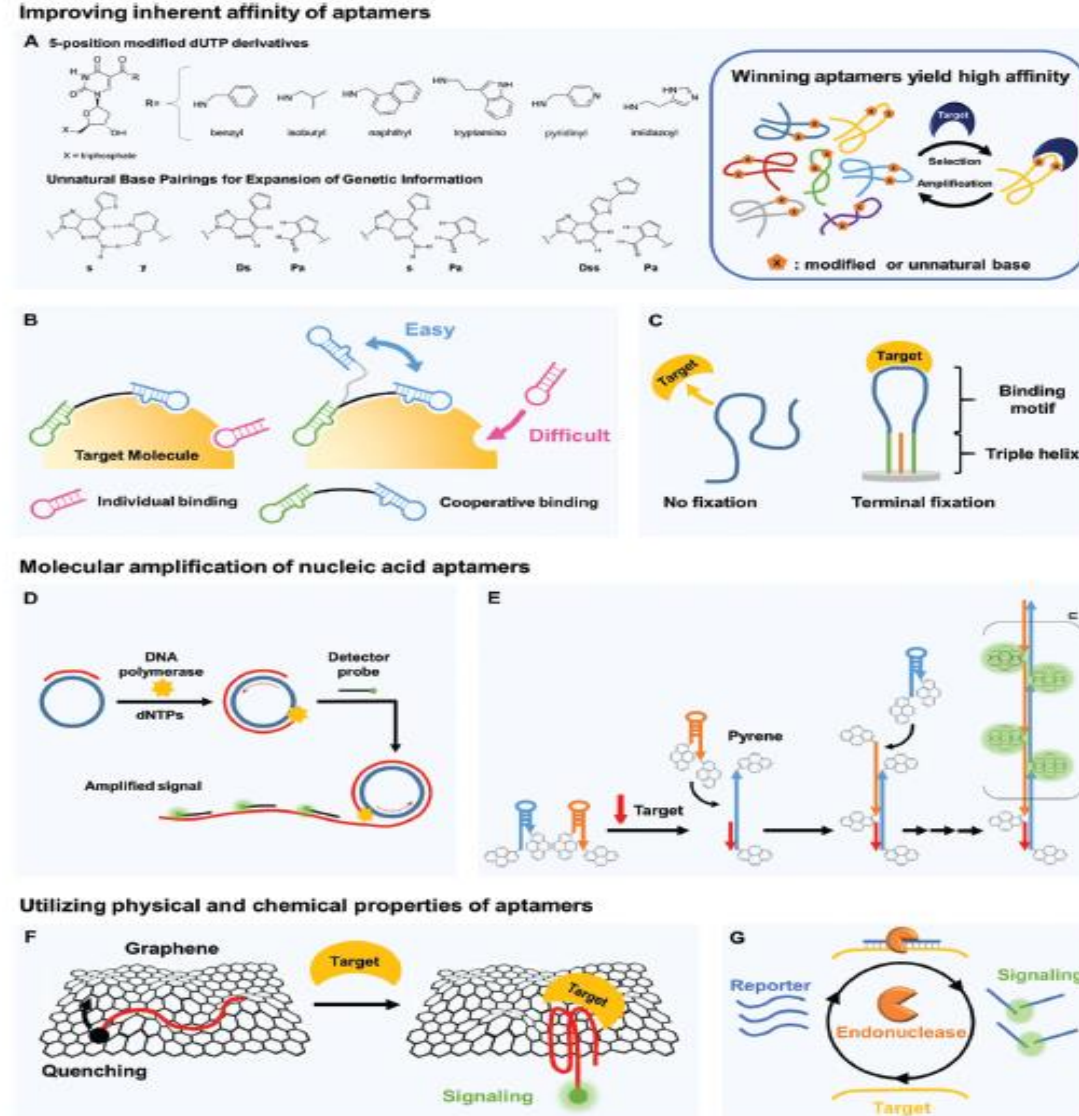


Fig. 2 Aptamers can be key components of biosensors to increase sensitivity in target detection. (A) The inherent binding affinity of aptamers can be strengthened by chemical modification of nucleic acids, e.g., by attaching hydrophobic moieties to nucleotides and by adding non-canonical pairing bases. (B) Multivalency by cooperative binding of multiple aptamers and (C) terminal fixation of folding structures can be also effective to improve the target binding capability of aptamers. (D) Molecular amplification techniques such as rolling circle amplification (RCA) can be useful to develop ultra-sensitive biosensors by significantly increasing detectable signals. [In RCA, primers are bound to circular templates; polymerases extend the primers to yield long single-stranded concatemers with tandem repeat structures, and the repeated hybridization of dye-labeled strands with tandem repeats produces amplified fluorescent signals.] (E) Hybridization chain reaction (HCR) can also be used to increase sensitivity. In HCR, introduction of DNA targets can trigger a hybridization cascade of signaling probes such as pyrene-conjugated hairpin probes and thereby facilitate ultra-sensitive target detection. (F) Unique physical properties of nucleic acid aptamers can contribute to highly sensitive target detection. By π - π stacking, single-stranded nucleic acids bind well to graphene surfaces, whereas the target-bound aptamers are released due to folding in tertiary structures. This folding change of aptamers yields changes in fluorescent or electrical signals, which can be easily detected. (G) Target-bound aptamers are less vulnerable to nuclease digestion than their target-free forms, and this feature can be applied to signal accumulation; the exonuclease-based, enzyme-assisted target recycling (EATR) technique can significantly decrease the limit of detection by summing fluorescence signals.

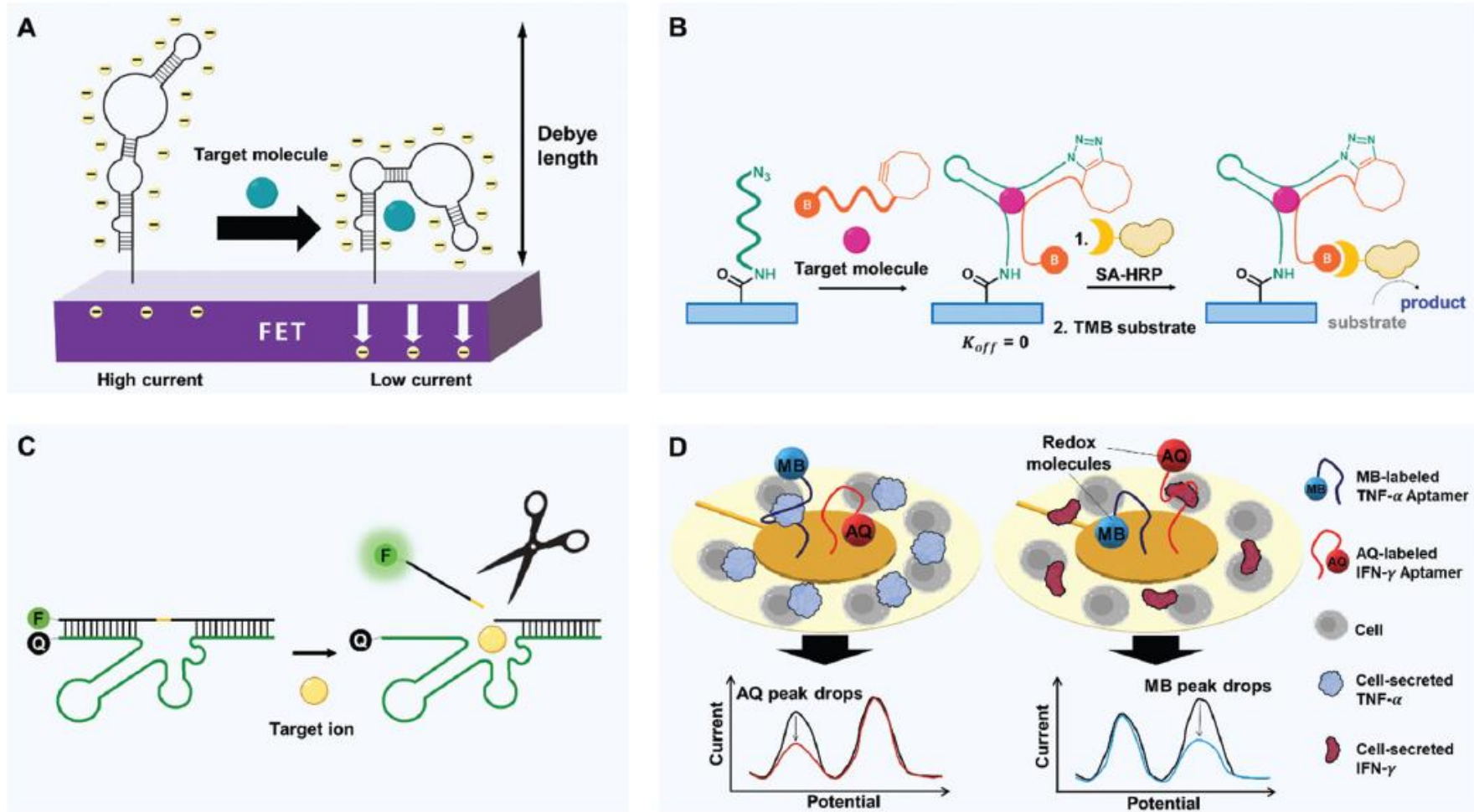
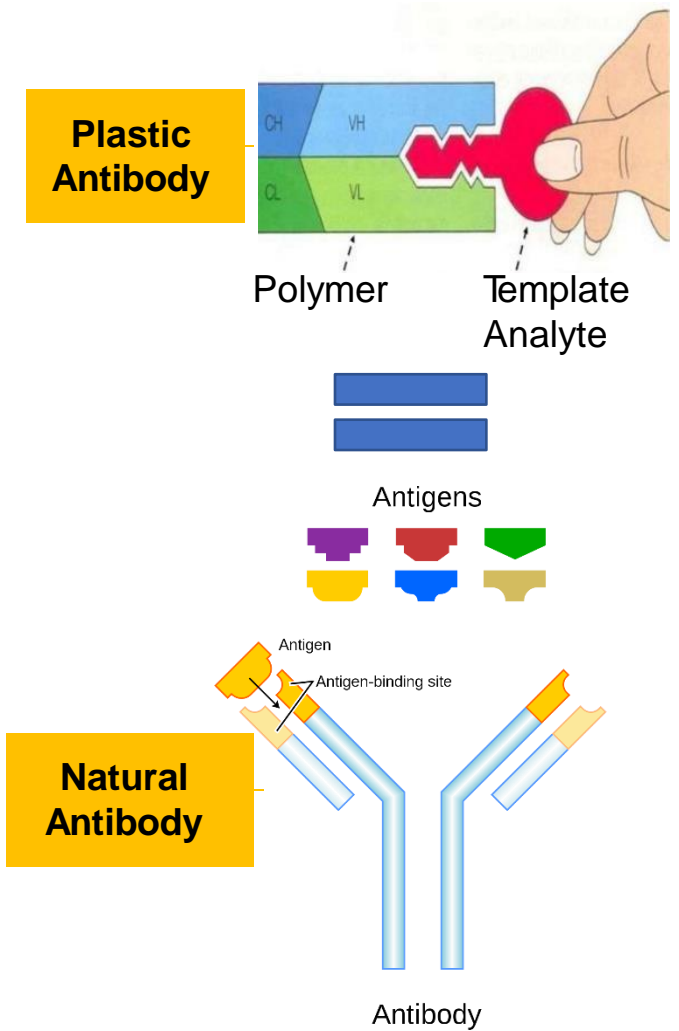
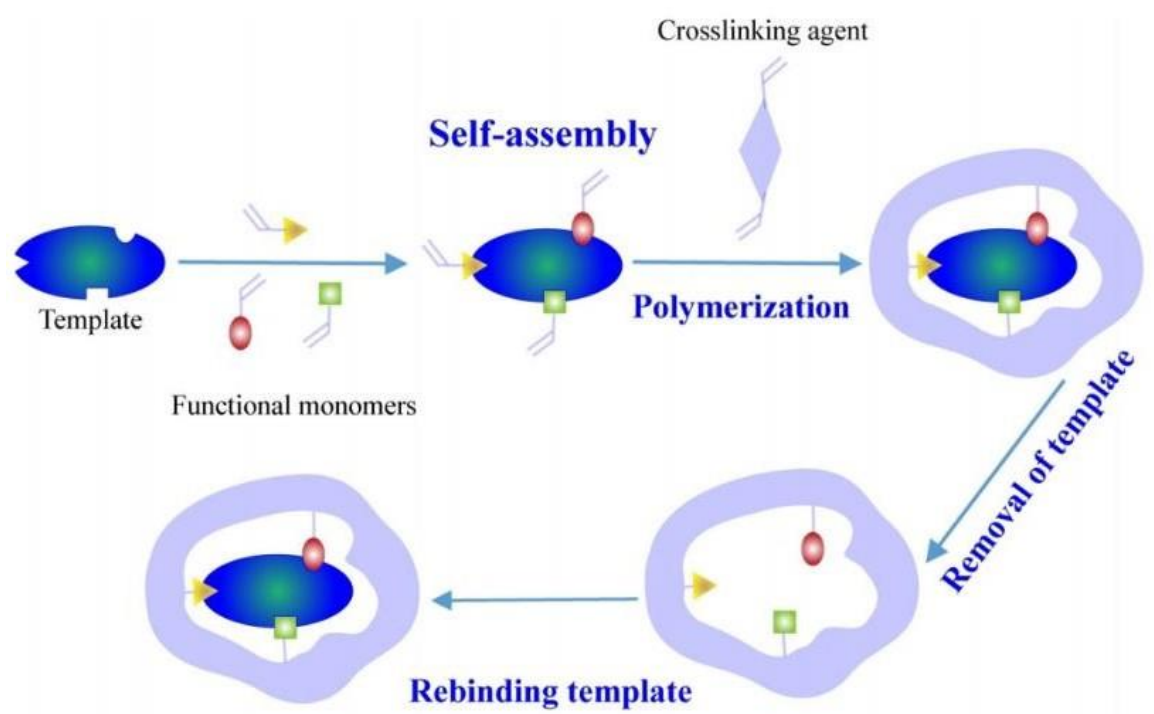


Fig. 3 Diverse strategies with aptamers to improve selectivity of biosensors. (A) Binding-induced self-conformational change of aptamers. FETs modified with target-specific structure-switching aptamers enable selective electronic target detection. Within or near the Debye length, target-induced reorientations of stem-loop aptamers near semiconductor channels deplete the channels electrostatically and thereby decrease transconductance. (B) Binding-induced hetero-conformational change of split aptamers. Upon target binding, split aptamers can be covalently linked to each other by click chemistry. When biotinylated aptamer fragments recruit streptavidin-horseradish peroxidase (SA-HRP), chromogenic substrates such as TMB can be oxidized to emit detectable signals. (C) Binding-activated catalytic reaction. By target binding-induced cleavage of aptazymes, the release of fluorophore-linked fragments can be activated to emit highly target-specific fluorescence by reducing physisorption-derived signaling. (D) High selectivity-driven multiplexing. A multiplex analysis can be conducted by aptamers that are linked to redox molecules. Surrounded by cells, Au electrodes can be modified with different aptamers-redox reporter constructs. Binding to cytokines (TNF- α and IFN- γ) causes target-dependent conformational changes that decrease electron-transfer efficiency and thereby decrease the current. Redox molecules with different potential enable the simultaneous detection of multiple targets.



Molecularly imprinted polymers (MIPs) are synthetic receptors for a targeted molecule. As such, they are analogues of the natural antibody–antigen systems

DOI: 10.1021/acs.chemrev.8b00171 Chem. Rev. 2019, 119, 94–119



Scheme 1. Schematic representation of the synthesis of molecularly imprinted polymers (MIPs).

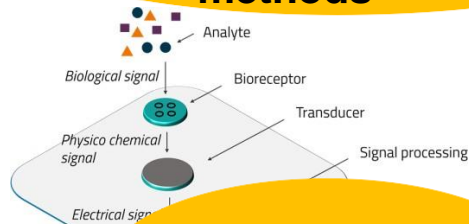
Abdellatif Ait Lahcen[a] and Aziz Amine*[a], 2018

MIP-State of the art

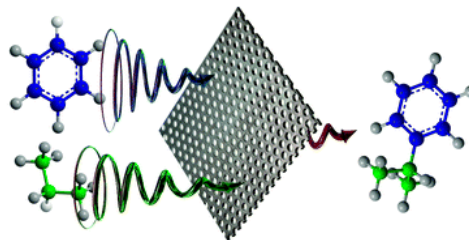
MIPs Applications

MIPs are excellent materials with high selectivity and are widely used for:

Sample preparation in bio analytical methods

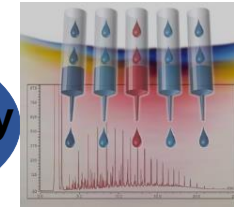


Sensors applications



Catalysis

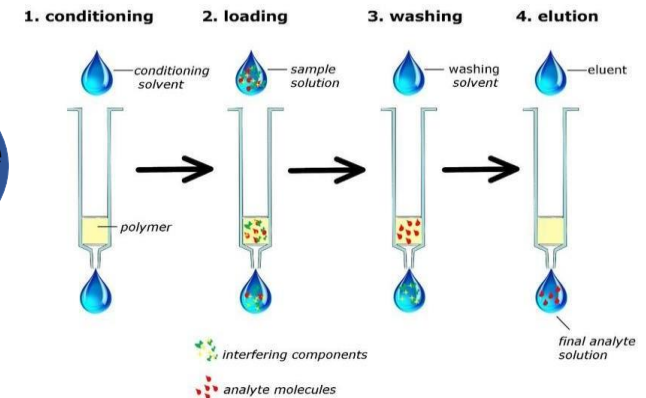
Chromatography



Drug delivery



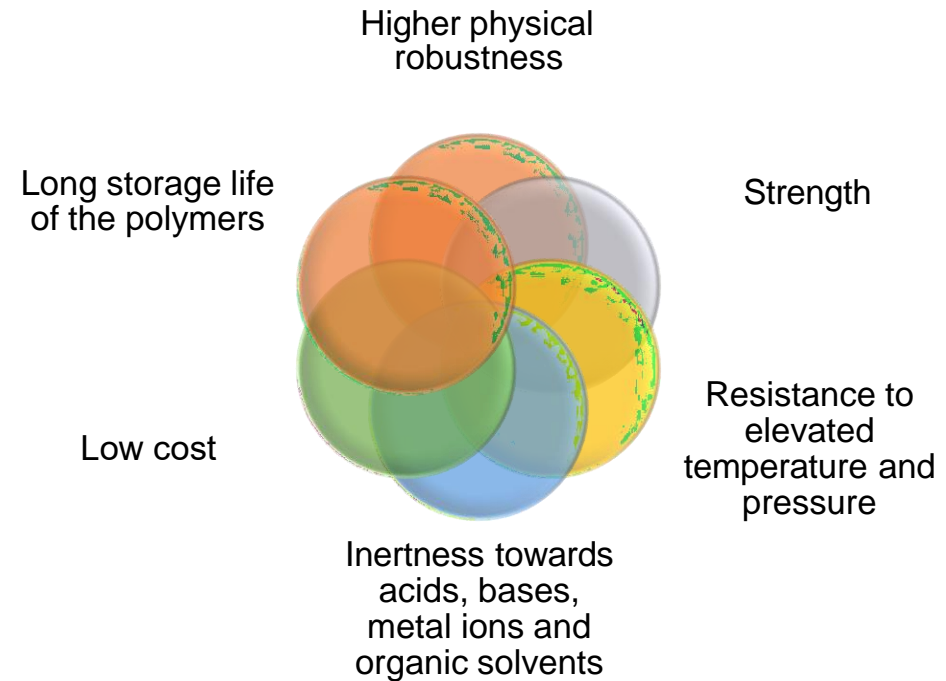
Solid phase extraction



Advantages of MIPs

- ❖ High **selectivity** and **affinity** for the **target molecule** used in the imprinting procedure.

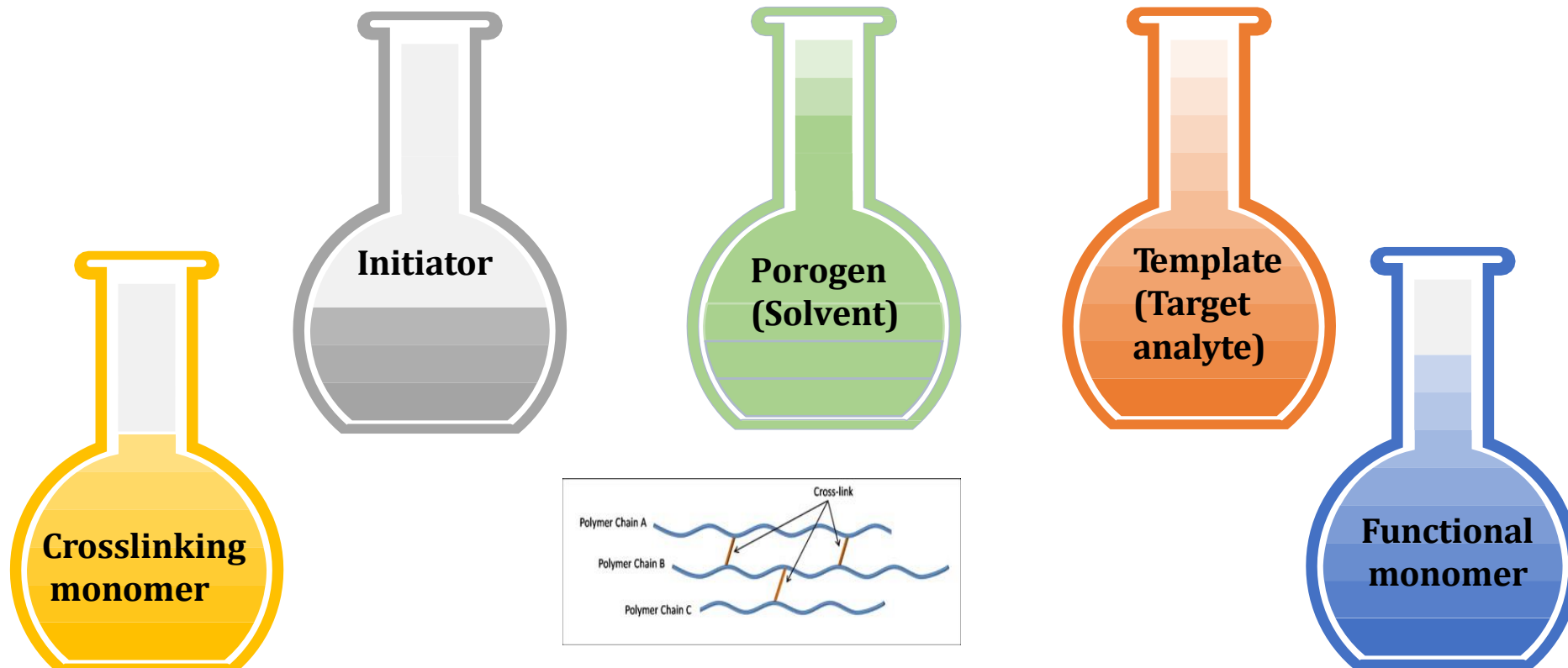
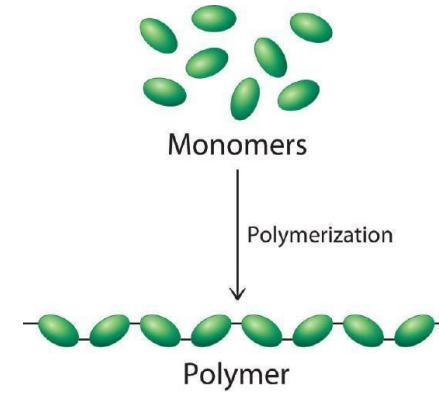
Compared to biological systems such as proteins and nucleic acids MIP has:



02 MIP-State of the art

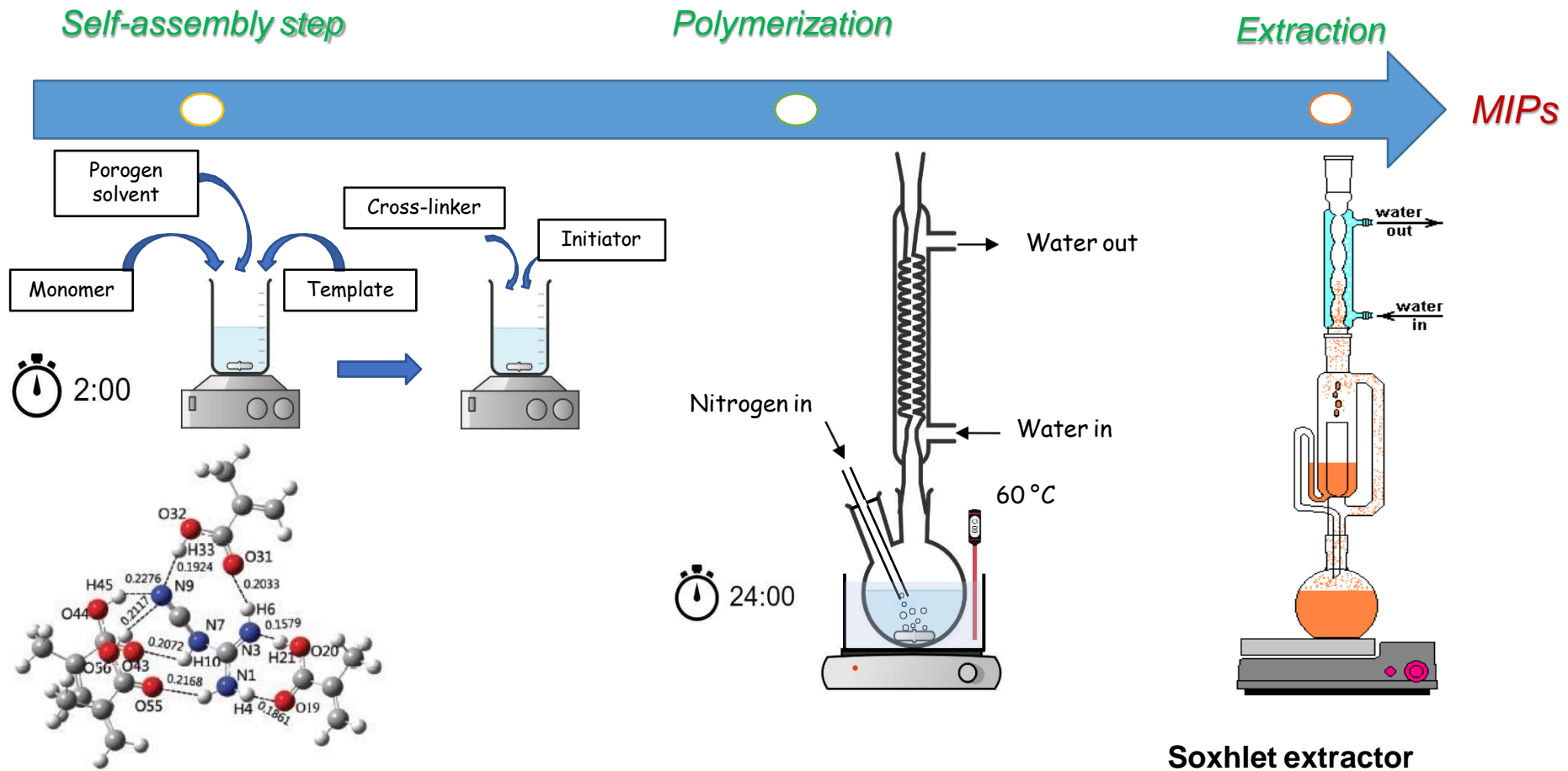
MIPs Synthesis

Components of MIP Mixture



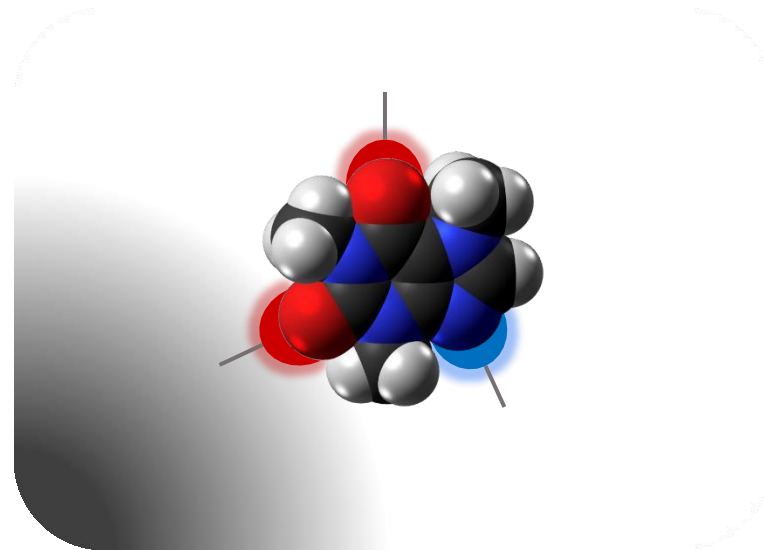
MIPs Synthesis

General procedure

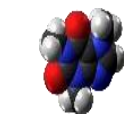


MIP synthesis

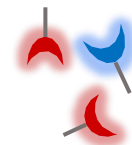
*Sulfamethoxazole
MIPs Synthesis*



Selective rebinding



**Template
(Sulfamethoxazole)**



Monomer (Methacrylamide MMA)

MIP-Synthesis

MIPs Synthesis

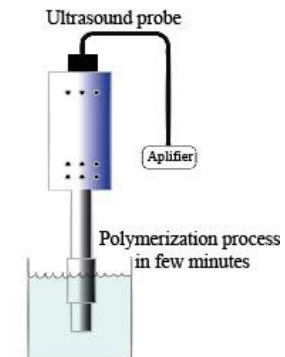
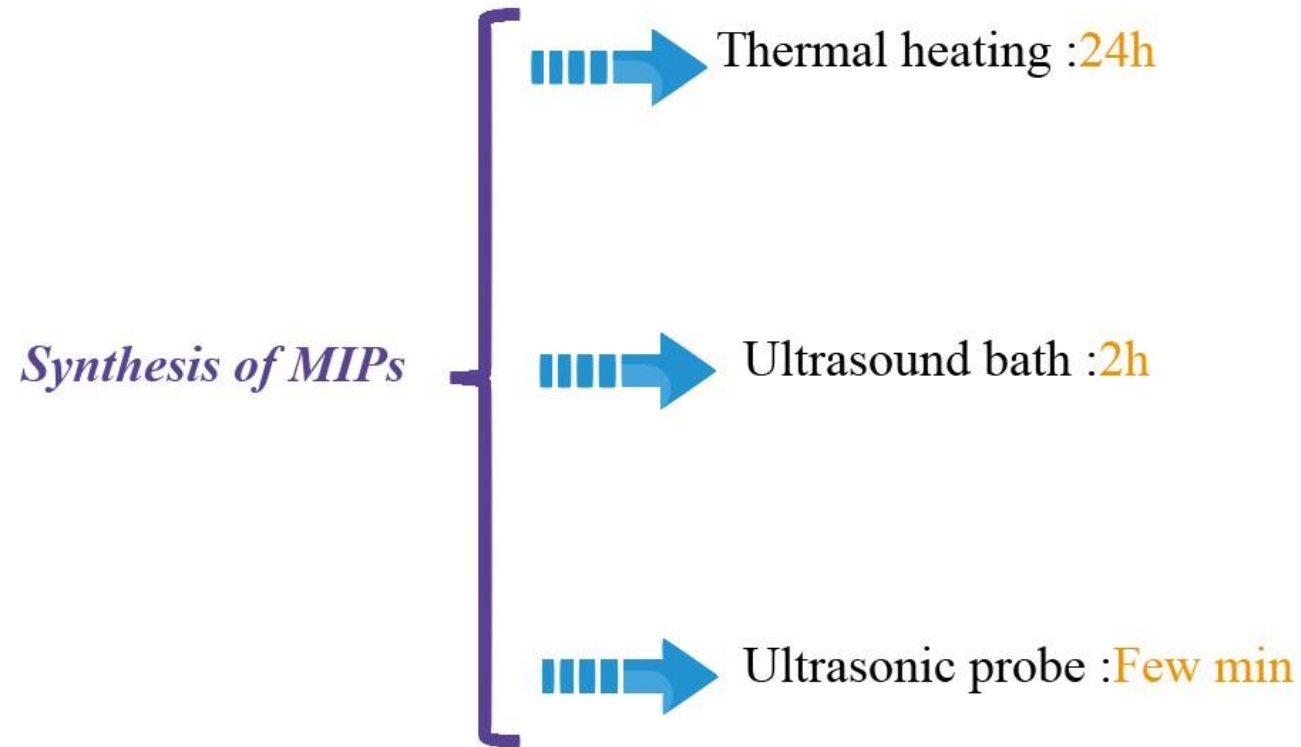


Figure : Synthesis of magnetic molecularly imprinted polymer

03 MIP-Synthesis

Theoretical optimizations prior to MIP s synthesis

Selection of the functional monomer

Prepolymer	E _{Monomer} (Hartree)	E _{Complex}	ΔE (kcal/mol)
Sulfamethoxazole:SMX	-1169.32	-	
SMX-Acrylamide	-245.92	-1415.29	-31.37
SMX- 4-vinyl pyridine	-323.88	-1493.25	-31.37
SMX-Methacrylic acid	-304.788	-1474.13	-13.80
SMX-Methacrylamide	-285.03	-1454.41	-37.65

Selection of the solvent

Complexes monomer-template-solvent	E _{complex} (Hartree)
SMX- Methacrylamide-ETOH	<u>-1608.60</u>
SMX- Methacrylamide-DMSO	<u>-2004.76</u>
SMX- Methacrylamide-DMF	<u>-1701.53</u>
SMX- Methacrylamide-ACETONE	<u>-1646.392</u>
SMX- Methacrylamide-ACETONITRILE	<u>-1586.45</u>
SMX- Methacrylamide-TOLUENE	<u>-1724.49</u>
SMX- Methacrylamide-WATER	<u>-1530.38</u>
SMX- Methacrylamide-METHANOL	<u>-1569.47</u>

Methacrylamide -SMX have highest interaction energy in DMSO solvent due to the formation of a more stable complex.

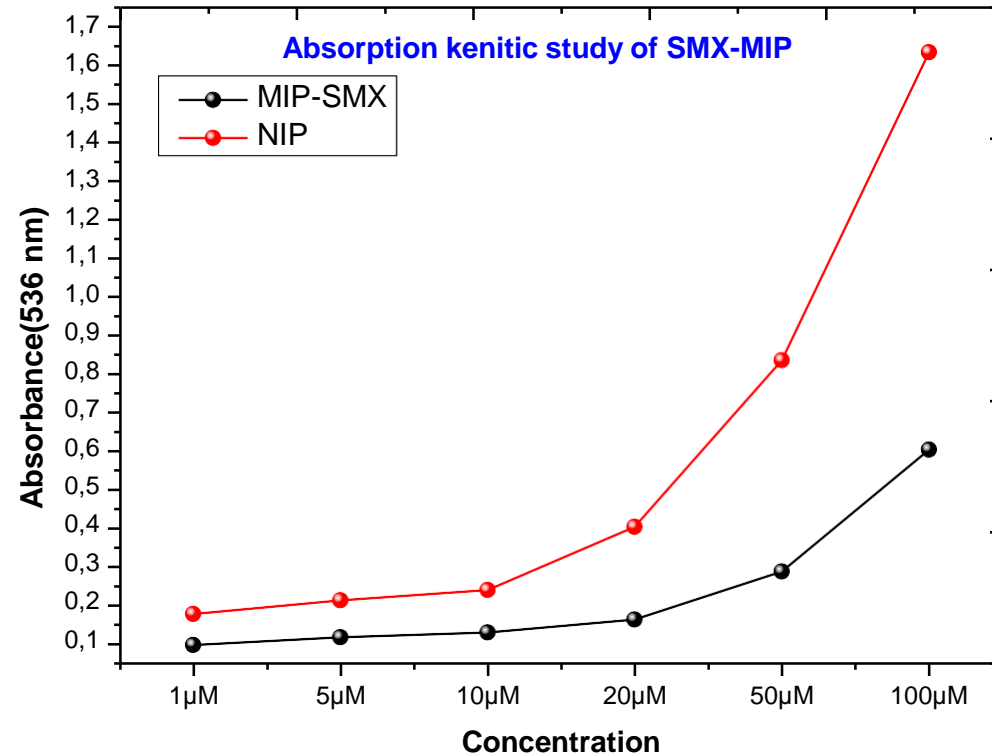
MIPs synthesis optimizations

Optimization of time and amplitude of synthesis was done to select the best parameters for MIP-Ultrasound probe synthesis

	Parameters	Comment	Polymer quality
MMA -MIP 22-07-2020	10 MIN /20A	Polymer was formed	++
MMA -NIP 22-07-2020	10 MIN /20A	Polymer was formed	++
MMA -MIP 23-07-2020	7.5MIN /30A	Polymer was formed	+++
MAA-NIP 23-07-2020	7.5MIN /30A	Polymer was formed	+++
MMA-MIP 23-07-2020	5 MIN /20A	Polymer was formed	++++
MMA-NIP 23-07-2020	5 MIN /20A	Polymer was formed	++++

5 min as time of synthesis and 20 as pulse amplitude was selected

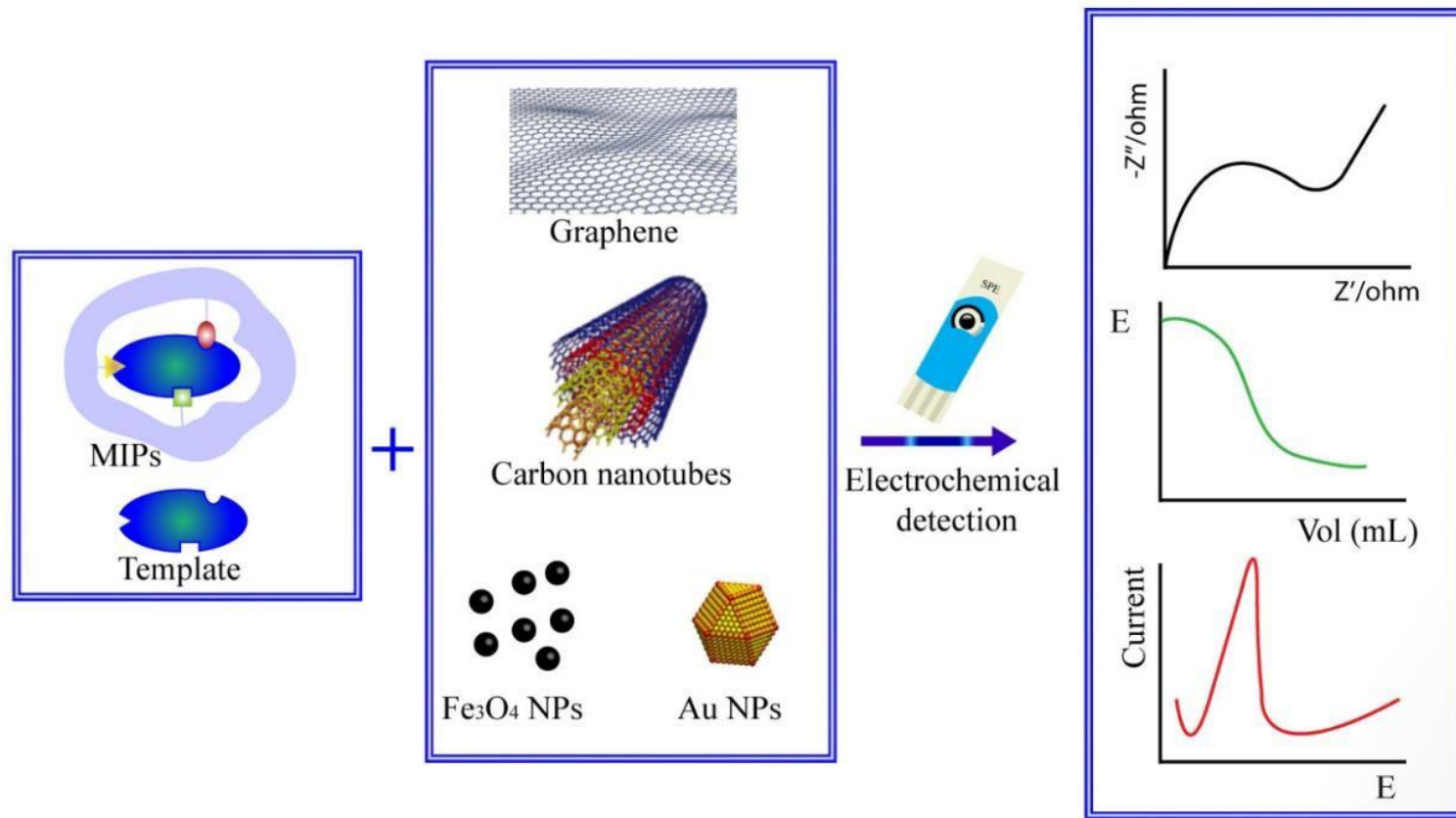
Graph of the un-retained template



MIP has higher capacity to capture the template compared to non imprinted polymer

02 MIP-State of the art

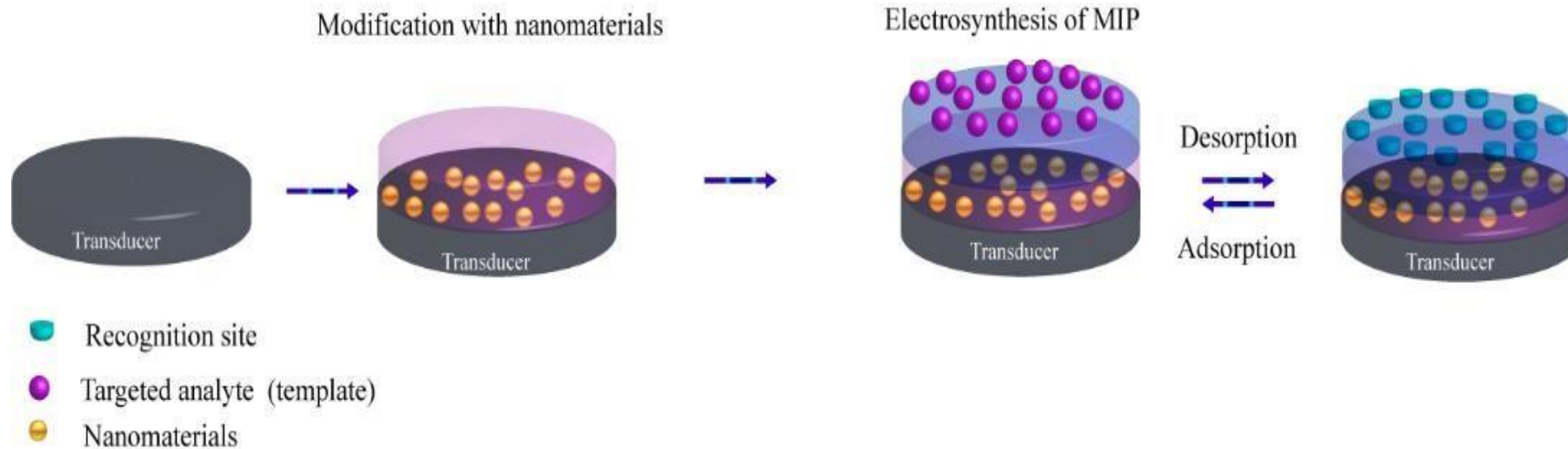
MIP based electrochemical sensors and nanomaterials



Scheme of MIP based electrochemical sensors and nanomaterials.

02 MIP-State of the art

*MIP based electrochemical sensors and
nanomaterials*
Electrosynthesis of MIPs



~~Initiator~~

~~Crosslinking
monomer~~

Template
(Target
analyte)



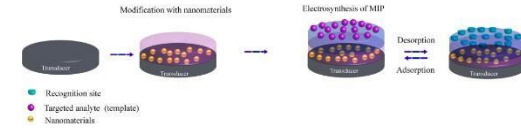
Porogen
(Solvent)
Buffer



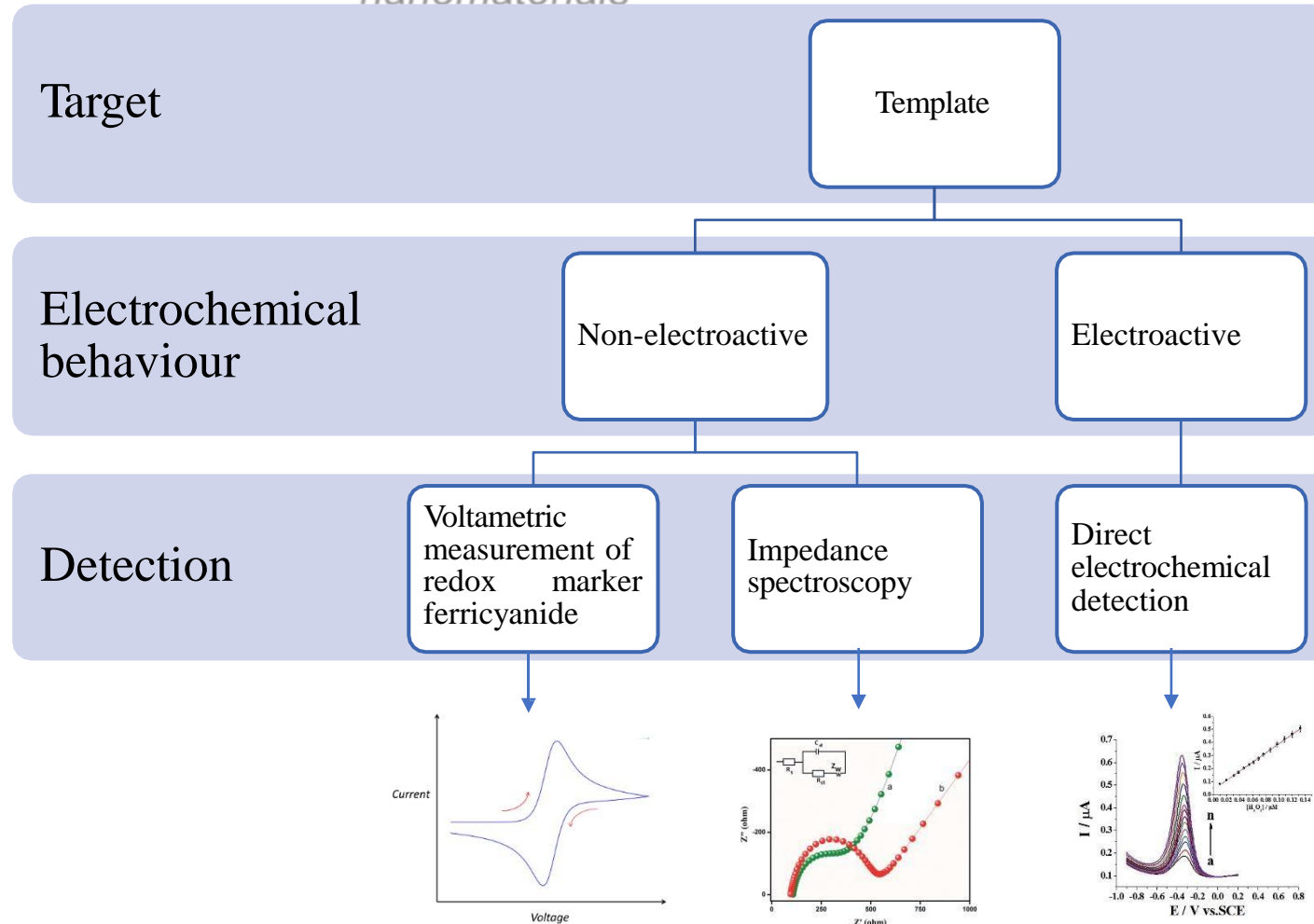
Functional
monomer



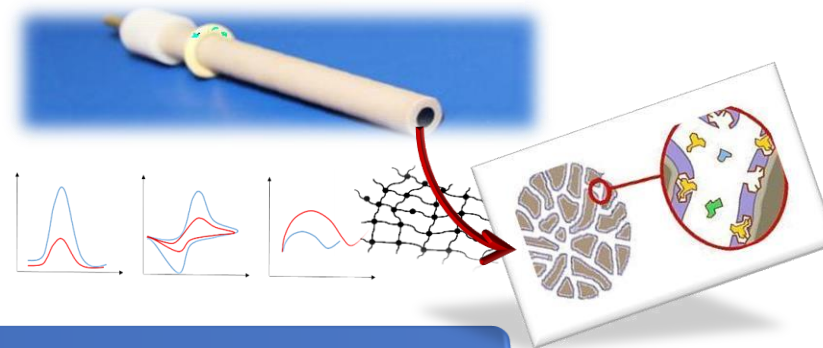
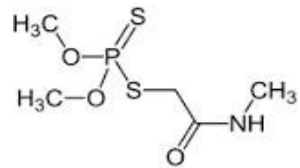
MIP-State of the art



MIP based electrochemical sensors and nanomaterials



MIP-MEPS based sensing strategy for the selective assay of dimethoate. Application to wheat flour samples



DIMETHOATE MONITORING IN WHEAT FLOUR

SAMPLE PREPARATION

ANALYTE DETECTION

MICROEXTRACTION BY PACKED SORBENT (MEPS)

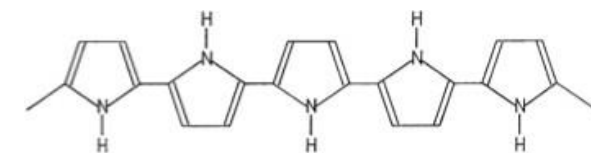
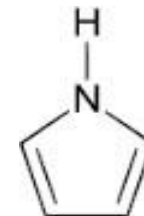
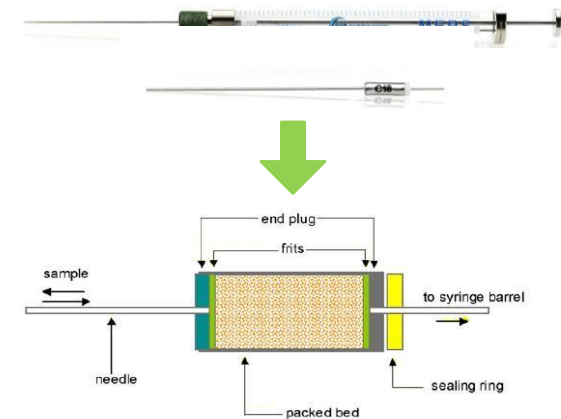
MIP-GLASSY CARBON ELECTRODE



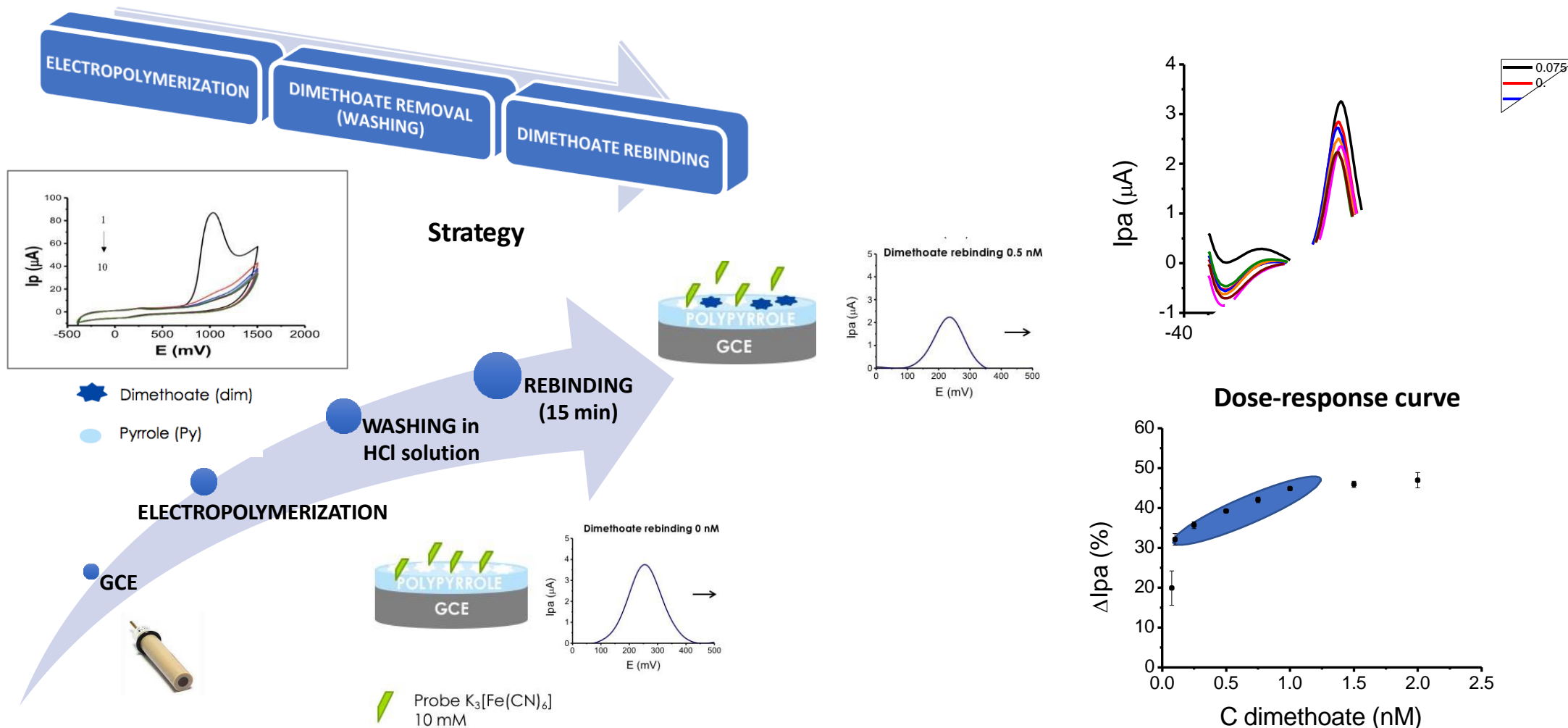
MIP-MEPS based sensing strategy for the selective assay of dimethoate. Application to wheat flour samples

D. Capoferri^a, M. Del Carlo^{a,1}, N. Ntshongontshi^b, E.I. Iwuoha^b, M. Sergi^a, F. Di Ottavio^a, D. Compagnone^{a,*,1}

^a Faculty of Biosciences and Technologies for Food, Agriculture and Environment, University of Teramo, via R. Balzarotti 1, 64100 Teramo, Italy
^b Sensor Lab, Department of Chemistry, University of the Western Cape, Bellville 7530, South Africa



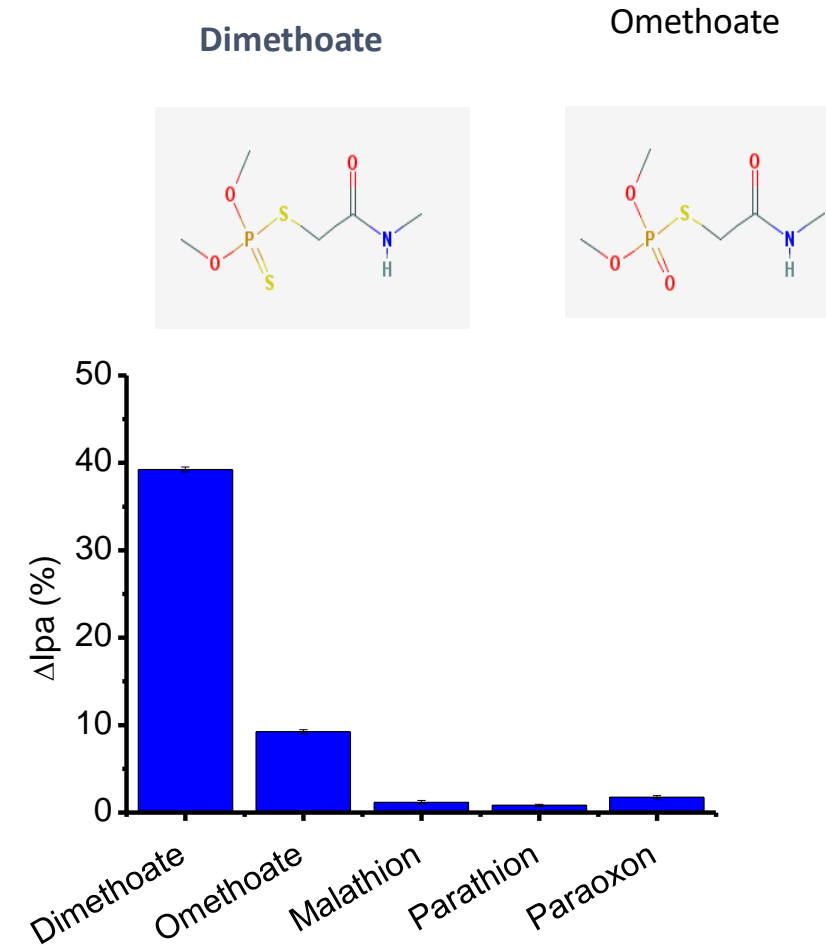
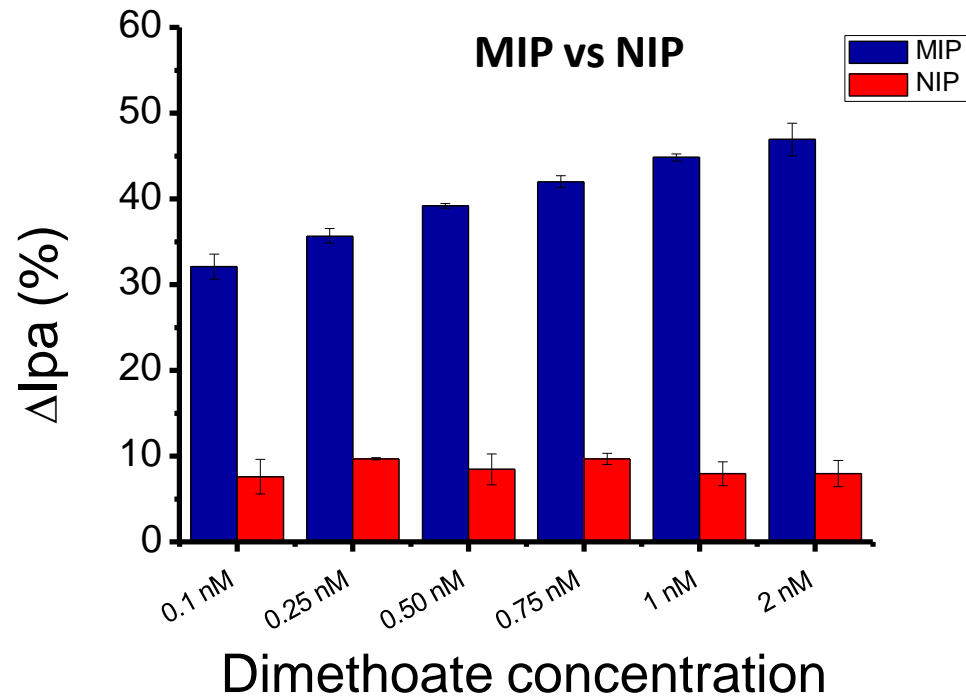
MIP-MEPS based sensing strategy for the selective assay of dimethoate. Application to wheat flour samples



MIP-MEPS based sensing strategy for the selective assay of dimethoate. Application to wheat flour samples

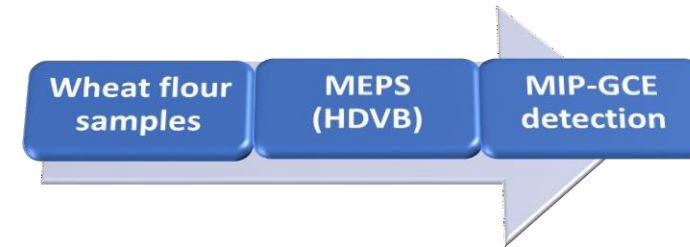
ΔI_{pa} (%)	Repeatability (RSD %)	Reproducibility (RSD %)
0.5 nM dimethoate (n=3)	0.68	2.72
1 nM dimethoate (n=3)	0.95	5.51

ΔI_{pa} (%) for malathion, parathion and paraoxon after the rebinding step was negligible; **omethoate** gave a response of **23%**.



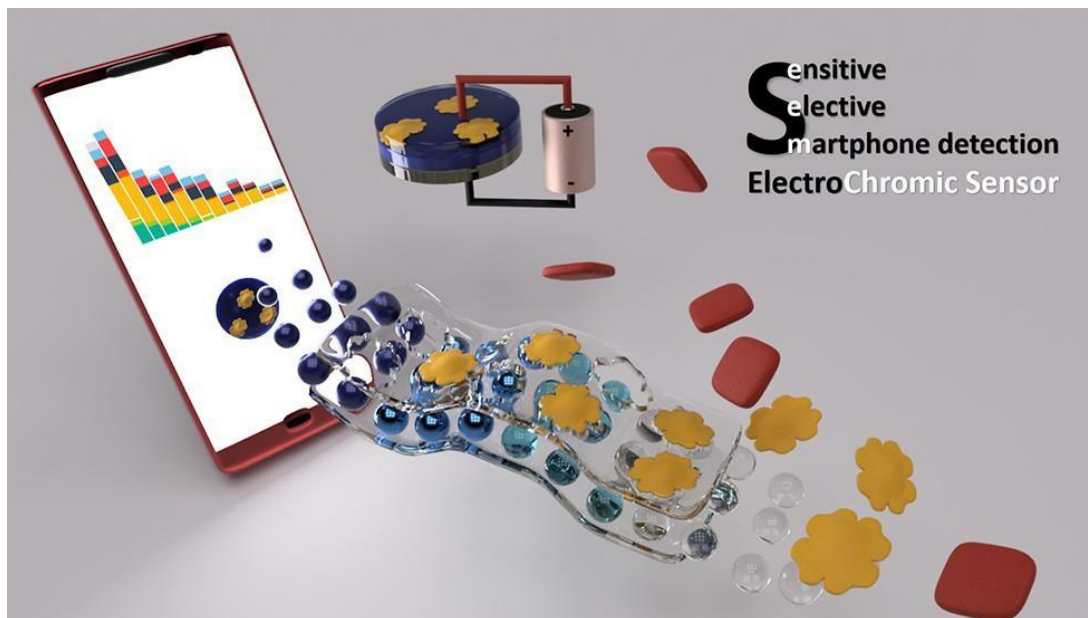
MIP-MEPS based sensing strategy for the selective assay of dimethoate. Application to wheat flour samples

Wheat flour samples: MIP vs. UHPLC-MS/MS

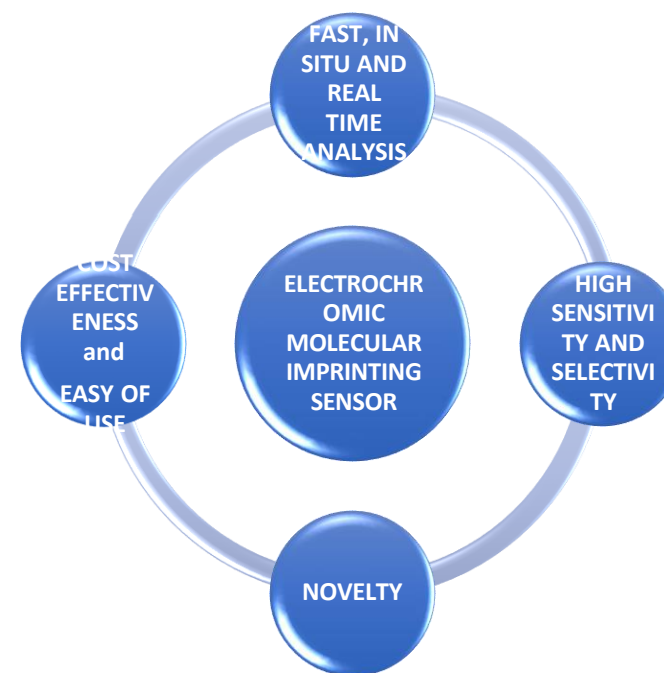


Samples	MIP-GCE RELATIVE ERROR (%) of dimethoate concentration ($\mu\text{g kg}^{-1}$)	MIP-GCE SD of dimethoate concentration ($\mu\text{g kg}^{-1}$)
Wheat flour spiked with dimethoate 0.5 MRL	+13.5	0.52
Wheat flour spiked with dimethoate 0.5 MRL + mix	+4.6	2.37
Wheat flour spiked with dimethoate MRL	-21.1	1.24
Wheat flour spiked with dimethoate MRL + mix	-21.2	1.36
Wheat flour spiked with dimethoate 1.5 MRL	+16.7	0.74
Wheat flour spiked with dimethoate 1.5 MRL + mix	-0.4	1.69
Wheat flour spiked with dimethoate MRL + omethoate (1:1)	+3.5	2.70
Wheat flour spiked with dimethoate MRL + omethoate (1:10)	-15.5	0.86

Electrochromic Molecular Imprinting Sensor for Visual and Smartphone-Based Detections



Sensitive
elective
smartphone detection
ElectroChromic Sensor



analytical
chemistry

Cite This: Anal. Chem. XXXX, XXX, XXX-XXX

Article

pubs.acs.org/ac

Electrochromic Molecular Imprinting Sensor for Visual and Smartphone-Based Detections

Denise Capoferri,^{†,‡,§} Ruslan Álvarez-Diduk,^{†,§} Michele Del Carlo,[‡] Dario Compagnone,[‡] and Arben Merkoçi^{*,†,||}

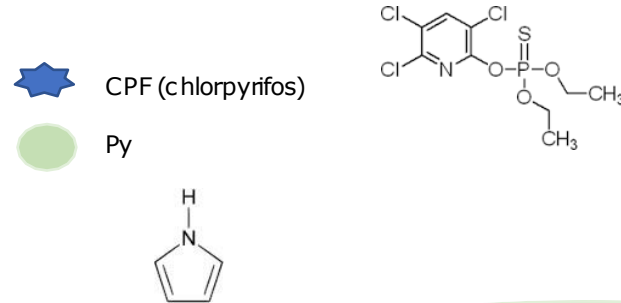
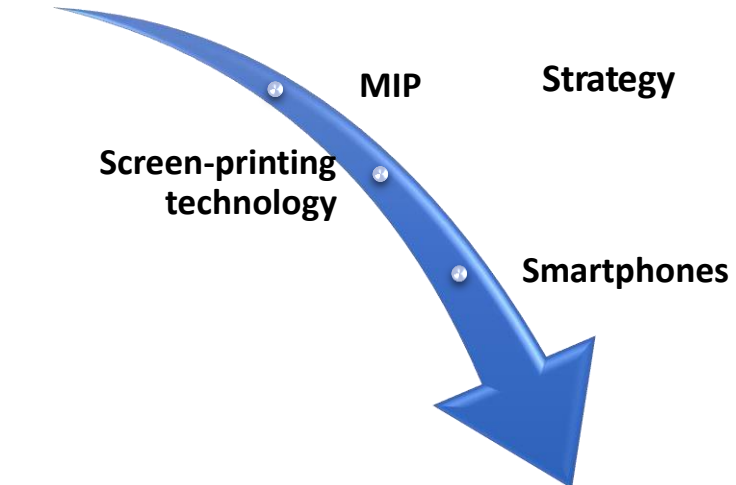
[†]Nanobioelectronics and Biosensor Group, Catalan Institute of Nanoscience and Nanotechnology (ICN2), CSIC, The Barcelona Institute of Science and Technology, Campus UAB, Bellaterra, 08193, Barcelona, Spain

[‡]Faculty of Biosciences and Technologies for Food, Agriculture and Environment, University of Teramo, via R. Balzarini 1, 64100 Teramo, Italy

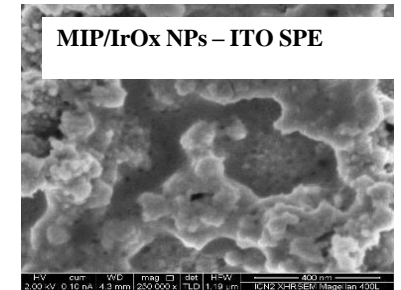
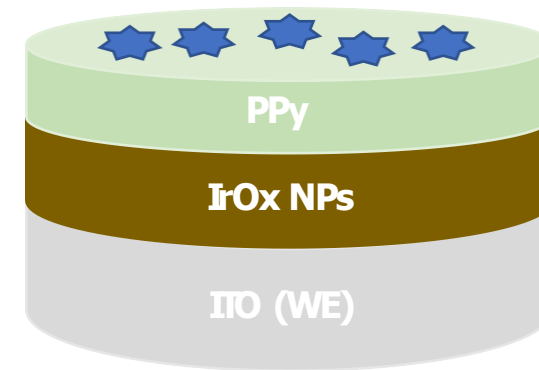
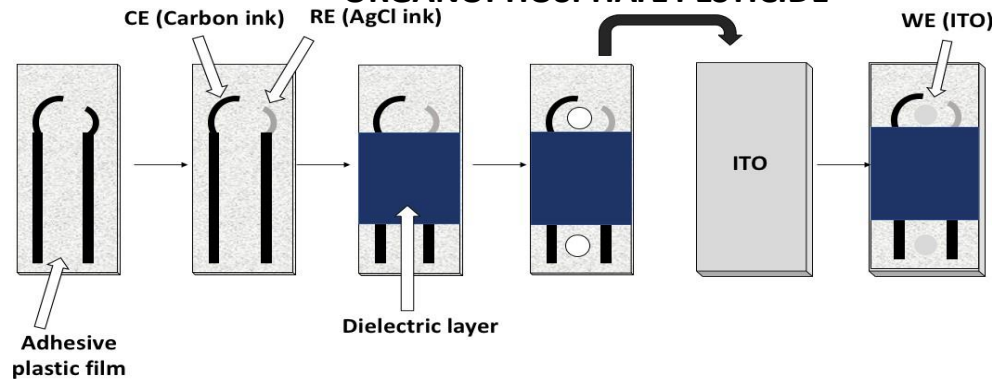
[§]Catalan Institution for Research and Advanced Studies (ICREA), Pg. Lluís Companys 23, 08010 Barcelona, Spain

Electrochromic Molecular Imprinting Sensor for Visual and Smartphone-Based Detections

Electrochromism

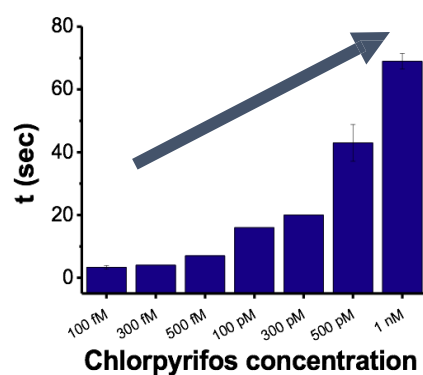
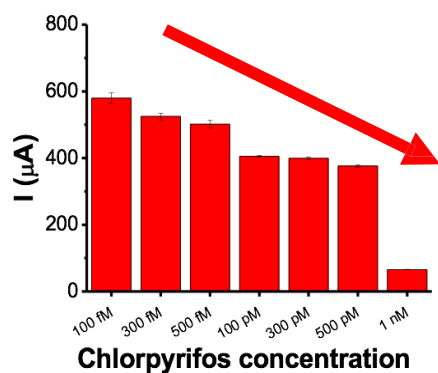
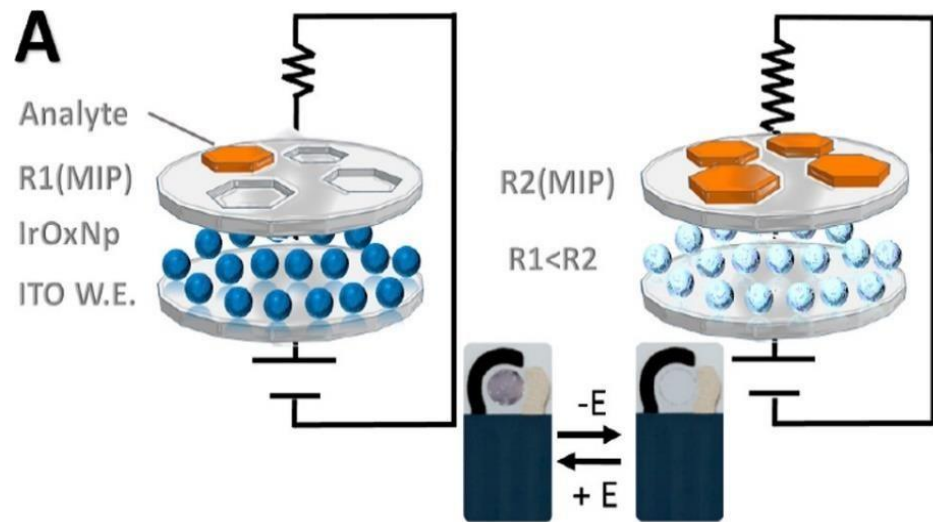


**ELECTROCHROMIC MOLECULAR
IMPRINTING SENSOR for an
ORGANOPHOSPHATE PESTICIDE**



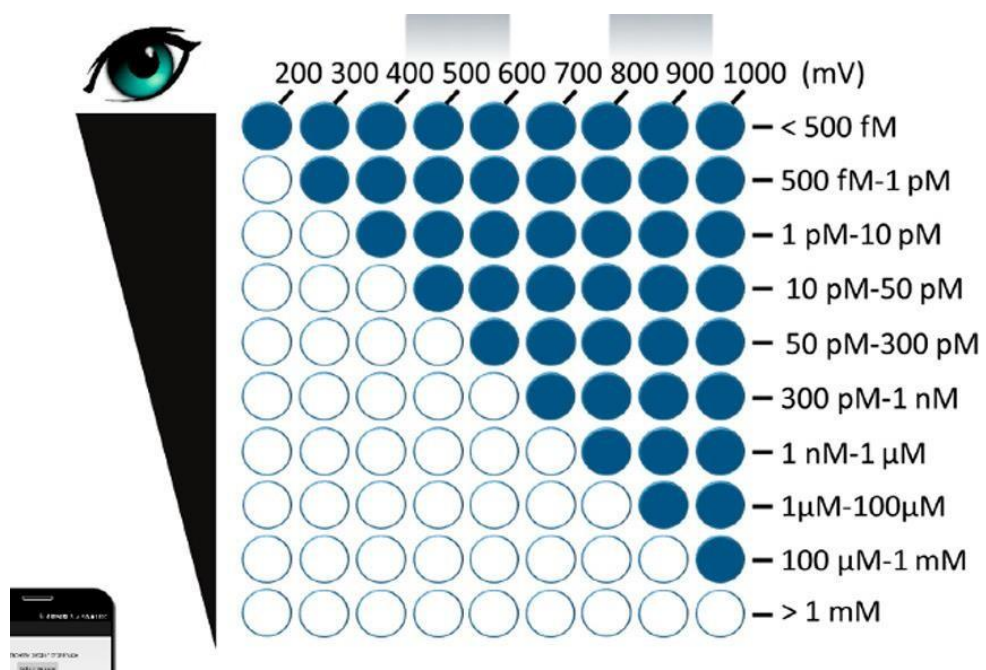
Electrochromic Molecular Imprinting Sensor for Visual and Smartphone-Based Detections

WORKING PRINCIPLE

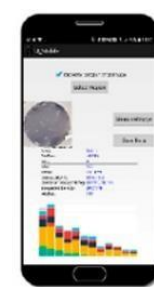
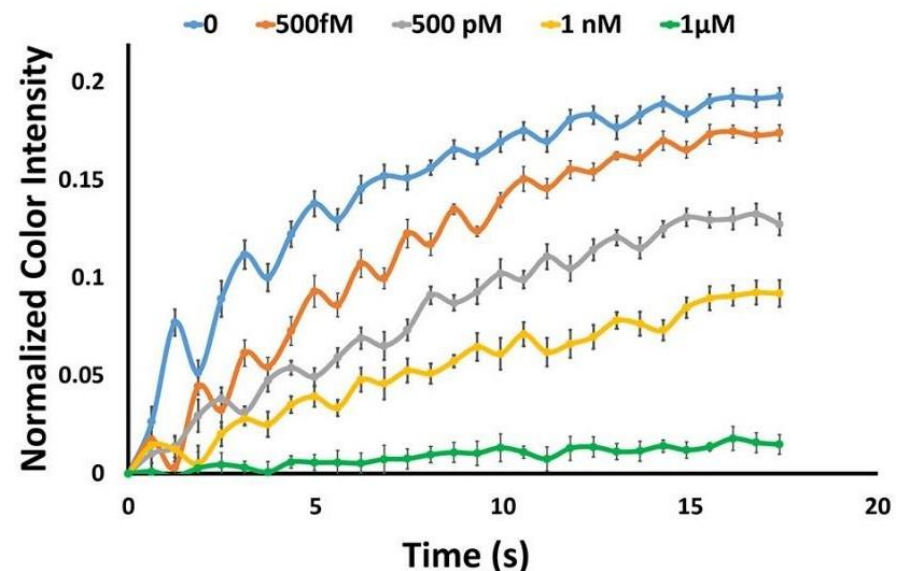


Electrochromic Molecular Imprinting Sensor for Visual and Smartphone-Based Detections

VISUAL APPROACH

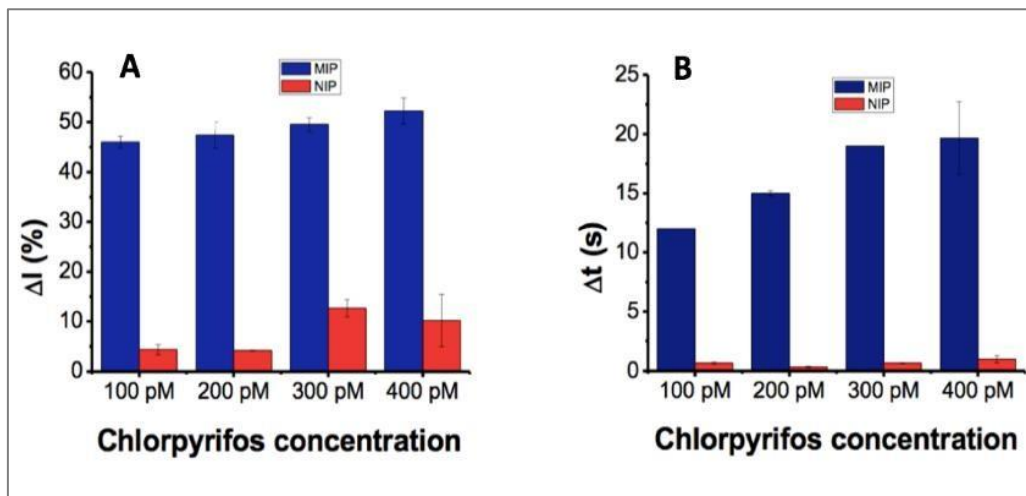


SMARTPHONE APPROACH



Electrochromic Molecular Imprinting Sensor for Visual and Smartphone-Based Detections

MIP vs NIP



Recovery values of chlorpyrifos in spiked drinking water samples (n = 3) using the current response

Added (Spiked)	Found	Recovery (%)	RSD (%)
500 fM	517.19 fM	103.44 ± 16.14	15.60
500 pM	471.45 pM	94.29 ± 17.92	19.00
1 nM	0.99 nM	99.50 ± 19.90	20.00
1 μM	0.98 μM	97.55 ± 25.87	26.52
1 mM	1.07 mM	106.57 ± 15.30	14.36

SELECTIVITY (500 mV-1000 mV)

